

**Metabolic Studies on 1-Cyclopropyl-4-phenyl-1,2,3,6-tetrahydropyridinyl
Derivatives by HPLC and LC-ESI/MS**

by

Xueqin Shang

Thesis submitted to the Faculty of the
Virginia Polytechnic Institute and State University
in partial fulfillment of the requirements for the degree of

MASTER OF SCIENCE

in

Chemistry

Dr. Neal Castagnoli, Jr., Chairman

Dr. Mark R. Anderson

Dr. Larry T. Taylor

July 28, 1999

Blacksburg, Virginia

Key words: cyclopropylaminyl radical cations, biotransformation,
cytochrome P450, single electron transfer, HPLC, LC/MS

Copyright 1999, Xueqin Shang

Metabolic Studies on 1-Cyclopropyl-4-phenyl-1,2,3,6-tetrahydropyridinyl Derivatives by HPLC and LC-ESI/MS

Xueqin Shang

(ABSTRACT)

The MAO-B catalyzed metabolic bioactivation of the parkinsonian inducing agent 1-methyl-4-phenyl-1,2,3,6-tetrahydropyridine (MPTP) to generate the neurotoxic 1-methyl-4-phenylpyridinium species (MPP⁺) is well documented. The N-cyclopropyl analog (CPTP) of MPTP is a mechanism based inactivator of MAO-B which presumably is processed by a single electron transfer (SET) pathway to generate a bioalkylating species. These results have prompted us to study how the cytochromes P450, the major liver drug metabolizing oxidases, interact with N-cyclopropyl analogs of MPTP. HPLC with diode array detection and LC-electrosprary ionization mass spectrometry (LC-ESI/MS) based methods have been developed for metabolite detection and characterization. From the UV spectral data and pseudomolecular ion species observed by LC-ESI/MS, we have identified N-oxide, C-hydroxylated, and pyridinium metabolites. For the *trans*-1-(2-phenylcyclopropyl) analog, cinnamaldehyde and *p*-hydroxycinnamaldehyde also were characterized.

Incubation of CPTP and its derivatives with cDNA expressed human hepatic cytochrome P450 has shown that CYP2D6 catalyzes the formation of cinnamaldehyde, the N-descyclopropyl, pyridinium and hydroxylated products. CYP3A4 is responsible for the formation of the N-descyclopropyl and pyridinium species and cinnamaldehyde but it does not mediate any hydroxylation reactions. Since both the α -carbon oxidation and N-descyclopropylation transformations are mediated by a single enzyme (either CYP2D6 or CYP3A4), we propose a common intermediate for both pathways, namely the cyclopropylaminyl radical cation generated by the SET pathway. This intermediate partitions between the α -carbon oxidation pathway leading to the dihydropyridinium and pyridinium species and the ring opening pathway leading to the N-descyclopropyl

metabolite and aldehyde species. The phenyl substituent on the cyclopropyl ring stabilizes the ring opened distonic radical cation and favors the ring opening pathway and results in the formation of less of the pyridinium species. The proton and methyl substituents on the cyclopropyl ring favor the α -carbon oxidation pathway and increased amounts of the pyridinium species are formed.

ACKNOWLEDGMENTS

I would like to express my gratitude to my advisor, Professor Neal Castagnoli, Jr., for his guidance, inspiration and encourage through this work. His profound knowledge, enormous enthusiasm and keen insight into chemistry have been, and will continue to be, a great resource of inspiration for me. In addition, I also would like to thank Mrs. Kay Castagnoli for all of her much appreciated help. Especially, I would like to thank both of them for encouraging me to go through some difficult times in my life.

Grateful acknowledgments are also made to Dr. Mark Anderson and Dr. Larry Taylor for their valuable advice and assistance.

I wish to thank the members of the Castagnoli research group for their suggestions, assistance and friendship. Special thanks to Dr. Estuko Usuki for helping me to start with LC/MS. I also wish to thank Dr. Phillippe Bissel, Mr. Sean Hislop, Dr. Simon Kuttab, Dr. Stephen Mabic, Dr. Geraldine Magnin and Dr. Zhiyang Zhao for their organic support.

Finally, my gratitude goes to my family members, especially my parents, for their love, understanding and support of my study.

I also wish to thank the Harvey W. Peters Research Center for supporting this research work.

TABLE OF CONTENTS

Chapter 1. Introduction	1
1.1. MPTP - A Parkinsonia Inducing Agent	1
1.2. CPTP - An MAO-B Inactivator	2
1.3.1. CPTP - How Does It Behave with Cytochrome P450 ?	4
Chapter 2. Literature Review and Research Proposal	7
2.1. Xenobiotic Biotransformation	7
2.2. Cytochrome P450	8
2.3. Mechanism of Amine Oxidation by Cytochrome P450	11
2.3.1. Oxidative N-Dealkylation of Tertiary Amine by Cytochrome P450	12
2.3.2. Mechanism of Inactivation of P450 by Cyclopropylamines	14
2.4. Research Proposal	17
Chapter 3. Characterize Metabolic Pathways of CPTP and Derivatives Incubated with Rat Liver Microsomes	20
3.1. Analytical Approaches	20
3.2. Experimental	21
3.3. CPTP	25
3.3.1. Results	25
3.3.2. Conclusions	43
3.4. MCPTP	45
3.4.1. Results	45
3.4.2. Conclusions	59
3.5. PCPTP	61
3.5.1. Results	61
3.5.2. Conclusions	91

Chapter 4. Metabolism of CPTP Derivatives Catalyzed by cDNA Expressed Forms of Human Hepatic Cytochrome P450	93
4.1. Introduction	93
4.2. Experimental	93
4.3. Results	94
4.4. Conclusions	104
Chapter 5. Conclusions	106
Chapter 6. References	108

LIST OF SCHEMES

Scheme 1	The MAO-B Catalyzed Bioactivation of 1-Methyl-4-phenyl -1,2,3,6-tetrahydropyridine	2
Scheme 2	Proposed SET Pathway for the MAO-B Catalyzed Oxidation of 1-Cyclopropyl-4-phenyl-1,2,3,6-tetrahydropyridine	3
Scheme 3	Proposed Pathways for the Cytochrome P450 Catalyzed α -Carbon Oxidation and Mechanism Based Inactivation of <i>N</i> -Benzylcyclopropylamine	5
Scheme 4	Proposed Mechanism of Oxidative N-Dealkylation of Tertiary Amines by P450	14
Scheme 5	Proposed Mechanism of Inactivation of MAO by <i>N</i> -Benzylcyclopropylamine	15
Scheme 6	Mechanism Postulated for the Inhibition of Cytochrome P450 by Cyclopropylamines	16
Scheme 7	Alternative Mechanism Proposed for the Inhibition of P450 by Cyclopropylamine	17
Scheme 8	Proposed Mechanism of Partition of the Cyclopropylaminyl Radical Cation	19
Scheme 9	<i>In vitro</i> Metabolic Fates of MPTP	26
Scheme 10	Predicted Metabolic Pathways of CPTP Catalyzed by Liver Microsomes	28
Scheme 11	Metabolic Pathways of Liver Microsomal Catalyzed Oxidation of CPTP	44
Scheme 12	Predicted Metabolic Pathways of MCPTP Catalyzed by Liver Microsomes	46
Scheme 13	Metabolic Pathways of Liver Microsomal Catalyzed Oxidation of MCPTP	60
Scheme 14	Predicted Metabolic Pathways of PCPTP Catalyzed by Liver Microsomes	62
Scheme 15	Fragmentation Generated from PCPTP	76

Scheme 16	The Fragmentation Generated from M23	77
Scheme 17	The Fragmentation Generated from M22	80
Scheme 18	The Fragmentation Generated from M21	80
Scheme 19	The Fragmentation Generated from M24	83
Scheme 20	The Fragmentation Generated from M20	84
Scheme 21	A Catalyzed Pathway Proposed to Account for the Formation of Cinnamaldehyde	85
Scheme 22	A Catalyzed Pathway Proposed to Account for the Formation of <i>p</i> -Hydroxycinnamaldehyde	90
Scheme 23	Metabolic Pathway of Liver Microsomal Catalyzed Oxidation of PCPTP	92
Scheme 24	Metabolic Pathway of PCPTP Catalyzed by CYP2D6	97
Scheme 25	Metabolic Pathway of PCPTP Catalyzed by CYP3A4	99
Scheme 26	Mechanism Proposed to Account for the α -Carbon Oxidation and N-Descyclopropylation	100
Scheme 27	Metabolic Pathway of CPTP Catalyzed by CYP3A4	102
Scheme 28	Metabolic Pathway of CPTP Generated by CYP3A4	103
Scheme 29	Proposed Partitioning of the Cyclopyoaminyl Radical Cation	105

LIST OF FIGURES

Figure 1	Structure of Ferric Protoporphyrin IX, the Prosthetic Group of Cytochromes P450	9
Figure 2	Catalytic Cycle of Cytochrome P450	11
Figure 4	HPLC-DA Analysis of CPTP Incubated with Liver Microsomes Supplemented with NADPH System for 60 min	30
Figure 5	HPLC-DA Analysis of CPTP Incubated with Liver Microsomes in the Absence of NADPH System for 60 min	31
Figure 6	UV Spectra of M2, M4 and S1	32
Figure 7	UV Spectrum of M1	33
Figure 8	UV Spectrum of M3	33
Figure 9	HPLC/MS/UV Analysis of Liver Microsomal Incubation Mixture of CPTP	35
Figure 10	Mass Spectrum of CPTP Obtained from LC-ESI/MS Analysis	36
Figure 11	LC-ESI/MS Spectrometric Analysis of Liver Microsomal Incubation Mixture of CPTP. Positive Ion TIC and Reconstructed Ion Current Chromatograms	37
Figure 12	Mass Spectrum of M3 Obtained from LC-ESI/MS Analysis of CPTP Incubation Mixture	38
Figure 13	Reconstructed Ion Current Trace of M1	39
Figure 14	Reconstructed Ion Current Chromatograms of the two Minor Metabolites M5 and M6	41
Figure 15	Proposed Structures of the two Minor Metabolites	42
Figure 16	The Structure of Deuterated CPTP-d ₄ and the Corresponding Predicted Metabolites	43
Figure 17	HPLC-DA Analysis of MCPTP Incubated with Liver Microsomes Supplemented with NADHP System for 60 min	48
Figure 18	HPLC-DA Analysis of MCPTP Incubated with Liver Microsomes in the Absence of NADPH System for 60 min	49
Figure 19	UV Spectra of M7, M8, M9 and S2	50

Figure 20	UV Spectra of M10 and M11	51
Figure 21	UV Spectra of M12 and M13	52
Figure 22	HPLC/MS/UV Analysis of Liver Microsomal Incubation Mixture of MCPTP	54
Figure 23	Mass Spectrum of MCPTP Obtained from LC-ESI/MS Analysis	55
Figure 24	Reconstructed ion Current Chromatograms from HPLC-ESI/MS Analysis of Liver Microsomal Incubation Mixture of MCPTP	56
Figure 25	Reconstructed Ion Current Chromatograms of the two Minor Metabolites M14 and M15	58
Figure 26	HPLC-DA Analysis of PCPTP Incubated with Liver Microsomes Supplemented with NADPH System for 60 min	64
Figure 27	HPLC-DA Analysis of CPTP Incubated with Liver Microsomes in the Absence of NADPH System for 60 min	65
Figure 28	HPLC Response of the Substrate PCPTP vs. Incubation Time	66
Figure 29	HPLC Responses of PCPTP Metabolites vs. Incubation Time	66
Figure 30	UV Spectrum of S3	67
Figure 31	UV Spectrum of M16	68
Figure 32	UV Spectrum of M17	68
Figure 33	UV Spectrum of M18	69
Figure 34	UV Spectrum of M19	69
Figure 35	UV Spectrum of M20	70
Figure 36	UV Spectrum of M21	70
Figure 37	UV Spectrum of M22	71
Figure 38	UV Spectrum of M23	71
Figure 39	UV Spectrum of M24	72
Figure 40	HPLC/MS/UV Analysis of Liver Microsomal Incubation Mixture of PCPTP	73
Figure 41	Reconstructed Ion Current Chromatograms of Liver Microsomal Incubation Mixture of PCPTP	74
Figure 42	Mass Spectrum of PCPTP	75
Figure 43	Mass Spectrum of M20	77

Figure 44	Mass Spectrum of the Mixture of M21 and M22	79
Figure 45	Mass Spectrum of M24	82
Figure 46	Mass Spectrum of Synthetic N-oxide PCPTP	82
Figure 47	Mass Spectrum of M20	84
Figure 48	HPLC-DA Chromatograms of Incubation Mixtures of PCPTP and Cinnamaldehyde and Authentic Cinnamyl Alcohol	87
Figure 49	Negative Ion Current Trace and Mass Spectrum of M16	89
Figure 50	Reconstructed Ion Current Chromatograms of two Minor Metabolites M25 and M26	91
Figure 51	HPLC-DA Chromatogram of Metabolic Fates of PCPTP by CYP2A6	95
Figure 52	HPLC-DA Chromatogram of Metabolic Fates of PCPTP by CYP2D6	96
Figure 53	HPLC-DA Chromatogram of Metabolic Fates of PCPTP by CYP3A4	98
Figure 54	HPLC-DA Chromatogram of Metabolic Fates of CPTP by CYP3A4	101
Figure 55	HPLC-DA Chromatogram of Metabolic Fates of MCPTP by CYP3A4	102
Figure 56	Comparison of the Pyridinium Metabolite Formation from CPTP and its Derivatives by CYP3A4	104

Chapter 1. Introduction

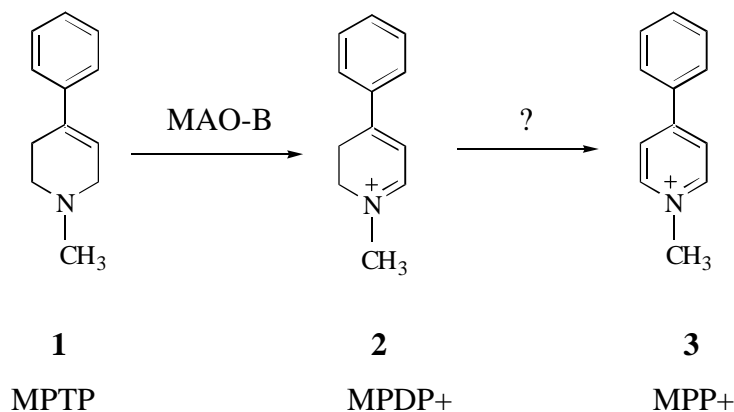
1.1. MPTP - A Parkinsonian Inducing Agent

Parkinson's disease is a chronic and progressive neurological disorder that affects the motor system and is characterized by symptoms such as muscular rigidity, tremor, shuffling gait, movement disorders and impaired balance and coordination [1]. The primary pathology is a lesion of dopaminergic neurons in the substantia nigra pars compacta leading to dopamine depletion in this region of the brain [2]. Depletion of dopamine causes the nerve cells of the striatum to fire out of control, resulting in the inability of patients to control their movement in the normal manner. The cause of this disease is unknown. Many researchers believe that oxidative damage, environmental toxins, genetic predisposition and accelerating age may cause this disease [3,4].

In recent years there has been much interest in the neurotoxin 1-methyl-4-phenyl-1,2,3,6-tetrahydropyridine (MPTP). MPTP first came to the attention of researchers when young drug addicts who had used a street drug, 1-methyl-4-phenyl-4-propionoxypiperidine (MPPP, a mepheridine analog) contaminated with MPTP, developed a parkinsonian syndrome [5]. MPTP was suspected as the causative agent. Later investigations of MPTP's toxicity have shown that MPTP was not the actual cause of neuronal cell death. Instead the ultimate toxin was shown to be the 1-methyl-4-phenylpyridinium species (MPP^+) [6]. Animal studies demonstrated that the neurotoxicity of MPTP was prevented by blocking MPP^+ formation by monoamine oxidase B (MAO-B) inhibitors [7-9].

The actual pathway leading to neurodegeneration is described in Scheme 1. MPTP (**1**) partitions into the brain where it is oxidized to the unstable dihydropyridinium species $MPDP^+$ (**2**) by MAO-B [10-12]. $MPDP^+$ undergoes further oxidation to MPP^+ (**3**) [13-15]. MPP^+ is actively transported into the dopaminergic neurons by the dopamine uptake system [16,17]. It is concentrated in the matrix of the mitochondria where it inhibits NADPH dehydrogenase and mitochondrial electron transport leading to cessation of oxidative phosphorylation, ATP depletion and neuronal death [18].

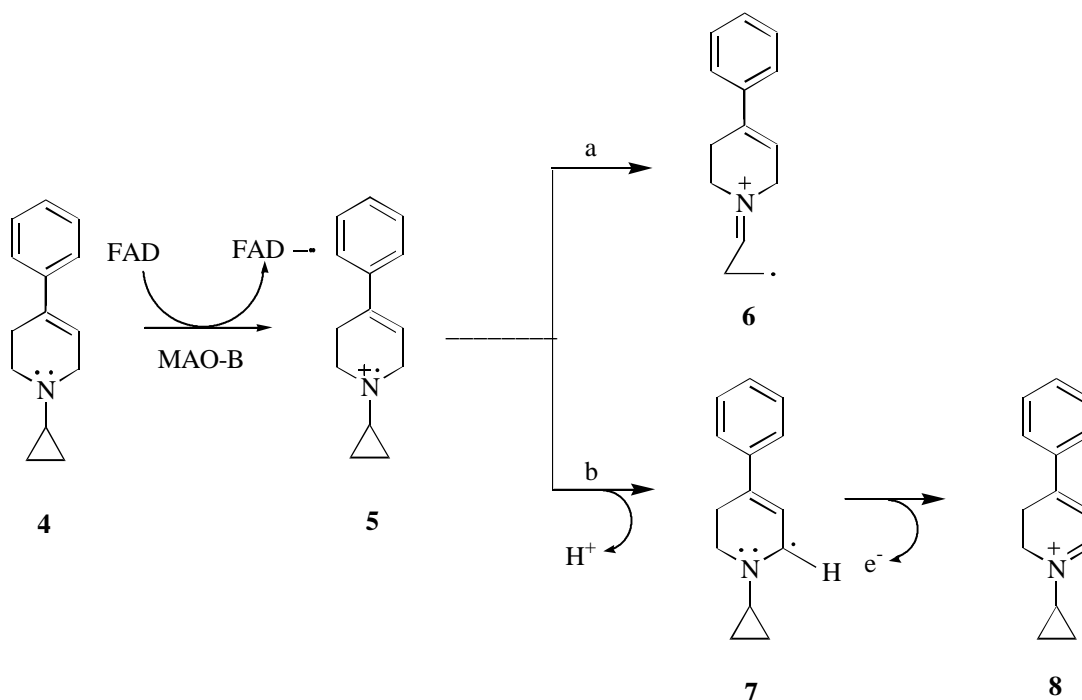
Scheme 1. The MAO-B Catalyzed Bioactivation of 1-Methyl-4-phenyl-1,2,3,6-tetrahydropyridine



1.2. CPTP - An MAO-B Inactivator

The finding that MPTP, a cyclic tertiary amine, has shown good MAO-B substrate properties was quite surprising since most substrates for this enzyme are acyclic primary and secondary amines such as dopamine or benzylamine. This interesting finding has prompted us to study the substrate properties of MPTP analogs. Silverman's studies have shown that primary and secondary amines (good MAO substrates) can be converted to mechanism based inactivators by introducing an N-cyclopropyl group [19-20]. In order to improve our knowledge about the interactions of MAO-B with tertiary amines, the N-cyclopropyl analog of MPTP, 1-cyclopropyl-4-phenyl-1,2,3,6-tetrahydropyridine (CPTP, **4**) was examined. The results have shown that CPTP is a mechanism based MAO-B inactivator [21].

Scheme 2. Proposed SET Pathway for the MAO-B Catalyzed Oxidation of 1-Cyclopropyl-4-phenyl-1,2,3,6-tetrahydropyridine (**4**)



A single electron transfer (SET) pathway (Scheme 2), analogous to that proposed by Silverman for N-benzylcyclopropylamine [22], has been postulated to account for the inactivation properties of CPTP. One-electron transfer from the nitrogen lone pair to FAD yields the cyclopropylaminyl radical cation **5**. This intermediate either forms the reactive distonic radical cation **6** by ring-opening (pathway a) or loses an α -proton to produce the carbon radical **7** (pathway b). This carbon radical undergoes a second one-electron transfer to produce the dihydropyridinium intermediate **8**. The distonic radical cation **6** is very reactive and can bind tightly with an active site functionality of MAO-B and inactivate the enzyme.

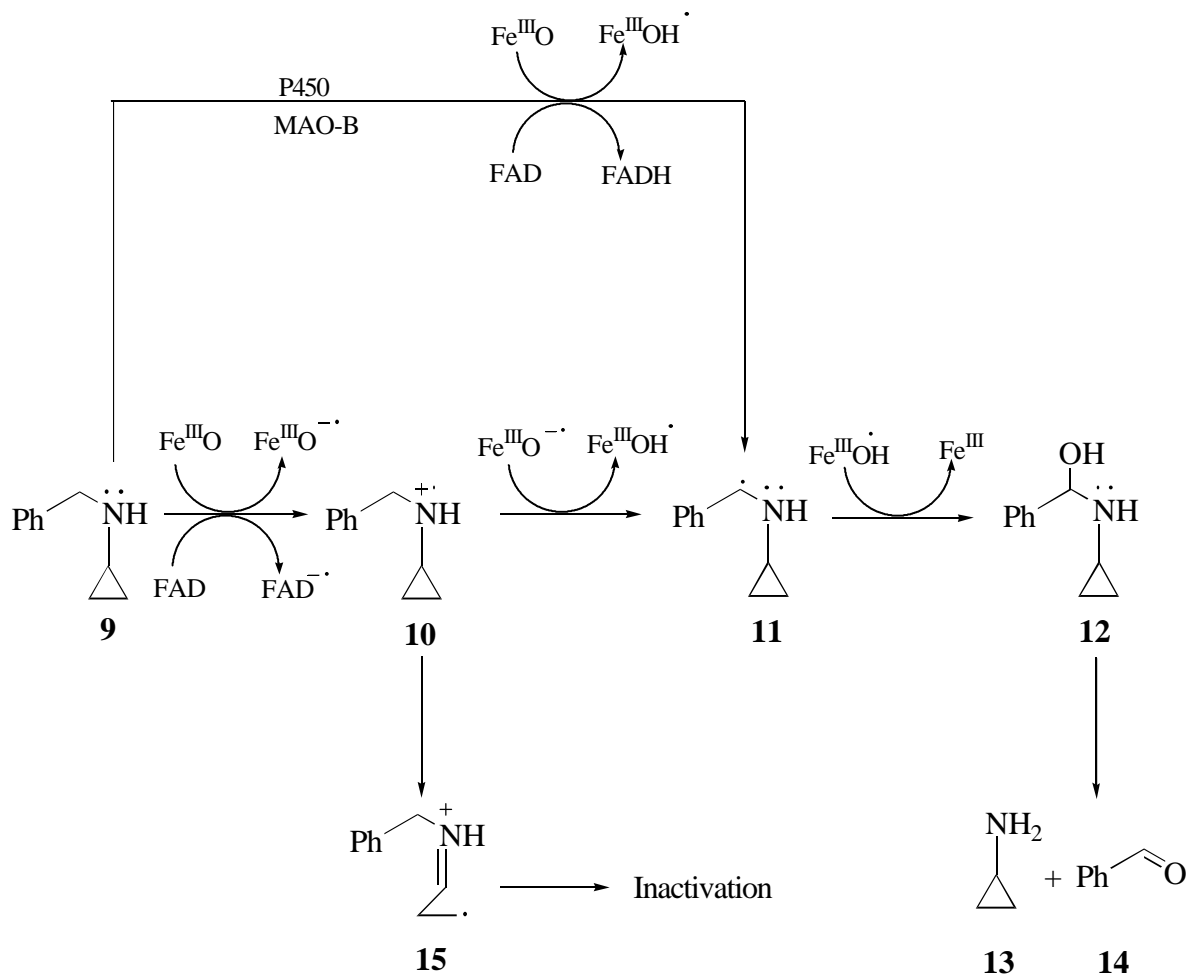
Kinetic studies have shown that cyclopropyl groups attached to a radical bearing atom undergo ring opening at a rate of $7 \times 10^{11} \text{ sec}^{-1}$ or faster [23]. Consistent with this behavior, the amounts of the dihydropyridinium metabolite **8** formed from CPTP were too low to detect, suggesting that the deprotonation pathway (b) does not compete effectively with the ring opening pathway (a).

1.3. CPTP - How Does It Behave with Cytochrome P450?

Since MAO-B is linked to Parkinson's disease as a result of degradation of brain dopaminergic neurons [24], compounds that selectively inhibit or inactivate MAO-B may be useful in the treatment of parkinson's disease [25]. The elucidation of the catalytic mechanism for the bioactivation of MPTP would aid in the design of potential new antiparkinsonian agents. The finding that CPTP is a mechanism based inactivator of MAO-B has prompted us to study its substrate properties with another class of important liver drug-metabolizing enzyme, the cytochrome P450s. As will be discussed, CPTP is a substrate of P450 instead of an inactivator. This result has suggested that the catalytic pathways for the two enzyme systems may be different despite claims to the contrary.

The cytochrome P450 catalyzed oxidation of cyclopropylamines has been extensively studied. The focus of these studies deals with mechanisms of N-dealkylation reactions [26,27]. The pathway of oxidative N-debenzylation of N-benzylcyclopropylamine (**9**), illustrated in Scheme 3 [33], has been proposed to proceed via an initial SET step from the nitrogen lone pair to the P450 iron oxo group followed by deprotonation of the resulting aminyl radical cation (**10**) to form an α -carbon radical (**11**). Radical recombination leads to a carbinolamine intermediate (**12**) that cleaves to yield the dealkylated amine (**13**) and an aldehyde (**14**). The evidence supporting the SET pathway has been summarized in a recent paper by Guengerich and Macdonald [28]. Particularly persuasive are the mechanism based inactivator properties of cyclopropylamines such as **9** [29-32]. In this case the SET generated cyclopropylaminyl radical cation **10** ring opens to form the primary carbon centered radical **15** that is thought to mediate the inactivation by alkylating an enzyme active site functionality. However, the SET pathway remains a subject of debate with some investigators favoring a hydrogen atom transfer (HAT) pathway (**9** \rightarrow **11**) which bypasses the radical cation intermediate **10** and leads directly to the α -carbon radical **11**.

Scheme 3. Proposed Pathways for the Cytochrome P450 Catalyzed α -Carbon Oxidation and Mechanism Based Inactivation of *N*-Benzylcyclopropylamine (9)



Our previous MAO-B related studies on a variety of 1-cyclopropyl-4-substituted-1,2,3,6-tetrahydropyridinyl derivatives did not allow us to distinguish between the SET and HAT pathways in this system [33]. Some of the analogs are mechanism based inactivators and the SET pathway appears to be favored. Other analogs display poor or no inactivator properties but instead are readily converted to the corresponding dihydropyridinium metabolites, behavior which may be more consistent with an HAT than an SET mechanism since the HAT pathway precludes the possibility of the ring opening reaction leading to enzyme inactivation.

Since CPTP is an efficient MAO-B mechanism based inactivator with very poor substrate properties, metabolite formation could not be detected spectrophotometrically. Its cytochrome P450 substrate properties would allow us to examine the metabolic fate and generate information on the metabolic profile which could be very useful in the elucidation of the catalytic mechanism. These considerations have led us to a series of metabolic studies of CPTP derivatives with cytochrome P450. We will examine pathways of CPTP derivatives with different substituents on the 2-position of the cyclopropyl ring. These will be discussed in more detail in the research proposal presented in the next chapter. We propose to characterize the metabolic pathways of CPTP and its derivatives and identify the responsible forms of P450. We hope that the results will give us a better picture relative to either cyclopropyl ring opening or dihydropyridinium formation. We also hope to provide fundamental insights that will lead to further investigations of the mechanism of the cytochrome P450 catalyzed oxidation of cyclopropyltetrahydropyridinyl derivatives.

Chapter 2. Literature Review and Research Proposal

2.1. Xenobiotic Biotransformation

Drug metabolism in its broadest sense may be considered as the absorption, distribution, biotransformation and excretion of drugs. During the past twenty years, important advances have been made in the development of new analytical techniques and in the recognition of the importance of metabolism and disposition in terms of the biological activities of drugs and other xenobiotics (compounds foreign to the body). Studies on the metabolism of drugs and other xenobiotics are often pursued in an effort to gain insights into the molecular mechanisms of the responsible metabolic pathways and the molecular events associated with the fate and pharmacological and toxicological properties of biologically active compounds.

Here we focus primarily on the biotransformation of xenobiotics. A foreign substance usually enters the body by being absorbed through mucous membranes, the skin, the digestive tract or the lungs. One factor that affects its absorption is its degree of lipophilicity. Lipophilic compounds tend to be easily absorbed into the body but not easily excreted from the body. Therefore, these compounds must be converted to hydrophilic compounds so that they can be eliminated before reaching toxic levels. Enzyme systems that catalyze metabolic reactions bring about structural modifications of xenobiotics that generally lead to more polar and biologically less active metabolites. This is the classical concept of metabolic detoxification. Liver has long been considered as the main site of xenobiotic detoxification. However, biotransformation of xenobiotics may produce metabolites with cytotoxic, mutagenic or carcinogenic properties as well [34-36]. In some case, xenobiotics may be metabolized to mitochondrial toxins that can lead to neurodegeneration [5].

Biotransformation is normally classified as Phase I (or functionalization reactions) and Phase II (or conjugation reactions). Phase I reactions include oxidation, reduction, hydrolysis and hydration. Phase II reactions include glucuronidation, sulphation, acetylation, methylation, conjugation with glutathione, amino acids and fatty acids. Phase I reactions create a reactive functional group on the molecule that can be modified by the phase II enzymes. Conjugates are more water-soluble than their

substrates and thus are rapidly excreted through the kidneys into the urine. Therefore, Phase II reactions are the true "detoxification" pathways [37].

The liver is the main organ responsible for Phase I and Phase II biotransformation reactions. Most of our fundamental knowledge regarding the molecular mechanisms of biotransformation has been derived from studies on liver enzymes. The Phase I oxidative enzymes are almost exclusively localized in the hepatic endoplasmic reticulum, along with the Phase II enzyme, glucuronyl transferase. In addition, other Phase II enzymes, including the glutathione-S-transferases, are found predominantly in the cytoplasm. Attempts to isolate the endoplasmic reticulum by tissue homogenization result in fragmentation to yield particles known as microsomes. The major components of the microsomes are its two electron transport chain systems: the NADPH-linked system [38-40], with cytochrome P450 [41,42] as the terminal oxidase, and the NADH-linked system [43,44], with cytochrome b₅ [45-47] as the electron acceptor. The main metabolic function of the NADPH-cytochrome P450 system is to participate in the Phase I reactions, mainly oxidation of drugs and other xenobiotics. On the other hand, the function of the NADH-cytochrome b₅ chain is not fully understood, although it appears to play a role in fatty acid desaturation. The catalytic mechanisms of the cytochrome P450 system have been extensively studied because this family of enzymes catalyzes the oxidation of a wide variety of steroids, fatty acids, eicosanoids, drugs, carcinogens and pesticides [48].

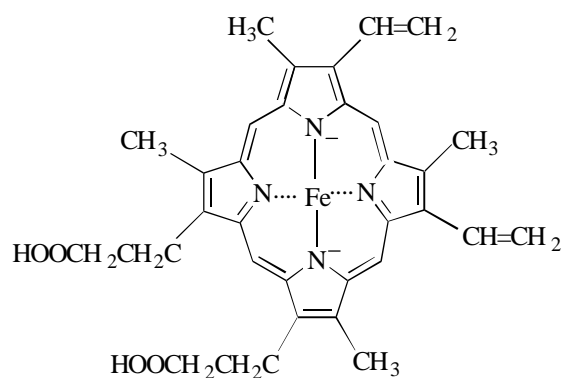
Two approaches to investigate the biotransformation of xenobiotics involve *in vitro* and *in vivo* methodologies. *In vitro* experiments are conducted with an isolated cell, cell fraction or purified enzyme. *In vivo* experiments take place within a living organism. By performing experiments *in vitro*, it may be easier to isolate metabolites and analyze the results. *In vivo* experiments are often confounded with other factors, making it difficult to isolate the biotransformation products of xenobiotics.

2.2. Cytochrome P450

Cytochrome P450 is the terminal oxidase component of the electron transfer system present in the endoplasmic reticulum and is classified as a hemo-containing enzyme, with iron protoporphyrin IX as the prosthetic group (Figure 1). The enzyme

consists of a family of closely related isoenzymes imbedded in the membrane of the endoplasmic reticulum. They exist in multiple forms with a monomeric molecular weight of approximately 45000-55000 Da. The heme is non-covalently bound to the apoprotein. The name cytochrome P450 is derived from the fact that the cytochrome exhibits a spectral absorbance at 450 nm when reduced and complexed with carbon monoxide.

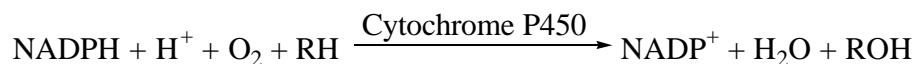
Figure 1. Structure of Ferric Protoporphyrin IX, the Prosthetic Group of Cytochromes P450



The isoforms of cytochrome P450 (CYP) are different enzymes classified according to amino acid sequence homology. P450 genes are classified into gene families with members of the same family having at least 40% amino acid sequence identity (e. g. CYP1, CYP2, etc). The number denotes the family. They are further divided into subfamilies (CYP1A, CYP2B, etc) with sequence identity of 55% [49]. The letter labels the subfamily. Individual genes can be labeled as CYP1A1, CYP1A2, etc [50,51]. In human liver, CYP2D6 and CYP3A4 seem to be the dominant isoforms mediating a variety of substrate oxidations [51]. Furthermore, the level of CYP3A4 is as high as 60% of the total P450. Methods to characterize P450 substrate selectivity have been developed in recent years. These methods include correlation studies, selective inhibition or induction studies, enzyme purification and reconstruction studies, and studies with expressed enzymes from cloned DNAs [52,53].

Cytochrome P450 is found in many tissues including the adrenal cortex [54], lung [55], skin [56] and kidney [57]. It is especially high in the liver [58]. Differential centrifugation of a liver homogenate yields several fractions that have been characterized in term of structures present in the intact cell. The principal fraction obtained at 10,000 x g sediment contains mitochondria. The 100,000 x g sediment contains the microsomal fraction. The 100,000 x g supernatant fraction contains the soluble enzymes such as the hydrolases, aldehyde oxidase and various dehydrogenases. Microsomal preparations contain the enzymes necessary for cytochrome P450 catalysis but must be supplemented either with NADPH or an NADPH generating system.

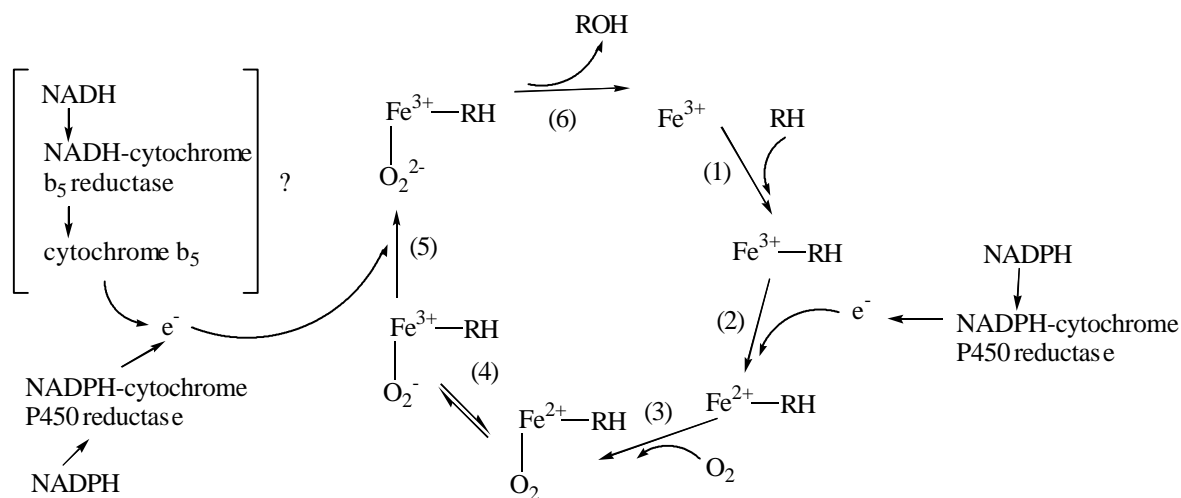
Cytochrome P450s form an important class of enzymes for the biosynthesis and metabolism of endogenous compounds such as fatty acids, steroids, eicosanoids, and vitamins and xenobiotics such as drugs, environment pollutants and industrial chemicals [59]. The common Phase I reactions catalyzed by cytochrome P450 are carbon hydroxylation, heteroatom oxygenation, oxidative N- and O-dealkylation, deamination and epoxidation [59]. Cytochrome P450s carry out oxidative reactions with typical mixed-function oxidase stoichiometry:



During the above mixed-function oxidation reaction, reducing equivalents derived from $\text{NADPH} + \text{H}^+$ are consumed and one atom of oxygen is inserted into the substrate whereas the other one is reduced to H_2O .

The primary source of electrons for the cytochrome P450s is the NADPH system which transfers electrons via the second enzyme system, NADPH-cytochrome P450 reductase. NADPH-cytochrome-P450 reductase is a flavoprotein consisting of one mole of flavin adenine dinucleotide (FAD) and one mole of flavin mononucleotide (FMN) per mole of apoprotein. Cytochrome P450 is both the substrate- and oxygen- binding locus of the mixed function oxygen reactions. The central features of the cytochrome P450 catalytic cycle are the ability of the hemo iron to undergo cyclic oxidation/reduction reactions in conjunction with substrate binding and oxygen activation [60-64] (Figure 2).

Figure 2. Catalytic Cycle of Cytochrome P450. RH Represents the Drug Substrate and ROH the Corresponding Hydroxylated Metabolite (Adapted from White, R. and Coon, M. J. *Ann. Rev. Biochem.*, 49, 315-56, 1980.).



Substrates undergo rapid and stoichiometric binding to the ferric enzyme [65]. This complex accepts one electron from the flavoprotein NADPH-cytochrome-P450 reductase [66,67] to form substrate-bound ferrous enzyme. The substrate-bound ferrous species binds oxygen rapidly to form an oxygenated complex [68]. This oxygenated complex may generate an activated iron-oxygen complex by accepting the second electron from the flavoprotein or possibly from cytochrome b_5 [63,69,70]. Oxygen is then added to the substrate. After that, the oxygenated product dissociates to leave the iron in the original ferric state.

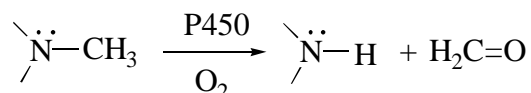
2.3. Mechanism of Amine Oxidation by Cytochrome P450

Because of the obvious importance of the P450s in the metabolism of xenobiotics, study of mechanism of P450's action has long intrigued chemists, biochemists, pharmacologist and toxicologists. Oxidation of amines is of considerable biological and pharmacological significance. Amine moieties are common in drug and other xenobiotics ingested into the body. N-dealkylation is a common means of degrading these molecules. They are often transformed into more polar compounds that are easy excreted from the

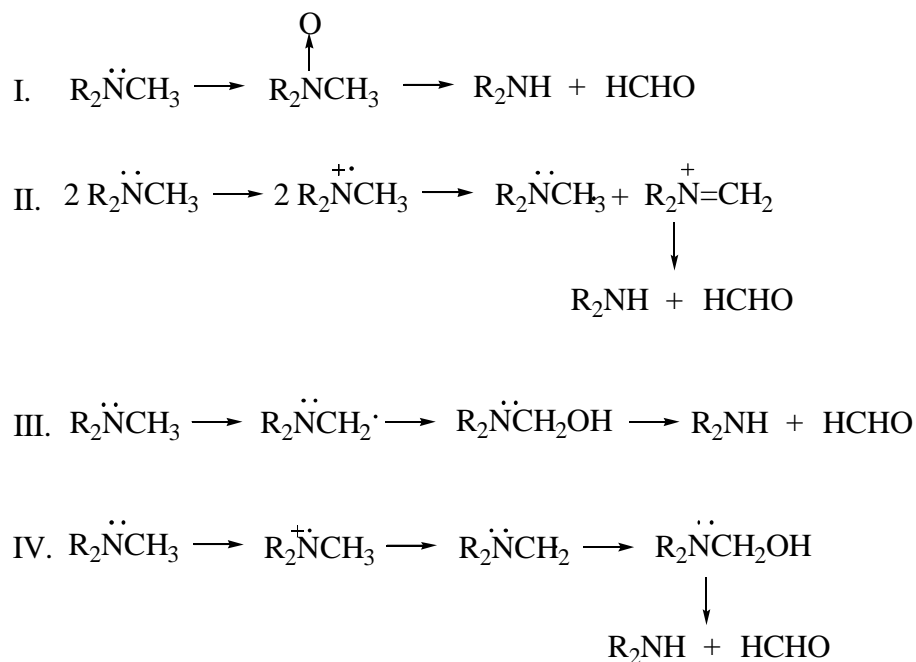
body due to enhanced solubility. Here we primarily focus our discussion on oxidative N-dealkylation by P450s since this pathway is related to the thesis work.

2.3.1. Oxidative N-Dealkylation of Tertiary Amines by Cytochrome P450

Oxidative N-dealkylation is an important reaction in the metabolism of numerous xenobiotic amines [71,72]. The overall reaction is shown below for an N-methyl amine.



At least four mechanisms have been considered (shown below) [28]



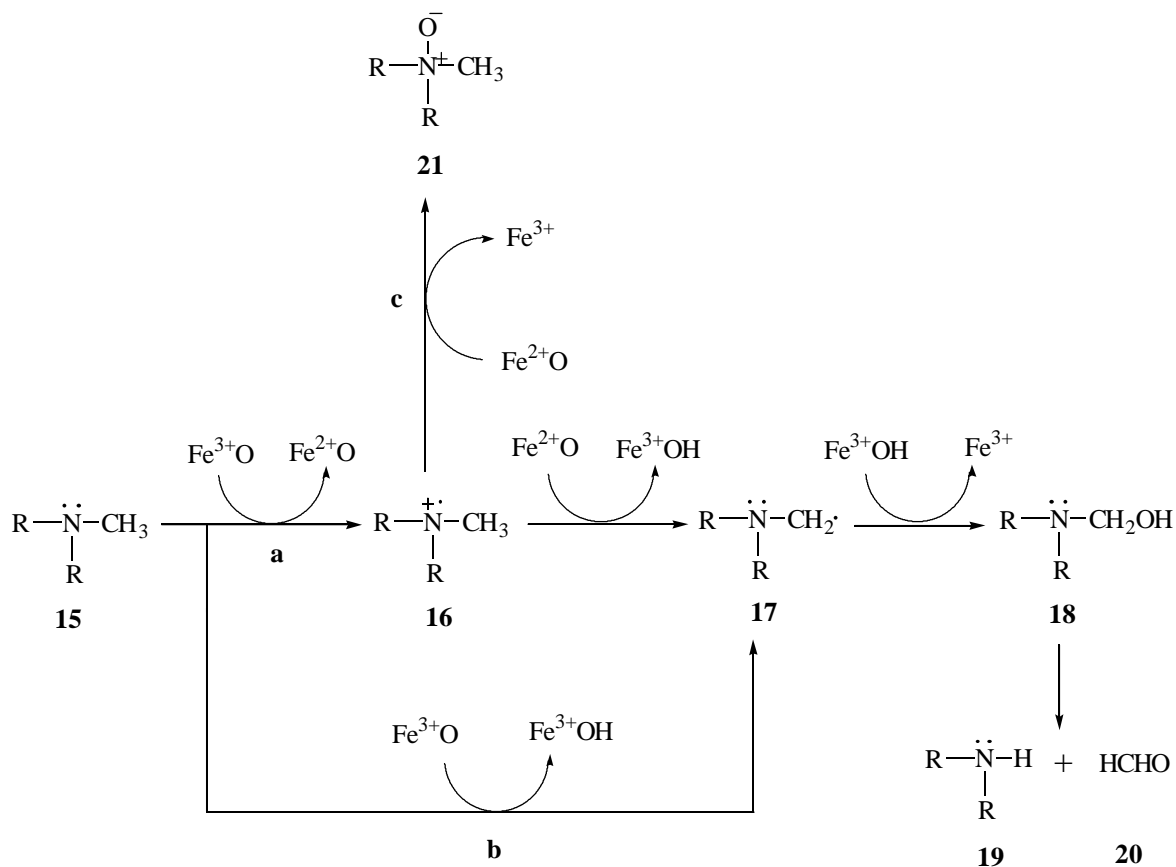
Reaction I involves the formation of an N-oxide and subsequent rearrangement to yield the dealkylated amine and carbonyl containing compound. This pathway is now considered highly unlikely due to the stability of most N-oxides [73,74].

Reaction II is generally accepted as the pathway utilized by peroxidases because oxidized peroxidase is generally recognized to be able to accept electrons but not to

transfer oxygen [75-77]. Initial one electron transfer from the substrate yields an aminium radical and the dismutation between two aminium radicals yields starting material and an iminium ion which hydrolyses to give the degraded amine and carbonyl containing moiety. Evidence against this pathway with P450s was the finding that the oxygen in the carbonyl product comes from O₂ not H₂O [78], in contrast with what would be expected from reaction II.

Reactions III and IV are generally accepted dealkylation pathways for P450 based on the fact that the oxygen in the aldehyde moiety generated from these two reaction sequences is derived from O₂ not H₂O. The formation of carbinolamines is catalyzed by P450. They are unstable intermediates that undergo subsequent non-enzymatic fragmentation to yield the dealkylated amine and aldehyde. Reactions III and IV are different in their initial intermediates, whether via single electron transfer (SET, route a) or hydrogen atom transfer (HAT, route b) as shown in Scheme 4. From route a, initial electron transfer from the substrate **15** nitrogen lone pair to the hemoprotein yields the aminium radical **16** and subsequent proton transfer yields the radical **17**. The HAT pathway (route b) bypasses the aminium radical **16** and directly yields radical **17**. The distinction between these two pathways is somewhat controversial because the radical **16** is too unstable to be detected. Perhaps the aminium radical **16** may help to rationalize the formation of N-oxides (route c). Attempts using kinetic isotope effects and linear free energy relationship to distinguish between these two pathways have been pursued. Some results support the single electron transfer mechanism [28] and others are in favor of hydrogen atom transfer mechanism [27]. The issue remains unsolved.

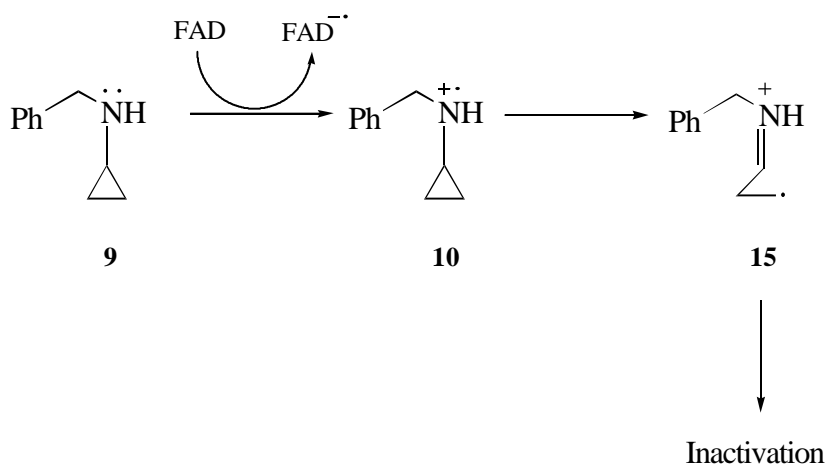
Scheme 4. Proposed Mechanism of Oxidative N-Dealkylation of Tertiary Amines by P450



2.3.2. Mechanism of Inactivation of P450 by Cyclopropylamines

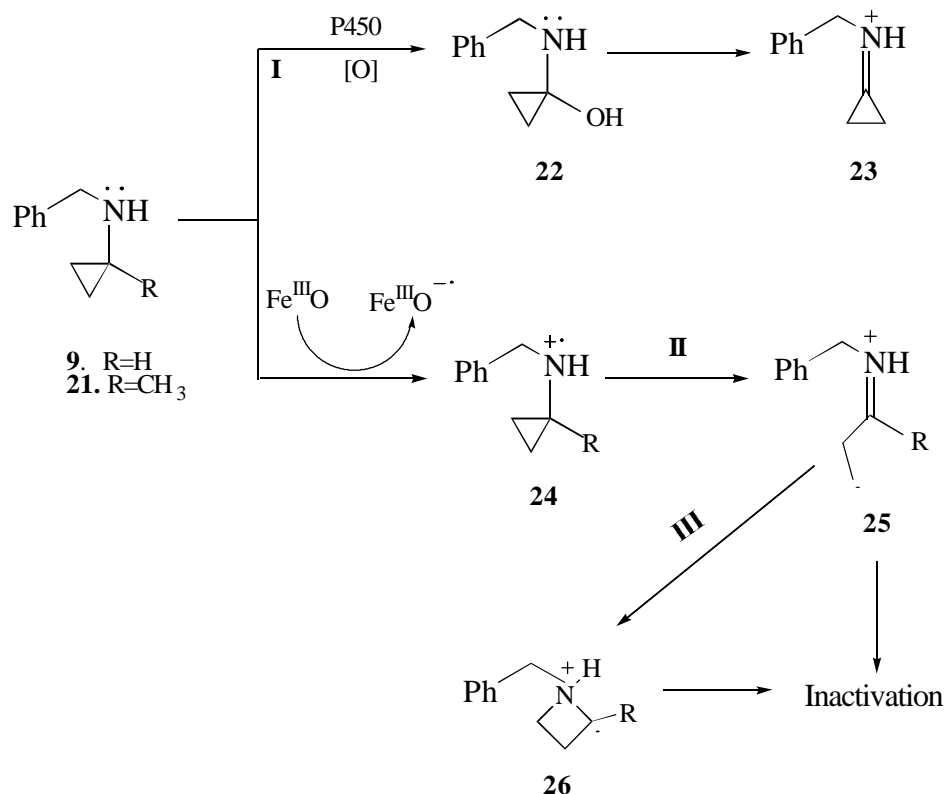
Cyclopropylamines have been extensively used as inhibitors of monoamine oxidase [22] and the mechanism of the inactivation process was interpreted as proceeding via the single electron transfer pathway to form a ring opened radical cation **15** which binds tightly with an active site functionality and inactivates the enzyme (Scheme 5).

Scheme 5. Proposed Mechanism of Inactivation of MAO
by N-Benzylcyclopropylamine



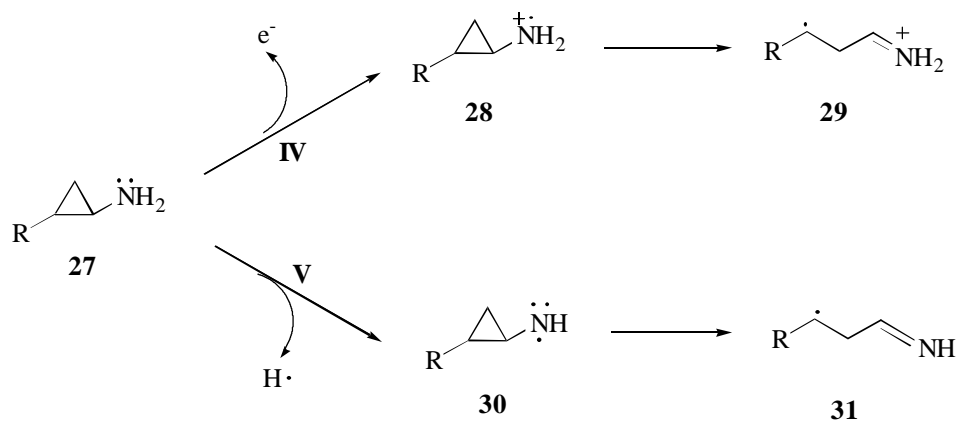
Cyclopropylamines are also mechanism-based inactivators of cytochrome P450 [79,80]. For N-benzylcyclopropylamine **9**, the inactivation process was initially proposed to proceed via α -carbon hydroxylation, to form cyclopropylcarbinolamine **22** which converts to the highly reactive iminium ion **23** that alkylates the enzyme [9] (Scheme 6, route I). Later findings have shown that compounds **21** with a methyl group at the α -carbon position which blocks the hydroxylation was an equally efficient inhibitor [80,81]. This suggested that route I was not valid. An alternative mechanism was proposed to be a consequence of initial amine nitrogen oxidation to generate a radical cation **24**, followed by rapid ring opening in the enzyme cavity to form a highly reactive carbon-centered radical **25** (route II) or rearrange to form ring expanded radical **26** (route III). The radicals formed in both pathways would destroy the hemo moieties of the enzyme [11]. This proposed mechanism can be best rationalized by single electron transfer chemistry and was supported by the unique chemistry of the cyclopropyl compounds, that is, the rapid rates of ring opening of the cyclopropylaminyl radical cations.

Scheme 6. Mechanism Postulated for the Inhibition of Cytochrome P450 by Cyclopropylamines



Dinnocenzo proposed that the mechanism based inactivation of P450 by cyclopropylamines can also be rationalized by either electron transfer (Scheme 7, route IV) or hydrogen atom transfer (route V). In the hydrogen atom transfer mechanism, the enzyme reaction with the cyclopropylamine forms the aminyl radical **30**, which undergoes ring opening to yield a neutral radical **31**. Radical **31** would inactivate the enzyme. The hydrogen atom transfer would not apply to tertiary cyclopropylamines.

Scheme 7. Alternative Mechanism Proposed for the Inhibition of P450
by Cyclopropylamine



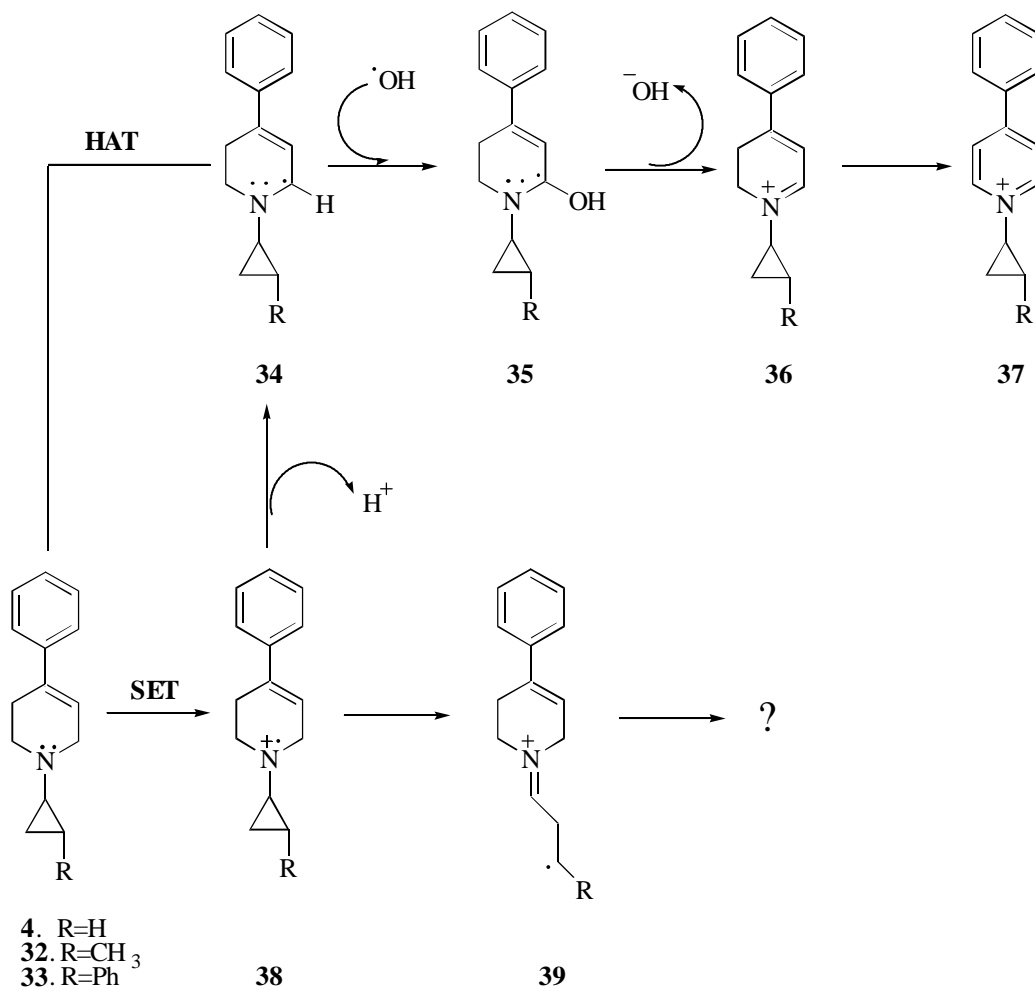
2.4. Research Proposal

Our interests in molecular mechanism underlying MPTP's neurotoxicity have led us to undertake a series of studies on MAO-B and cytochrome P450 substrate activity relationships. The N-cyclopropyl analog CPTP is an efficient MAO-B inactivator and demonstrates poor substrate properties [21]. The mechanism of inactivation is thought to proceed via the SET pathway. Alkylation of an active site functionality by the highly reactive distonic iminium radical formed following the rapid ring opening of the SET generated cyclopropylaminyl radical cation is thought to result in the inactivation of the enzyme. The poor MAO-B substrate properties of CPTP obviate the possibility of characterizing the biotransformation because metabolites could not be detected spectrophotometrically. This may not be the case with cytochrome P450. Our initial studies with cytochrome P450 have shown pyridinium metabolite formation by a process that does not involve significant inactivation of the enzyme, suggesting that ring opening is not a main pathway [89]. The formation of the pyridinium metabolite was proposed to proceed via the dihydropyridinium intermediate by the P450 catalyzed α -carbon oxidation pathway (Scheme 8). The mechanism proposed to account for the formation of the dihydropyridinium species **36** (R=H) can be via either SET or HAT pathway.

In order to get a better understanding about the partitioning between ring opening vs. α -carbon oxidation, i.e., SET vs. HAT and MAO-B vs. P450, we propose to examine the P450 catalyzed metabolism of CPTP derivatives with different substituents (hydrogen, methyl, phenyl) on the 2-position of the cyclopropyl ring. The CPTP derivatives we will employ in this study are *trans*-1-(2-methylcyclopropyl)-4-phenyl-1,2,3,6-tetrahydropyridine [MCPTP, (**32**)] and *trans*-1-(2-phenyl-cyclopropyl)-4-phenyl-1,2,3,6-tetrahydropyridine (PCPTP, **33**). We anticipate that the cytochrome P450 catalyzed oxidation of CPTP derivatives is initiated by the SET generated cyclopropylaminyl radical cation **38**. The cyclopropylaminyl radical cation is expected to partition between the α -carbon deprotonation and hydroxyl radical recombination pathway to form dihydropyridinium **36**, and the ring opening pathway to form the distonic carbon centered iminium radical **39** which may undergo further modification which will be investigated in this study. We expect that the phenyl group on the 2-position will stabilize the ring opened radical **39** which would favor ring opened metabolites, while the proton and methyl groups on the 2-position would favor the α -carbon oxidation pathway leading to the formation of the dihydropyridinium species **36**. Alternatively, the HAT pathway bypasses intermediate **38** and would only account for the α -carbon oxidation generated dihydropyridinium species but not any ring opening products.

We propose to characterize the metabolic pathways of CPTP derivatives. The structural characterizations will be pursued by using HPLC coupled with mass spectrometry and HPLC equipped with a diode array detector. We also hope to identify the forms of P450 that catalyze the oxidation of these compounds. We are particularly interested in finding one form of P450 that would mediate both the α -carbon oxidation and ring opening pathway. This would provide an opportunity to gain evidence to evaluate the SET pathway since the intermediate of aminyl radical cation **38** generated by SET would be the common intermediate involved in the two pathways. We hope that this investigation will provide fundamental insights that will lead to further investigations of the mechanism of the cytochrome P450 catalyzed oxidation of tetrahydropyridinyl derivatives.

Scheme 8. Proposed Mechanism of Partition of the Cyclopropylaminyll Radical Cation



Chapter 3. Characterization of Metabolic Pathways of CPTP and Derivatives Incubated with Rat Liver Microsomes

3.1. Analytical Approaches

Our interest in studying the molecular mechanism of the cytochrome P450 catalyzed oxidation of CPTP and derivatives requires a careful documentation of their metabolic profiles. Traditional chromatographic isolation is time consuming and labor intensive and requires a large amount of analyte. On-line GC/MS was attempted in earlier studies. As might be expected, some of the metabolites are thermally labile and could not be properly identified. Since the biological matrix is complex, tedious extraction is needed to run GC/MS. The harsh acidic and basic extraction conditions may modify the structure of metabolites. In consideration of these drawbacks, we elected to focus our efforts on high performance liquid chromatography in conjunction with mass spectrometry.

With the advent of atmospheric pressure ionization, coupling high-performance liquid chromatography with mass spectrometry (LC-MS) has become the primary tool in the identification and quantitation of biotransformation products of xenobiotics in biological matrices [82,83]. Detection of metabolites can be accomplished by direct analysis of a biological sample with minimal sample preparation. Pseudomolecular ions generated from the atmospheric pressure soft ionization mode can be easily detected in full scan mode followed, if needed, by selected ion analysis. Since the major routes of biotransformation mediated by cytochromes P450 are common Phase I reactions such as oxidative N-dealkylation, pseudomolecular ions acquired from LC/MS are very useful in evaluating the biotransformation process. For example, metabolites whose parent ions are 16 amu higher than those of the starting drugs are likely to arise from the introduction of an oxygen atom. Metabolites whose parent ions are 2 amu lower may arise from a two-electron oxidation involving the loss of two hydrogens. Unfortunately, because of the lack of MS/MS capability on our instrument, we can only get the limited mass spectral data from a single quadrupole MS system. These data do not provide an opportunity for obtaining product ion scans that would differentiate isomeric structures. We must use some other techniques, such as stable isotope analysis and UV absorption characteristics

obtained by HPLC equipped with diode array detectors, to provide complementary information.

By using stable isotopically labeled substrates, the mass spectral data of metabolites obtained from LC/MS analysis would also yield very useful information for locating the site of metabolic change that will help to characterize the biotransformation process. Additional structural information can also be provided by UV spectral analysis acquired from the HPLC equipped with the diode array detector. Some metabolites may dramatically change their chromophore after oxidation or reduction. Dihydropyridinium and pyridinium metabolites generated from two or four-electron oxidations of the 4-phenyl-1,2,3,6-tetrahydropyridinyl species have characteristic UV chromophores which are significantly different from their starting substrates [84]. Addition of some functional group, such as a hydroxyl group, into the substrate may shift the maximum absorbance.

Since the metabolites we study here are polar or ionic, LC coupled with electrospray mass spectrometry (LC-ESI/MS) offers the best analytical approach. Separation of metabolites is achieved on conventional analytical columns such as 4.6 mm x 250 mm, Zorbax SB-C8, 5 μ m. Since electrospray is a low flow technique, post-column splitting is required to achieve a reduced flow into the MS system. The combination of LC/MS and LC/DAD-UV is a useful approach to solve identification problems. Matching target analyte retention time and associated mass and UV spectra with those from reference standards will produce unambiguous evidence for the identification of metabolites.

3.2. Experimental

Chemicals. CH₃CN (EM scientific, Gibbstown, NJ), CH₃OH, glacial CH₃COOH (Fisher Scientific, Fair Lawn, NJ) and ammonium acetate (Fisher Scientific, Fair Lawn, NJ) were HPLC grade. Mono and dibasic potassium phosphate (Fisher Scientific, Fair lawn, NJ), ethylenediamine tetraacetic acid (EDTA) (Sigma Chemical Co., St. Louis, MO), MgCl₂ (Fisher Scientific, Fair Lawn, NJ), trisodium isocitrate (Sigma Chemical Co., St. Louis, MO), β -nicotinamide adenine dinucleotide phosphate (NADP) (Sigma Chemical Co., St. Louis, MO) and isocitrate dehydrogenase (Sigma Chemical Co., St. Louis, MO) were purchased as indicated. CPTP, MCPTP and PCPTP, N-oxide of

PCPTP, *trans*-1-(2-phenyl-cyclopropyl)-4-phenylpyridinium were synthesized in our lab by Dr. Simon Kuttab. *p*-Hydroxycinnamaldehyde was synthesized by Mr. Sean Hislop, 1-cyclopropyl-4-phenyl-1,2,3,6-tetrahydropyridine-d₄ was synthesized at our lab by Dr. Philippe Bissel.

Liver microsomal preparation. The livers of four rats were perfused with cold (4 °C) 0.9% saline solution containing 0.1 mM EDTA immediately after collection. After adequate perfusion (the dark red livers change to brown) to remove residual blood from the tissues, the livers were then placed in cold 0.9% saline solution to completely rinse out residual blood. The livers were homogenized in 24 mL 1.15% KCl containing 10 mM EDTA. The homogenates were centrifuged at 10,368 x g (11,500 rpm at $R_{av} = 70$ mm) for 10 min, using a Beckman J2 high speed centrifuge tubes (JA-20 rotor). The supernatant was transferred to an ultracentrifuge and spun at 111,406 x g (35,000 rpm at $R_{av} = 81.2$ mm) for 60 min using a Beckman preparative ultracentrifuge (with 50.2 Ti rotor). The precipitate was resuspended and homogenized in 25 mL 0.1 M pH 7.4 sodium pyrophosphate containing 1 mM EDTA, and was centrifuged at 111,406 x g for another 60 min. The precipitate was resuspended and homogenized with 3 mL 20% glycerol in 20 mM potassium phosphate buffer (pH 7.4) containing 0.1 mM EDTA. This fraction is called the liver microsomal preparation

Protein assay. Standard BSA solution (1 mg/ml) in 20% glycerol, 20 mM potassium phosphate buffer pH 7.4 containing 0.1 mM EDTA was prepared and was diluted to 0.2, 0.4, 0.6 and 0.8 mg/mL to make a calibration curve. Each diluted solution (100 μ L) was pipetted into 12x100 mm test tubes. 5 mL Bradford reagent was added to each tube and the contents was mixed by vortexing. The absorbance at 595 nm was taken after 6 min against the blank prepared from 100 μ L buffer and 5 mL Bradford reagent. The standard calibration curve ($y = 0.01166 + 0.42215 x$, $R^2 = 0.991$) was plotted by using the absorbance vs. the corresponding concentration of BSA.

The liver microsomal preparation (10 μ L) was added to 390 μ L buffer and the resulting mixture was vortexed. The diluted liver microsomes (100 μ L) was used to measure the absorbance of protein according to the above method. The reading of absorbance was 0.2178, and the protein concentration of the original liver microsomes was calculated to be 19.5 mg/mL.

Liver microsomal incubations. A 40 mM stock solution of CPTP in methanol, 50 mM pH 7.4 potassium phosphate buffer with 0.1 mM EDTA and a 10 mM NADPH generating system (50 mM MgCl₂, 50 mM trisodium isocitrate, 10 mM NADP⁺, and 5 unit isocitrate dehydrogenase) was prepared. The protein concentration of the rat liver microsomes was 20 mg/mL. Typical microsomal incubations were conducted in an incubation system consisting of 1 mg/mL protein in a final volume of 1 mL 50 mM potassium phosphate buffer at 37 °C. Substrate (10 µL of 40 mM solution in methanol) was added to the incubation mixture to make a final concentration of 400 µM CPTP. The reaction was initiated by the addition of 100 µL of the NADPH generating system to maintain a steady state concentration of 1 mM NADPH in the incubation mixture. Aliquots (150 µL) taken at 0, 20, 40 and 60 min were quenched by adding an equal volume of acetonitrile. The incubation mixtures were then centrifuged at 10,000 g for 6 min. The supernatants were applied to HPLC-DA (50 µL). Samples injected into the LC-ESI/MS system were concentrated twice under dry N₂. The concentrated supernatants (200 µL) were injected onto the LC-ESI/MS. Control incubations were conducted in the absence of either drug or the NADPH generating system or enzyme system under which conditions no evidence of metabolite formation was observed.

Incubations of MCPTP and PCPTP were conducted in the same manner. The final concentration of MCPTP in 1 mL incubation mixture was the same with that of CPTP (400 µM) while the final concentration of PCPTP was reduced to 250 µM due to its limited solubility.

HPLC-DA/UV assay. HPLC was performed on a Hewlett Packard 1100 HPLC system equipped with a UV/VIS diode array detector (G1315A), a Rheodyne 7725I injector and a quaternary pump (GB11A). Chromatography was done on a 250 mm x 4.6 mm Zorbax SB-C8 5 µm column, with an in-line pre-column filter (2 µm, Upchurch Scientific Inc., Oak Harbor, WA) using isocratic condition at 56% acetonitrile and 44% water containing 10 mM ammonium acetate, pH 5.0. We used 5 different wavelengths to detect the possible metabolites: 215 nm, 230 nm, 260 nm, 290 nm and 310 nm.

HPLC-ESI/MS assay. HPLC-ESI/MS was performed on a Micromass VG Platform mass spectrometer equipped with a thermal pneumatic nebulizer and single quadrupole analyzer coupled to a 1050 HP HPLC system. The mass spectrometer was

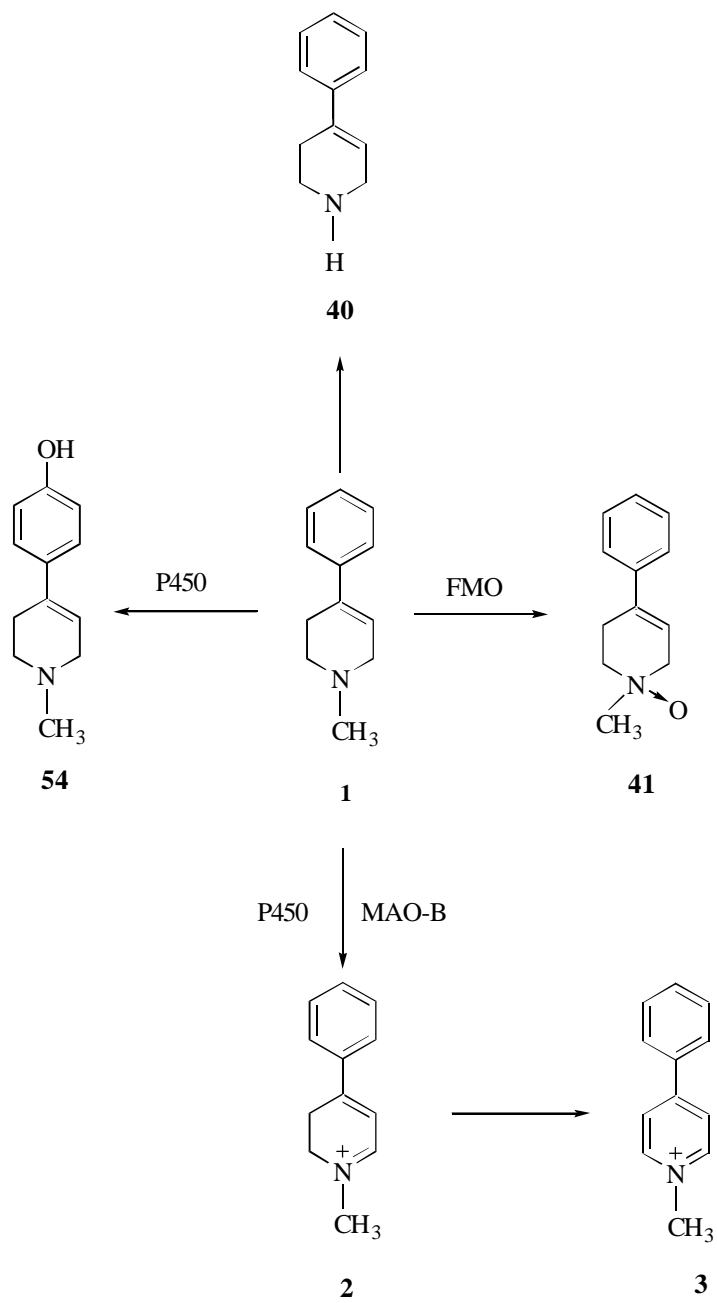
operated in the ESI positive or negative ion mode with a source temperature at 110 °C. The nebulizer gas was set to 20 L/hour and the dry gas was set at 400 L/hour. To achieve good sensitivity, the cone voltage was set at 30 V. The HP 1050 HPLC system was equipped with a UV/VIS detector, a Rheodyne 7725I injector with a 200 µL loop and a quaternary pump. Chromatography was done on a 250 mm x 4.6 mm Zorbax SB-C8 5 µm column, with an in-line pre-column filter using isocratic conditions at 56% acetonitrile and 44% water containing 30 mM ammonium acetate, pH 5.0. The HPLC flow rate was set at 1 mL/min. A split was used to direct the HPLC effluent to the MS inlet at 250 µL/min. A 200 µL aliquot of sample was injected on the column.

3.3. CPTP

3.3.1. Results

The common biotransformation reactions mediated by cytochrome P450 are Phase I reactions such as hydroxylation, N-oxidation, and N- or O-dealkylation. For the cyclic tertiary amine species MPTP (**1**), the α -carbon two-electron oxidation is catalyzed by both MAO-B and cytochrome P450 to form the dihydropyridinium MPDP⁺ species (**2**). Compound **2** undergoes a secondary two-electron oxidation to the pyridinium species MPP⁺ (**3**) [85, 86, 87]. The UV chromophores of MPDP⁺ and MPP⁺ are significantly different from MPTP. MPTP, MPDP⁺ and MPP⁺ display their distinctive UV chromophores at 245 nm, 345 nm and 299 nm, respectively, and are readily detected by HPLC-diode array analysis. The N-desmethyl (**40**), N-oxide (**41**) and hydroxyl (**54**) metabolites generated via the common Phase I reactions have been identified in the NADPH-supplemented liver microsomal incubation mixture of MPTP [88] (Scheme 9). The N-oxide metabolite is generally thought to be formed by a reaction catalyzed by the flavin-containing monooxygenase (FMO) present in the liver microsomal preparations [88].

Scheme 9. *In vitro* Metabolic Fates of MPTP



Our interest here is to examine the metabolic profile of CPTP mediated by liver microsomes. CPTP is an MPTP analog in which the N-methyl group is substituted by a methyl group. Cyclopropylamines have been well documented as inactivators of both MAO and P450 [22,79,80]. CPTP is being investigated because of the presence of the cyclopropyl group which is metabolized differently when incubated with MAO-B and liver microsomes. When incubated with MAO-B, CPTP was shown to be a mechanism based inactivator [21], As discussed in Chapter 1, the distonic radical cation resulting from the ring opening reaction leads to the inactivation. When incubated with liver microsomes, no significant inactivation was observed. Instead the molecule was extensively metabolized. In light of these earlier results, we expected that there would be several metabolic pathways operating through the interactions with P450. These anticipated pathways are due to the presence of both the phenyltetrahydropyridinyl moiety and the N-cyclopropyl moiety (Scheme 10). The substrate may undergo α -carbon oxidation to form the dihydropyridinium species CPDP⁺ (**8**) and pyridinium species CPP⁺ (**42**). Alternatively, it may undergo the ring opening reaction via the cyclopropylaminyl radical cation **5** to form the distonic radical cation **6** which may lead to inactivation of the enzyme or may undergo subsequent radical recombination to form **46** and cleavage to generate N-descyclopropyl species **40** and aldehyde **44**. Besides these reactions, CPTP may undergo the common Phase I reaction, to form N-oxide **45**, and the hydroxylated products **46**, **47**, and/or **48**. Carbinolamine **48** is unstable and should undergo further fragmentation to form N-descyclopropyl product **40** and ketone **49**. The final metabolic profile might be the result of the competition between these pathways. The next few paragraphs will discuss our studies on characterizing these metabolic pathways.

CPTP was incubated with a rat liver microsomal preparation which had been supplemented with an NADPH generating system. Samples were analyzed by HPLC-diode array at 0, 20, 40 and 60 min at 37 °C to see if these metabolites are generated and if so, if their formation is time dependent. CPTP was also incubated with rat liver microsomes in the absence of NADPH. The HPLC-diode array system was used to analyze the incubation mixture. We selected the following five wavelengths to monitor the incubation mixture: 215 nm, 230 nm, 255 nm, 290 nm and 325 nm. This allowed us to detect simultaneously the unchanged substrate and the suspected metabolites including, but not limited to, the N-descyclopropyl and pyridinium species. Short wavelengths (215 nm and 230 nm) can be used to detect almost all compounds since most of them have UV absorbance at the short wavelength. However, the noise level at 215 nm was very high because of the biological background. The noise level at 230 nm was less. The 255 nm can be used to detect the unchanged substrate and metabolites with similar UV properties to those of the substrate such as N-descyclopropyl species. The 290 nm channel can be used to detect the pyridinium metabolites while the 325 nm can be used to detect metabolites which have absorbance at longer wavelengths.

The incubation mixture was analyzed by the HPLC-diode array as described in the Experimental Section. Four new peaks (M1-M4) besides the substrate (S1) appeared and their intensities were shown to gradually increase with the time of incubation. The intensity of the substrate gradually decreased with the time of incubation. These results indicated that the substrate was consumed and metabolites formed. Figure 4 depicts the HPLC-DA tracing of the CPTP liver microsomal incubation preparation supplemented with an NADPH generating system at 60 min. The HPLC/DA analysis of the control sample (containing no NADPH) showed only one peak which would be assigned to the unchanged substrate (Figure 5). This established that the substrate was chemically stable under these conditions. Based on these data, the formation of the new peaks M1-M4 is likely to be cytochrome P450 mediated.

Figure 4. HPLC-DA Analysis of the CPTP Incubated with Liver Microsomes
Supplemented with NADPH System for 60 min

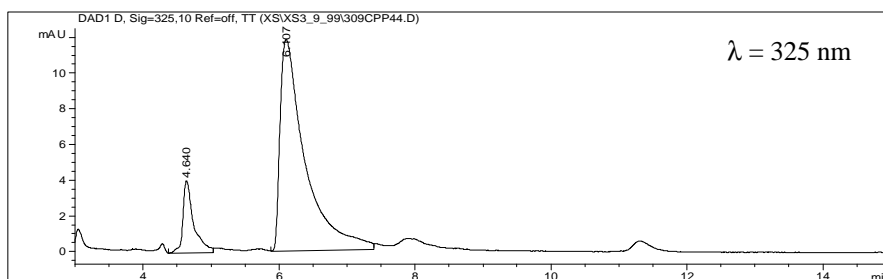
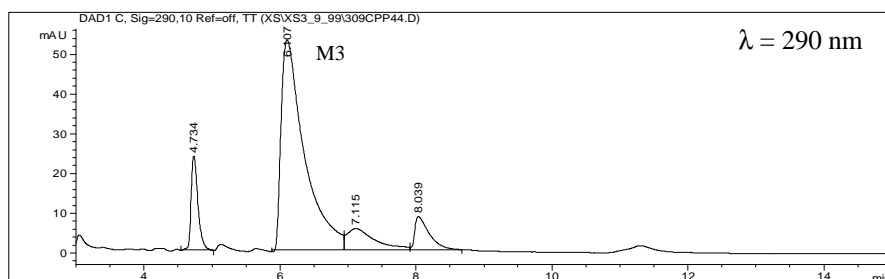
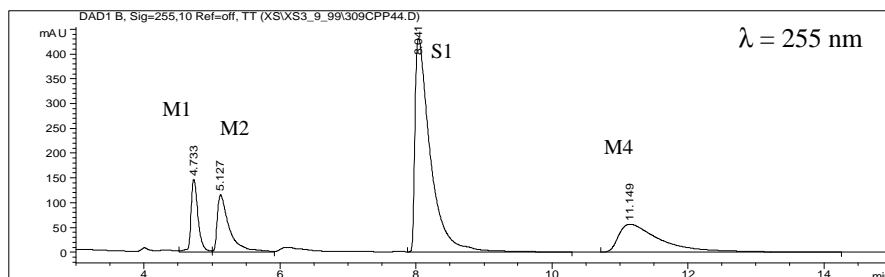
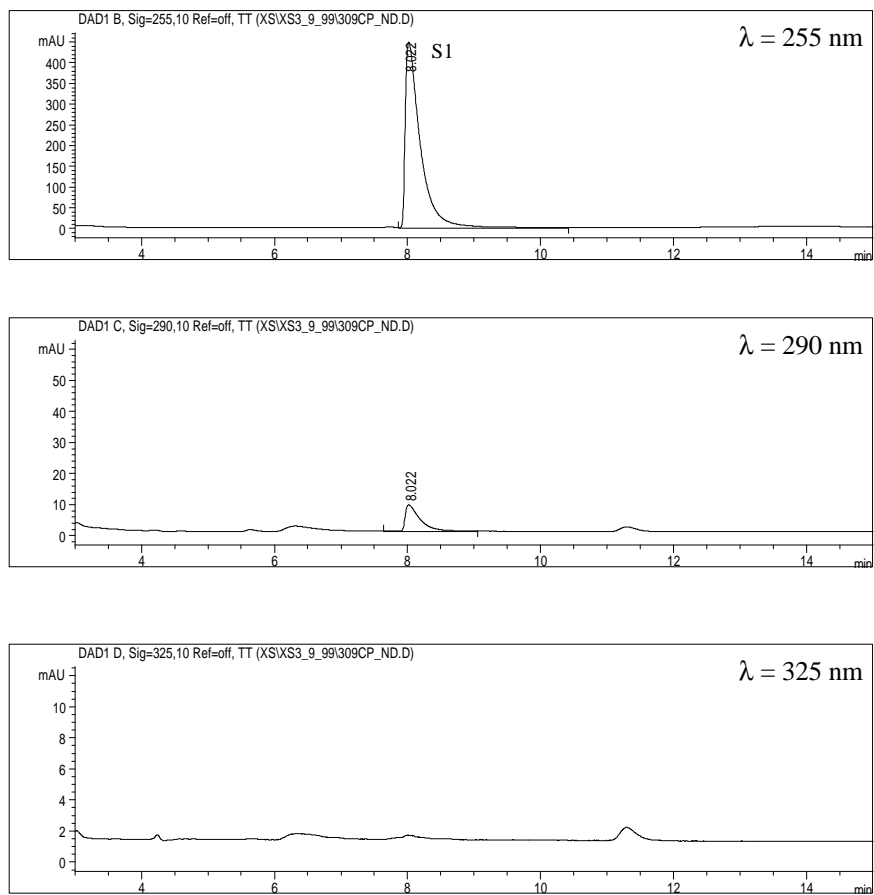


Figure 5. HPLC-DA Analysis of CPTP Incubated with Liver Microsomes
in the Absence of NADPH System for 60 min



The substrate (S1) eluted at 8.04 min and the diode array analysis of this peak displayed a UV spectrum with λ_{max} 245 nm (Figure 6), which is due to the styrene moiety present in the 4-phenyl-1,2,3,6-tetrahydropyridine. M1 eluted at 4.2 min and displayed a UV chromophore at 260 nm (Figure 7). M2 eluted at 5.13 min and displayed a UV chromophore at 245 nm (Figure 6). M3 eluted at 6.10 min and displayed a UV chromophore at 299 nm (Figure 8). M4 eluted at 11.15 min and displayed a UV chromophore at 245 nm (Figure 6). The two metabolites M2 and M4 have the same UV chromophores as that of the substrate CPTP, suggesting that the electronic feature of styrene moiety remained unchanged in these metabolites. Possible structures are the N-descyclopropyl **40** and N-oxide **45** products. Some evidence suggests that UV chromophore of the N-oxide of MPTP is the same as MPTP itself [88]. The 299 nm chromophore of M2 led us to suspect that this metabolite might be the 1-cyclopropyl-4-phenylpyridinium species **42** since MPP^+ has a UV chromophore at 299 nm [88].

Figure 6. UV Spectra of M2, M4 and S1

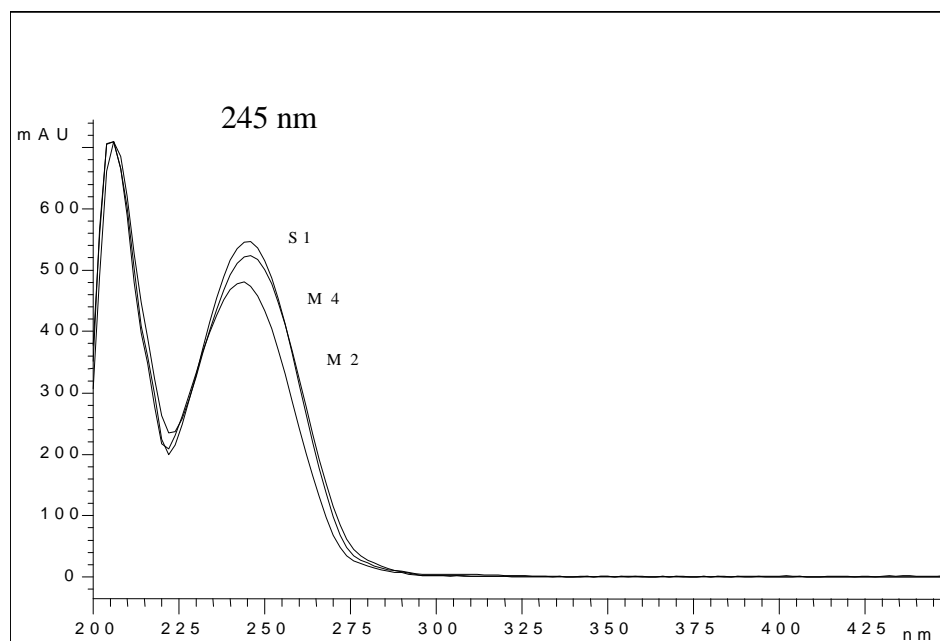


Figure 7. UV Spectrum of M1

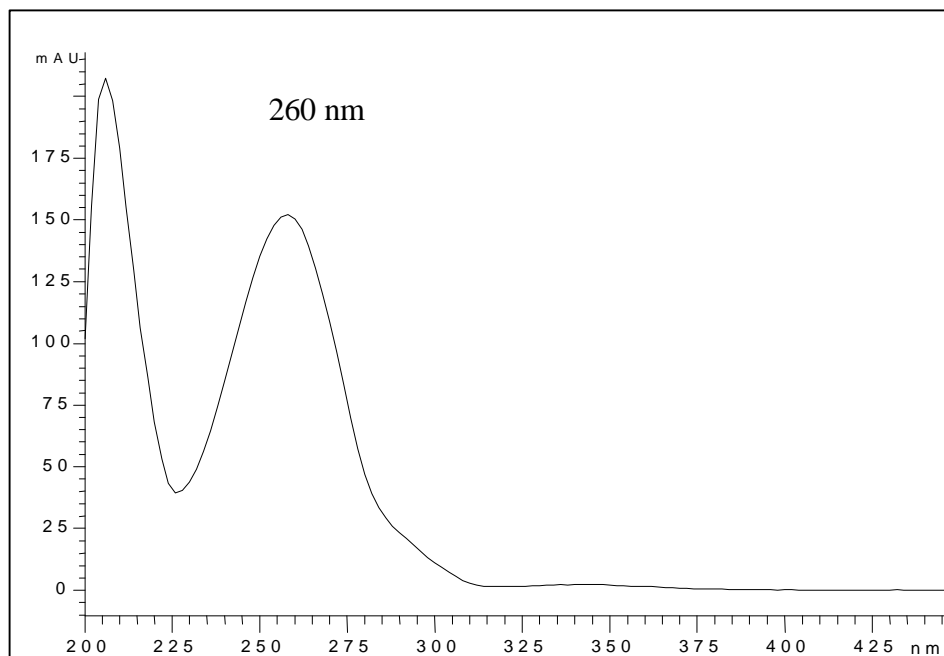
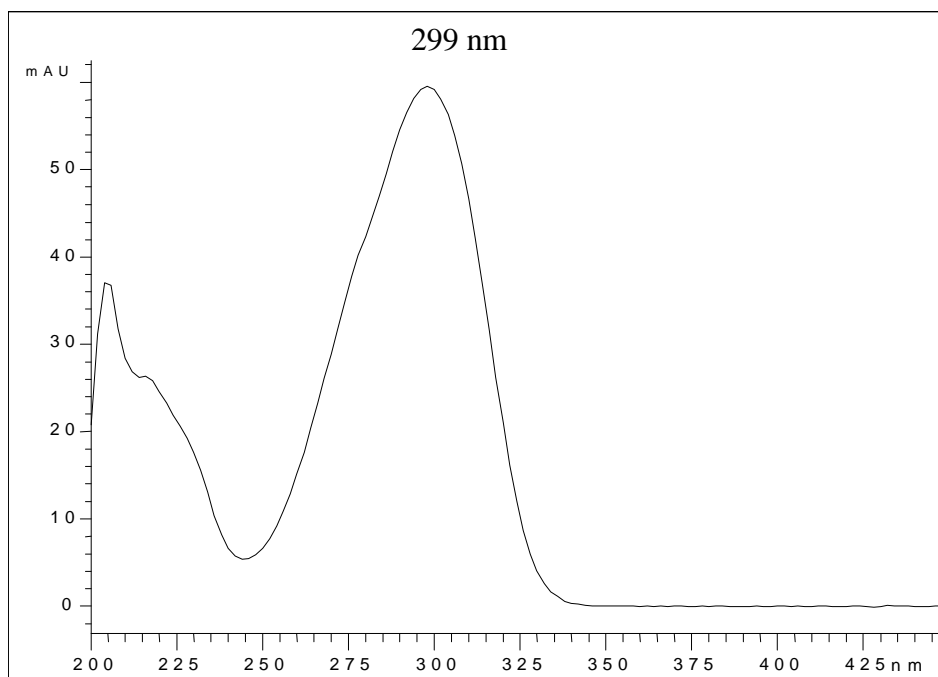


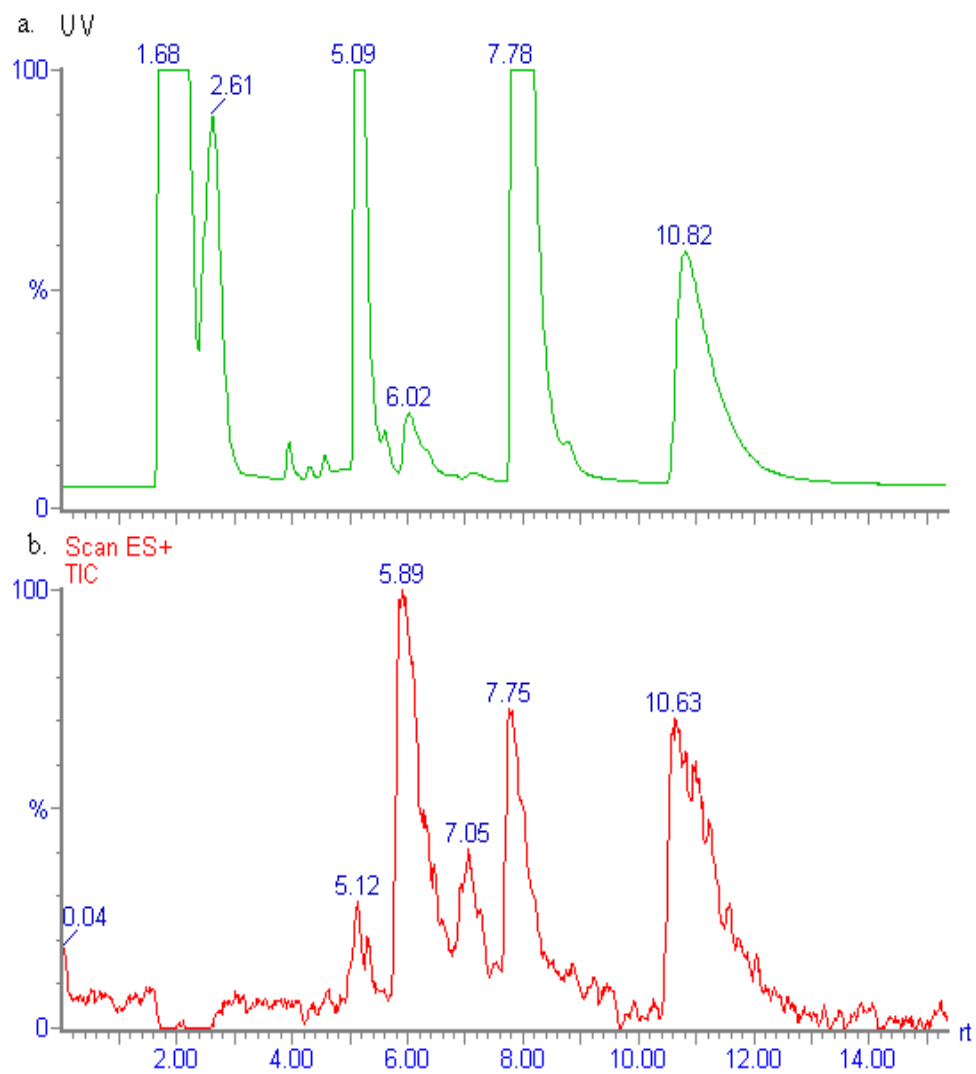
Figure 8. UV Spectrum of M3



In order to obtain additional structural information, LC-ESI/MS/UV analysis was attempted. Since the UV detector we employed here is not a diode array detector, we only could select one wavelength to monitor the chromatographic peak. We chose 250 nm to observe the unchanged substrate and possible metabolites M1, M2 and M4. However, metabolite M3 does not absorb at 250 nm and it could not be detected at this wavelength. The HPLC/UV chromatogram served as a resource to let us correlate the retention times of the peaks between the HPLC/DA chromatogram and the total ion current (TIC) traces from HPLC-ESI/MS analysis of the incubation mixtures. Figures 9a and 9b depict the HPLC-UV chromatogram and the positive ion TIC chromatogram obtained from a full scan LC-ESI/MS analysis of the incubation mixture of CPTP. We can see that the sensitivities of metabolite responses toward electrospray mass spectrometry detector and DA-UV detector are different. M1 was sensitive to the DA-UV detector and HPLC-UV trace displayed an intense peak. However, this compound was barely detectable by LC-ESI/MS because of its insensitivity toward electrospray mass spectral analysis (poor ionization efficiency). The retention time of the peaks in the TIC chromatogram are slightly different from the HPLC/DA analysis because they were acquired with a different system. We are still able to correlate the peaks from HPLC/DA and from the LC/MS by comparing the metabolic profiles obtained from HPLC/DA and HPLC/UV analysis.

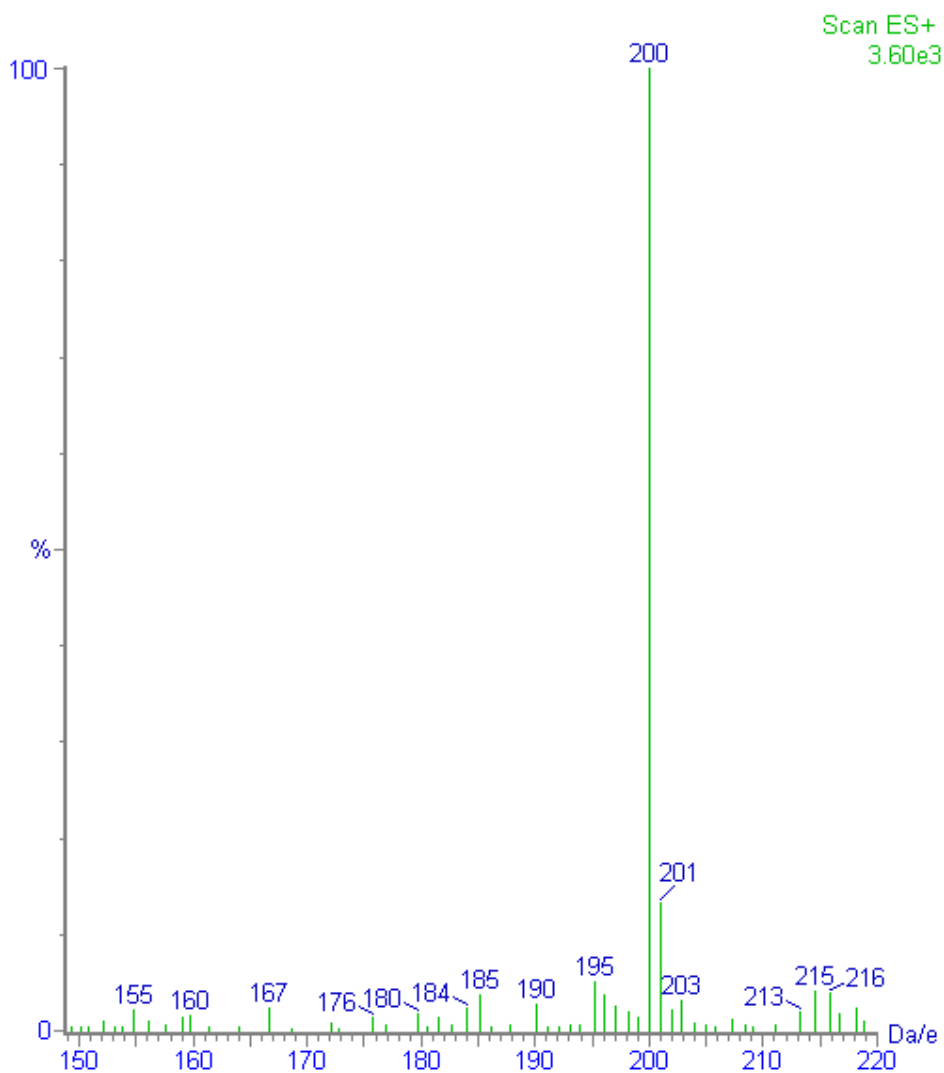
Figure 9. HPLC/MS/UV Analysis of Liver Microsomal Incubation Mixture of CPTP.

a. HPLC/UV Chromatogram, b. TIC Obtained from LC-ESI/MS



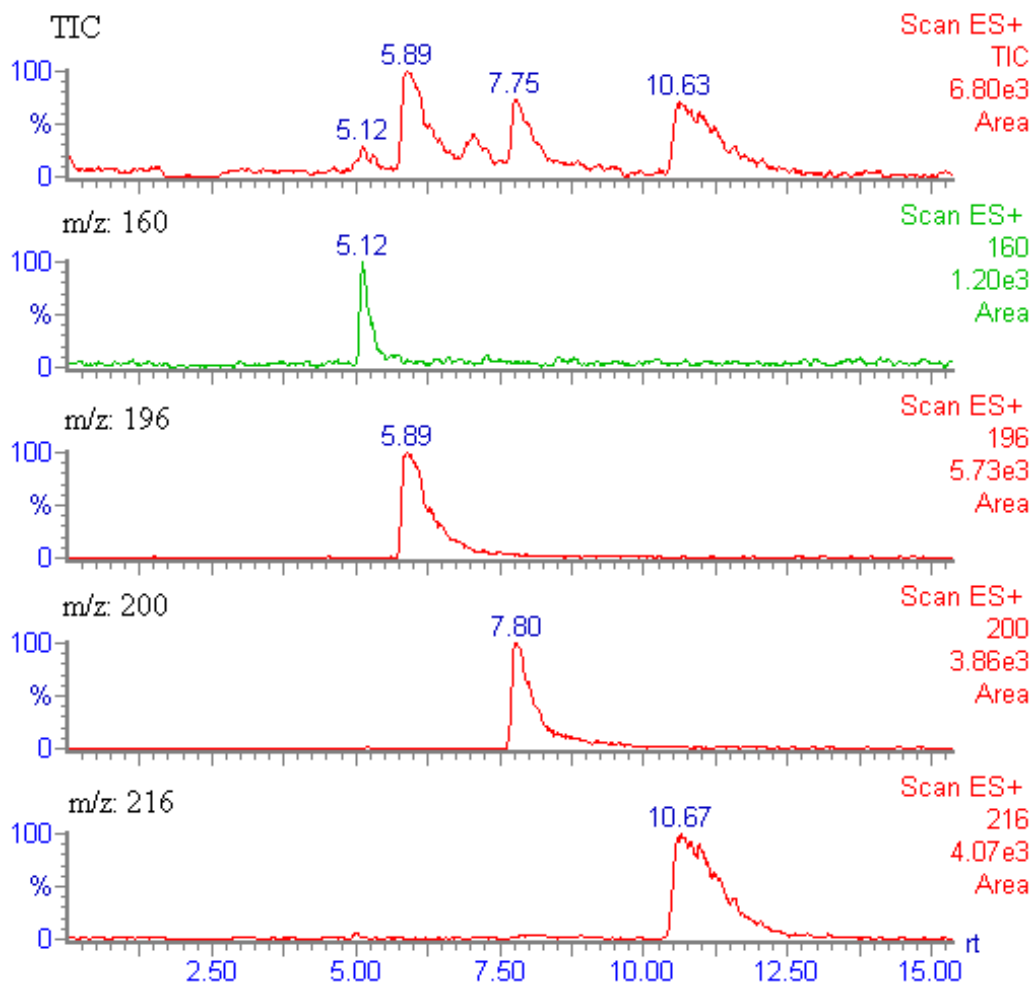
Electrospray mass spectrometry is a soft ionization technique and, in the positive ion mode, it usually generates protonated pseudomolecular ions (MH^+). Figure 10 displays the mass spectrum of the substrate CPTP which shows only one peak (m/z 200) corresponding to MH^+ of CPTP.

Figure 10. Mass Spectrum of CPTP Obtained from LC-ESI/MS Analysis



Single-ion current traces were extracted in the search of chromatographic peaks generated from base ion peaks and from pseudomolecular ions of likely metabolites (Figure 11). Our search results gave several single ion traces with MH^+ values of 160, 196, 200 and 216 Da. Characterization of these metabolites was sought by examining the extracted ion current chromatograms which monitored specific pseudomolecular ions.

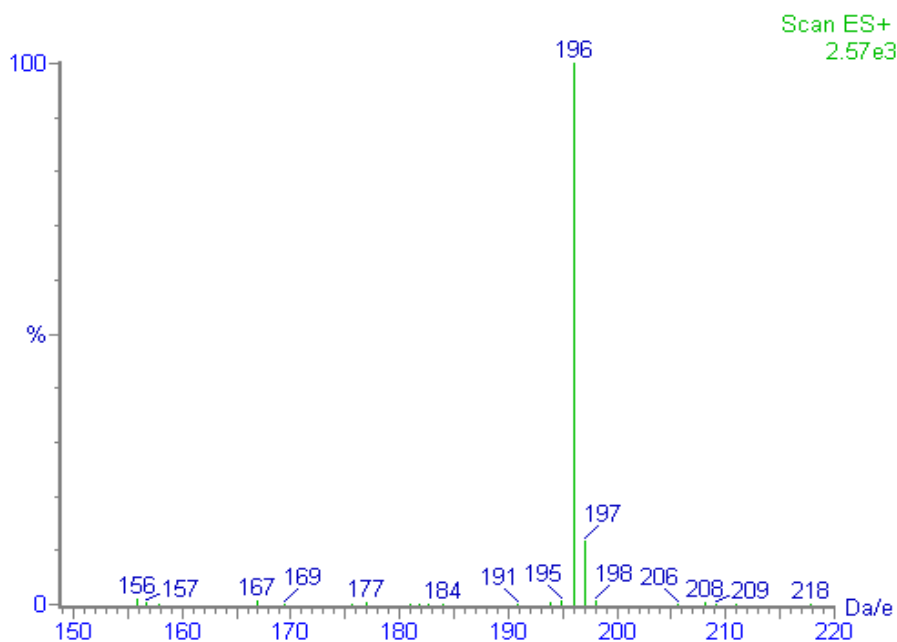
Figure 11. LC-ESI/MS Spectrometric Analysis of Liver Microsomal Incubation Mixture of CPTP. Positive ion TIC (top) and Reconstructed Ion Current Chromatograms.



Obviously, the ion peak at m/z 200 corresponded to the substrate CPTP. The ion peak at m/z 160 (M2, $t_R = 5.1$ min) corresponded to 4-phenyl-1,2,3,6-tetrahydropyridine (PTP, **40**), a metabolite generated by the pathway of N-descycloproplation. This assignment was based on its matched retention time, mass spectrum and UV spectrum (λ_{max} 245 nm) with the standard PTP (commercially available).

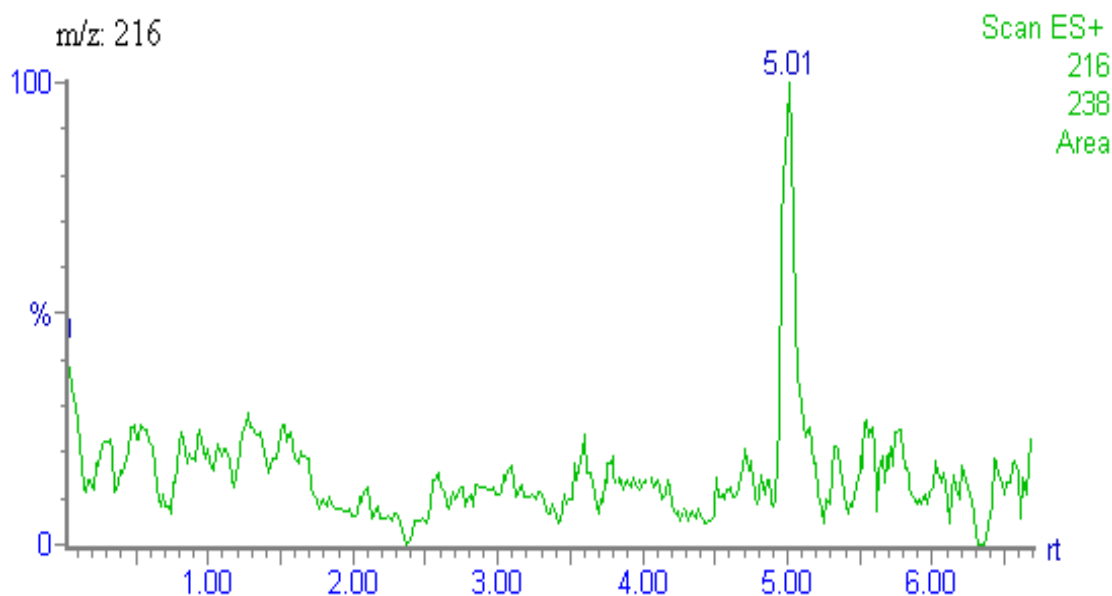
M3 displayed a single ion peak at m/z 196 ($t_R = 5.8$ min), 4 amu lower than of the parent drug and indicative of the loss of four hydrogens, suggesting that this metabolite was the pyridinium species **42** generated by the 4 electron oxidation of CPTP. Figure 12 depicts the mass spectrum of M3 which showed only the molecular ion peak. Its distinctive UV chromphore at 299 nm confirms this assignment (Figure 8). Our search of the single-ion current trace at m/z 198 corresponding to the ion trace of dihydropyridinium species **8**, a possible precursor of pyridinium metabolite, failed. No chromatographic and spectroscopic evidence for the dihydropyridinium was obtained. This is likely to be due to the fact that the dihydropyridinium species is unstable and is quickly oxidized to the corresponding pyridinium metabolite [89].

Figure 12. Mass Spectrum of M3 Obtained from LC-ESI/MS Analysis of CPTP Incubation Mixture



M4 displayed a protonated parent at m/z 216, 16 amu higher than the substrate (200), indicative of a monooxygenated product. Since C-hydroxylation and N-oxidation are common pathways of cytochrome P450 catalyzed oxidations, we expected to observe several monooxygenated metabolites e.g. **45**, **46**, **47** and **48** in consideration of the structure of CPTP. But only one intense ion peak at 10.67 min (corresponding to M4) was observed (Figure 11) and this might be because the intensity of the ion current of M4 was so overwhelming that it overshadowed other peaks. In our attempts to search for these peaks, one additional peak at 5.04 min was located by being displayed as a narrowed band (Figure 13). This ion peak corresponded to M1 from HPLC diode array analysis (Figure 4).

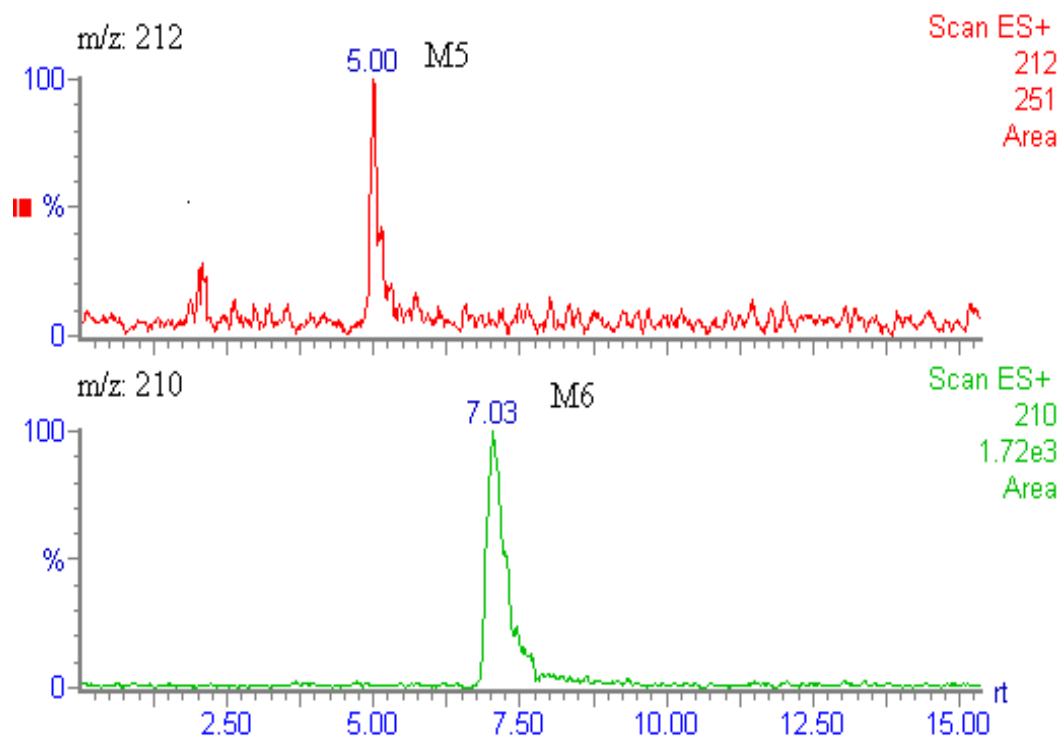
Figure 13. Reconstructed Ion Current Trace of M1



Now we have two monooxygenated products which have different chromatographic retention behavior and different UV chromophores. M1 elutes much earlier (5.0 min) and has a longer wavelength chromophore at 260 nm. M4 elutes later at 10.7 min with the identical UV chromophore (245 nm) as the substrate CPTP. Since the N-oxide metabolite of MPTP (**41**), which was identified from the liver microsomal incubation mixtures of MPTP, displayed the same UV chromophore with the substrate MPTP [88], we expected that the formation of this N-oxide would not change the chromophore of 4-phenyl-1,2,3,6-tetrahydropyridine moiety. This suggests that the N-oxide product **45** is one possible structure for M4. The other monooxygenated metabolite, M1, has a UV chromophore at 260 nm. Besides N-oxidation, C-hydroxylation is another possibility to add one atom oxygen into the substrate. This is also a common pathway mediated by cytochrome P450. But there are several sites for C-hydroxylation including the phenyl moiety and the cyclopropyl moiety. Hydroxylation in the *para*-position of the 4-phenyl moiety would result in a hypsochromic shift of the chromophore of the 4-phenyl-1,2,3,6-tetrahydropyridine moiety. M1 was proposed to have the structure of 1-cyclopropyl-4-*p*-hydroxyphenyl-1,2,3,6-tetrahydropyridine (**47**). Our assignments of M1 and M4 as the hydroxyl and N-oxide metabolites, respectively, are consistent with their chromatographic retention behavior. The hydroxyl metabolite is more polar than the N-oxide and elutes earlier in reserved phase HPLC. In order to identify these metabolites unambiguously, the corresponding synthetic standards were examined [33]. Our assignments were confirmed by their matched chromatographic and spectroscopic properties with those of the corresponding synthetic standards.

Searching the base ion peaks from the TIC also yielded two additional peaks, M5 and M6, at m/z 212 and 210 (Figure 14), respectively. The mass of M5 ($m/z = 212$, $t_R = 5.1$) is 12 amu higher than the substrate S1 ($m/z = 200$), and the mass of M6 ($m/z = 210$, $t_R = 7.1$) is 10 amu higher than the substrate.

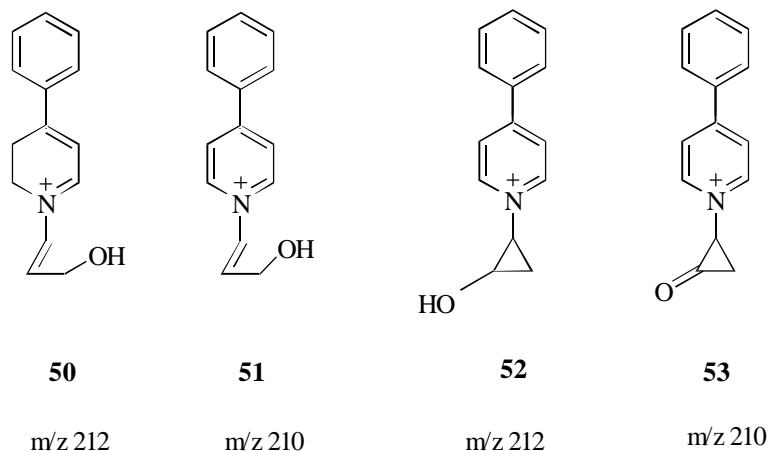
Figure 14. Reconstructed Ion Current Chromatograms of the two Minor Metabolites M5 and M6



This unexpected finding is difficult to be rationalized in terms of biotransformation reactions that would yield such products. We think these two peaks are real metabolites rather than false peaks generated from the background noise because, as will be discussed later, we have found similar ion peak patterns related to the corresponding substrates of MCPTP and PCPTP. However, we were not able to locate the corresponding peaks in the HPLC-DA tracing, possibly due to the limited sensitivity of UV detector for these compounds and/or spectroscopic interferences. Possible structures **50** and **51** or **52** and **53** (Figure 15) were proposed based on the masses. Compounds **50** and **51** are not likely due to the expected chemical instability of the dihydropyridinium moiety. The pyridinium species **52** and **53** are relatively stable and are very responsive under ESI conditions. That the two minor metabolites were observed by mass spectrometry and not by UV might suggest they are pyridinium species **52** and

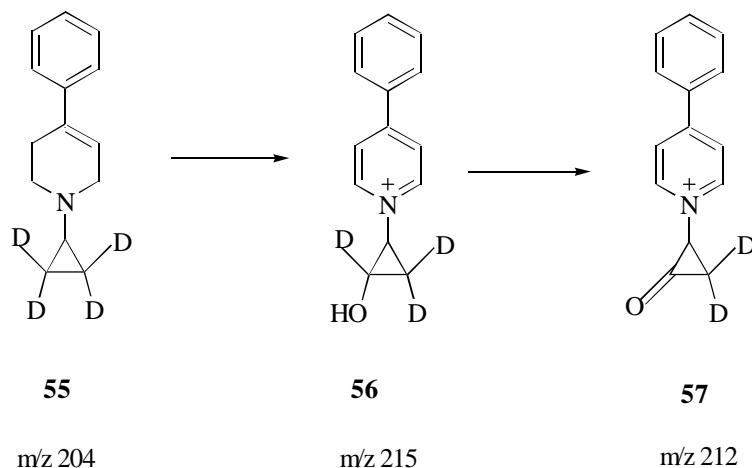
53. However, with only molecular ion information, we can not confirm these assignments.

Figure 15. Proposed Structures of the two Minor Metabolites



In order to find out if hydroxylation occurred on the cyclopropyl moiety, additional experiments involving the isotopically labeled substrate 1-cyclopropyl-4-phenyl-1,2,3,6-tetrahydropyridine- d_4 (**54**) were proposed. If **52** and **53** are correct assignments, the metabolites generated from this CPTP- d_4 compound would yield the metabolites **55** and **56** with m/z 215 and m/z 212, 11 and 8 amu higher than the substrate (Figure 16). The deuterated substrate 1-cyclopropyl-4-phenyl-1,2,3,6-tetrahydropyridine- d_4 was synthesized in our lab by Dr. Phillippe Bissel. LC/MS analysis of an incubation mixture of CPTP- d_4 did not reveal ion peaks of these two minor metabolites, probably because their concentrations are too low to be detected. I only used 0.6 mg/mL enzyme (made 1 year ago) in the incubation mixture instead of 1 mg/mL. This experiment needs to be repeated with a freshly prepared liver microsomal preparation. Compounds **52** and **53** are tentatively proposed for these two unexpected metabolites.

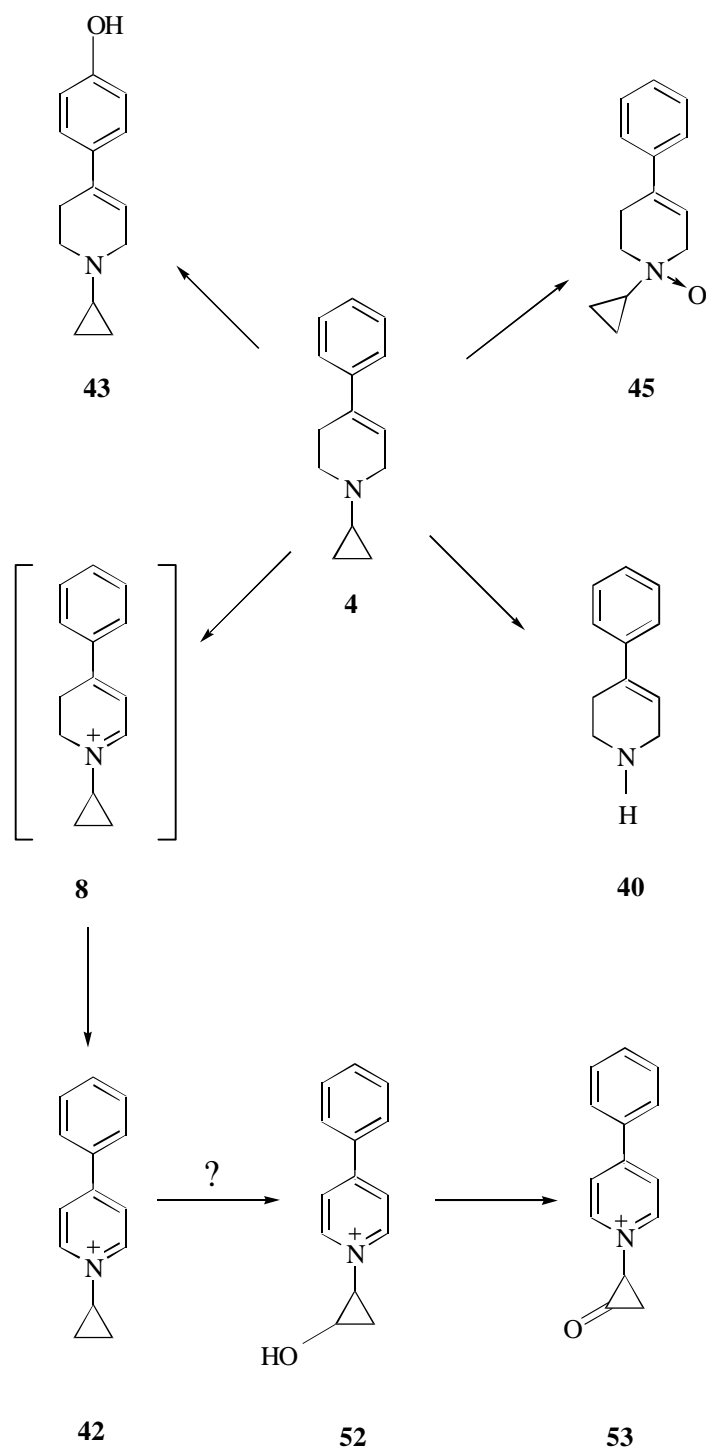
Figure 16. The structure of Deuterated CPTP-d₄ and the Corresponding Predicted Metabolites



3.3.2. Conclusions

Incubation of CPTP with rat liver microsomes generated several metabolites with no evidence of significant inactivation. These metabolites were identified by using HPLC coupled with electrospray mass spectrometry and by HPLC equipped with diode array-UV detection. Our results indicate these metabolites are NADPH-dependent and are catalyzed by cytochromes P450. The pathways of these biotransformations are depicted in Scheme 11. CPTP undergoes four major pathways: 1) N-decyclopropylation to form PTP **40**, 2) hydroxylation to yield the *p*-hydroxyphenyl-1,2,3,6-tetrahydropyridinyl metabolite **42**, 3) N-oxidation to generate the N-oxide **45**, and 4) ring α -carbon oxidation to yield pyridinium species **8** and **42**. The formation of the two minor metabolites may involve hydroxylation of the cyclopropyl moiety present in the pyridinium metabolite to form **52** and further oxidation of **52** to form the keto metabolite **53**. Although no cyclopropyl ring opened metabolites were observed, the conversion of CPTP to descyclopropyl **40** may proceed via the ring opening pathway depicted in Scheme 10.

Scheme 11. Metabolic Pathways of Liver Microsomal Catalyzed Oxidation of CPTP

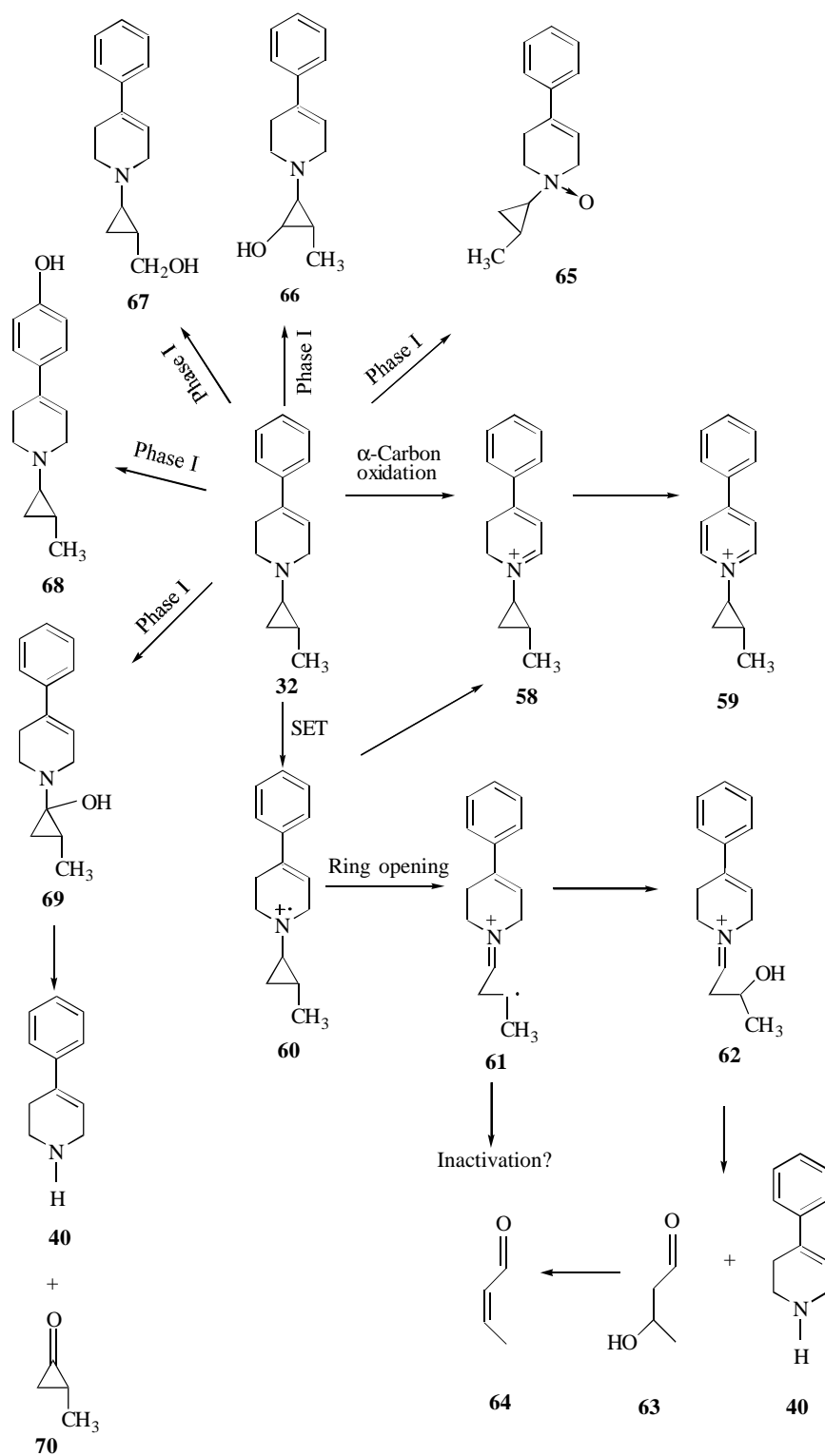


3.4. MCPTP

3.4.1. Results

Our studies on the liver microsomal catalyzed oxidation of CPTP did not provide a clear distinction between the SET and HAT pathways. Although the formation of the N-descyclopropyl product **40** can be rationalized to proceed via the ring opening pathway initiated by SET, the lack of direct observation of the fate of the cyclopropyl moiety limits our ability to describe this pathway. The liver microsomal catalyzed oxidation of the CPTP analog, MCPTP (**32**), was examined next. MCPTP was synthesized at our lab by Dr. Simon Kuttub [90] and was obtained as a mixture of *cis* and *trans* isomers. The compound we used here is the pure *trans* isomer: *trans*-1-(2-methylcyclopropyl)-4-phenyl-1,2,3,6-tetrahydropyridine (**32**). We expected that the methyl substituent on the cyclopropyl ring would stabilize the ring opened radical cation and favor the ring opening pathway. The metabolic pathways analogous to that shown in Scheme 10 are proposed for MCPTP (Scheme 12). The substrate **32** may undergo α -carbon oxidation to form the dihydropyridinium species **58** and pyridinium species **59**. Alternatively it may undergo the ring opening reaction via the cyclopropylaminyl radical cation **60** to form the distonic radical cation **61** which may lead to the inactivation of the enzyme or may undergo subsequent radical recombination to form **62** and cleavage to form N-descyclopropyl **40** and 3-hydroxybutanol (**63**). Compound **63** can undergo dehydration to form crotonaldehyde (**64**). Besides these reactions, CPTP may undergo the common phase I reactions to form the N-oxide **65** and the hydroxylated products **66**, **67**, **68** and (or) **69**. Carbinolamine **69** is unstable and should undergo fragmentation to form the N-descyclopropyl product **40** and ketone **70**. The final metabolic profile might be the result of the competition between these pathways. We will discuss our experimental results on characterizing these metabolic pathways below.

Scheme 12. Predicted Metabolic Pathways of MCPTP Catalyzed by Liver Microsomes



MCPTP was incubated with a rat liver microsomal preparation which had been supplemented with an NADPH generating system at 37 °C. The samples were analyzed by HPLC-diode array at the incubation times of 0, 20, 40 and 60 min to see if any metabolites were generated and if their formation was time dependent. MCPTP was also incubated with rat liver microsomes in the absence of NADPH. As we discussed in the CPTP section, the following five wavelengths were employed to monitor the incubation mixture: 215 nm, 230 nm, 255 nm, 290 nm and 325 nm. This allowed us to detect simultaneously the unchanged substrate and the anticipated metabolites.

The incubation mixture was analyzed by the HPLC-DA assay as described in the Experimental Section. Figure 17 depicts the HPLC-DA results in the presence of the NADPH generating system. Seven new peaks, M7 to M13, besides the substrate S2, appeared and their intensities were shown to gradually increase with the time of the incubation. The intensity of the substrate peak gradually decreased during this time. The HPLC-DA analysis of the control sample (containing no NADPH) showed only the substrate peak S2 which eluted at about 14 min (Figure 18). This established that the substrate was chemically stable under these conditions. Based on these data, the formation of M7 to M13 is likely to be cytochrome P450 mediated.

Figure 17. HPLC-DA Analysis of MCPTP Incubated with Liver Microsomes
Supplemented with NADHP System for 60 min

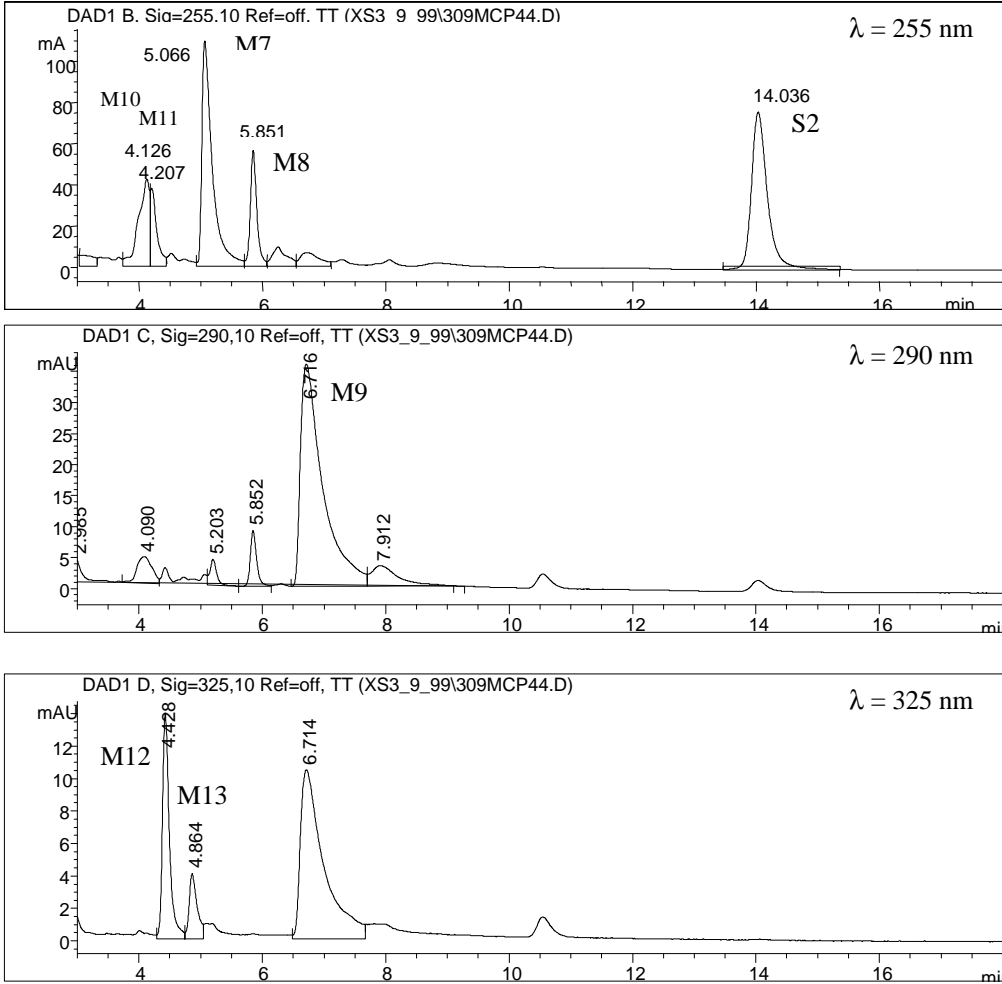
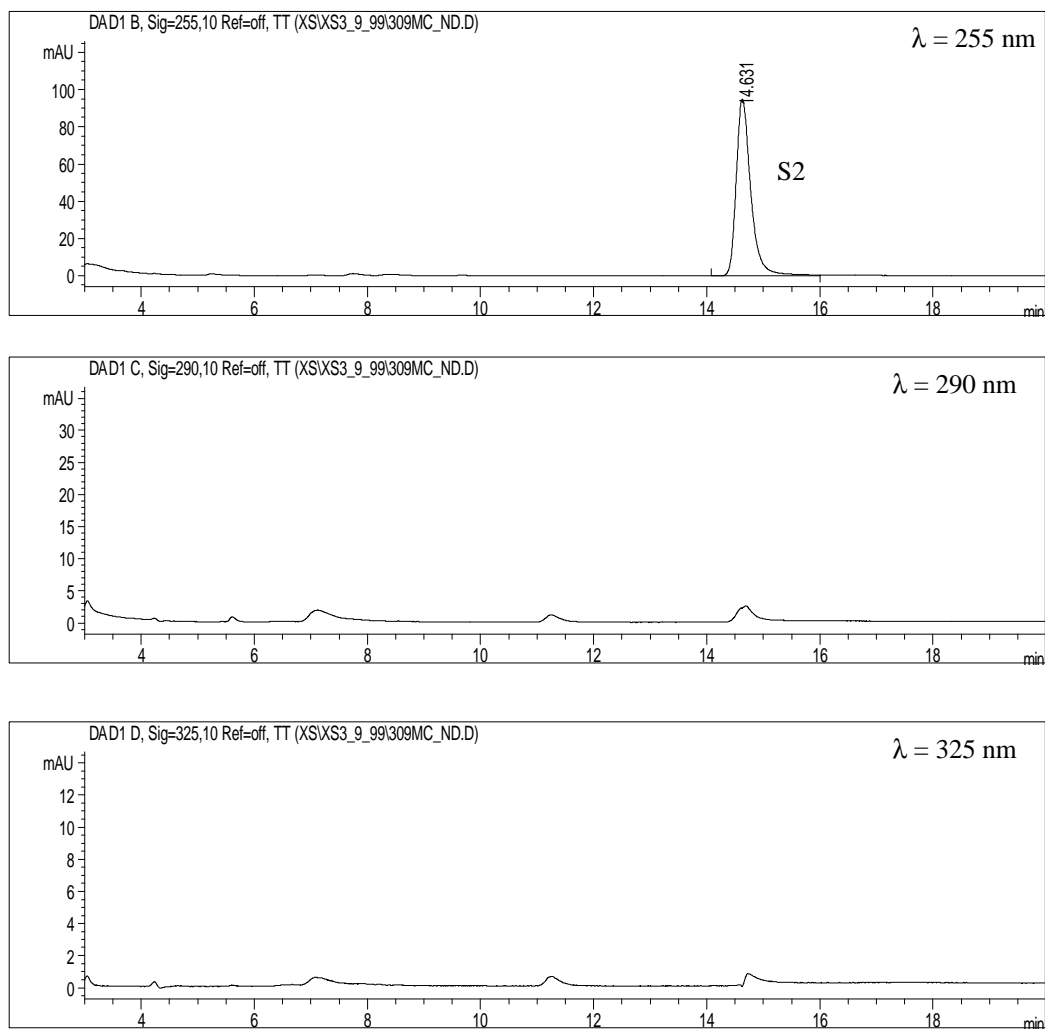
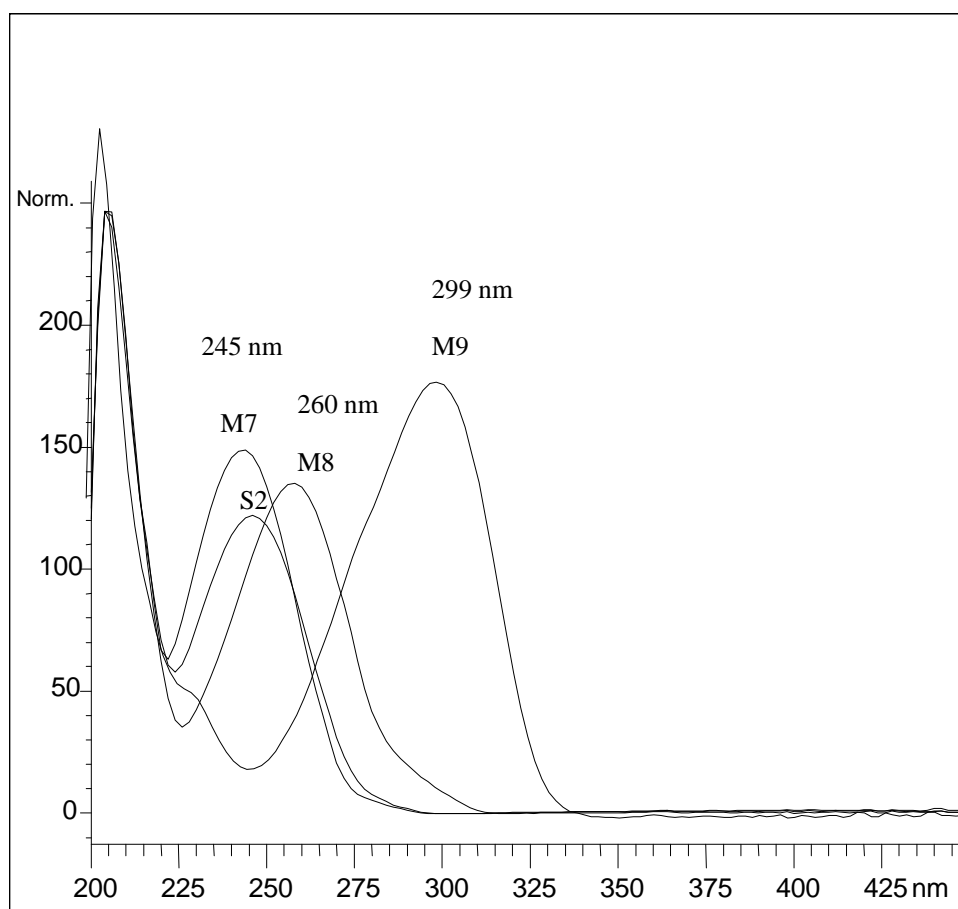


Figure 18. HPLC-DA Analysis of MCPTP Incubated with Liver Microsomes in the Absence of NADPH System for 60 min



The substrate MCPTP (S2) eluted at 14.6 min and displayed a chromophore at 245 nm (Figure 19). Three major metabolites, M7 to M9, were well resolved by HPLC. M7 eluted at 5.1 min and displayed a UV chromophore at 245 nm. M8 eluted at 5.8 min and displayed a UV chromophore at 260 nm. M8 eluted at 6.7 min and displayed a UV chromophore at 299 nm (Figure 19). This metabolic profile was similar to that observed with CPTP except that there were some new peaks, M10-M13, present in this tracing.

Figure 19. UV Spectra of M7, M8, M9 and S2



M10 and M11 almost coeluted and displayed identical UV chromophores at 250 nm (Figure 20). M12 and M13 were well resolved and have an identical UV chromophore at 345 nm (Figure 21). However, the chromophores are very weak, as we can see from Figure 21, and are different from that of the dihydropyridinium species which generally has a very strong absorbance at about this wavelength.

Figure 20. UV Spectra of M10 and M11

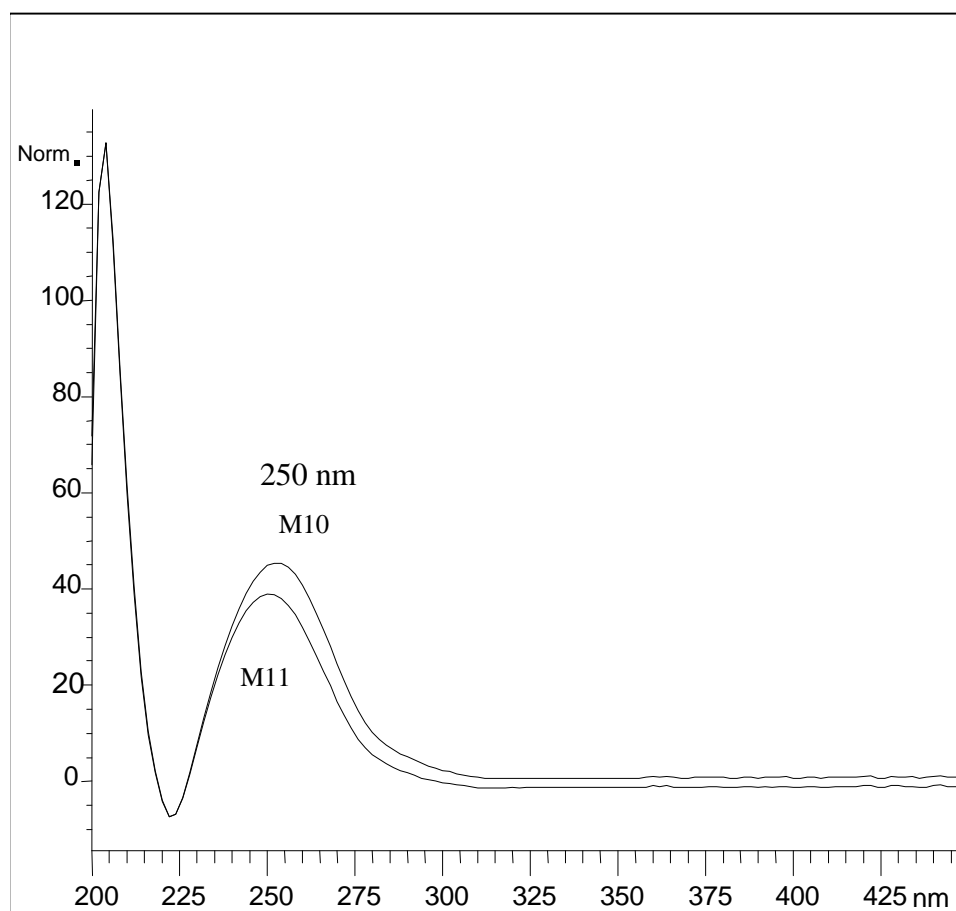
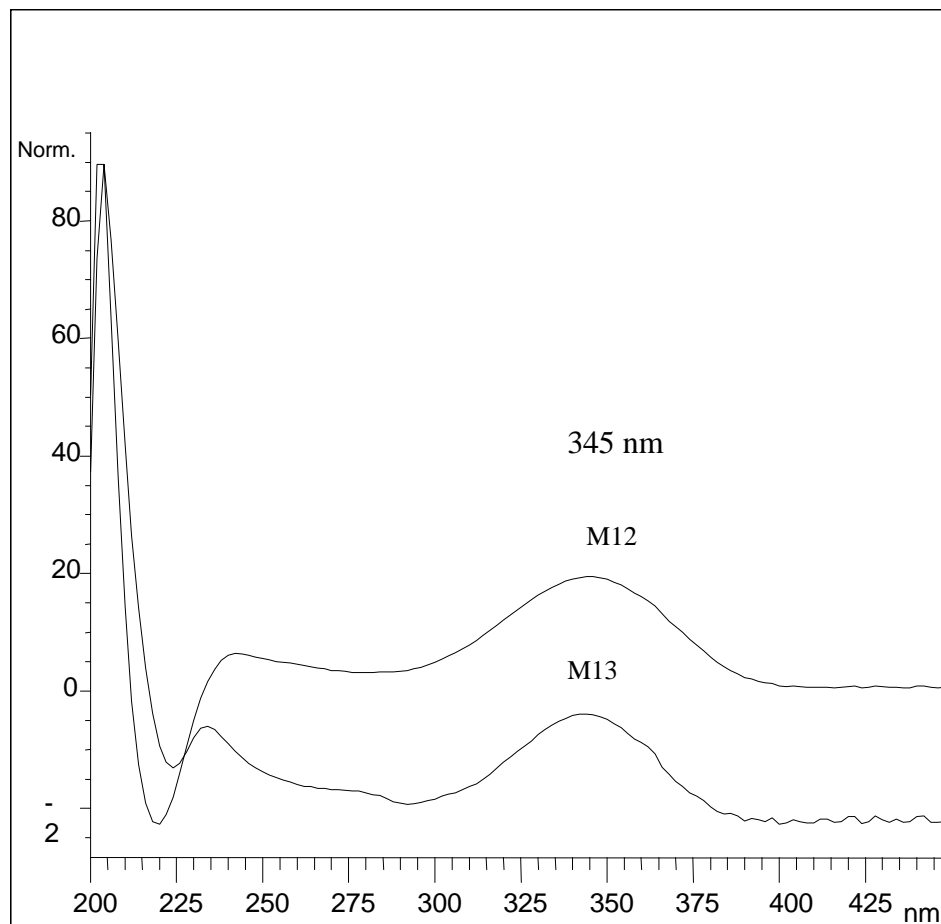


Figure 21. UV Spectra of M12 and M13



Based on our findings with CPTP metabolite formation, the 245 nm chromophore of M7 led us to suspect that this metabolite might be the N-descyclopropylated product PTP (**40**). The 260 nm chromophore of M8 led us to suspect that it might be *trans*-1-(2-methylcyclopropyl)-4-*p*-hydroxyphenyl-1,2,3,6-tetrahydropyridine (**68**). The 299 nm chromophore led us to suspect that this metabolite might be the *trans*-1-(2-methylcyclopropyl)-4-phenylpyridinium (**59**) species. It is very difficult to link M10-M13 with any structures. From Scheme 12, crotonaldehyde might be one possible metabolite. HPLC analysis of freshly prepared crotonaldehyde showed that it eluted at 3.5 min and displayed a UV chromophore of 254 nm. Neither the retention time nor the UV

chromophore matched with any of the peaks from M10-M13. It was found that crotonaldehyde was extremely sensitive to air and moisture. Even if crotonaldehyde was produced, its instability under the assay conditions precludes the possibility of its detection.

HPLC-ESI/MS/UV analysis was attempted next in the hope that it would provide additional structural information from mass spectral data. As discussed in the CPTP section, the HPLC/UV chromatogram obtained from the online UV detector served as a resource to let us correlate the retention times of the peaks between the HPLC/DA chromatogram and the TIC from HPLC-ESI/MS analysis of the incubation mixtures. Figures 22a and 22b depict the HPLC-UV chromatograms and the positive ion chromatogram obtained from a full scan LC-ESI/MS analysis of the incubation mixture of MCPTP. The ion peak eluting at 14.2 min corresponded to the substrate MCPTP. Figure 23 displays the mass spectrum of MCPTP obtained from LC-ESI/MS analysis which shows only one peak (m/z 214) corresponding to MH^+ of MCPTP.

Figure 22. HPLC/MS/UV Analysis of Liver Microsomal Incubation Mixture of MCPTP.

a. HPLC/UV Chromatogram, b. TIC Obtained from LC-ESI/MS

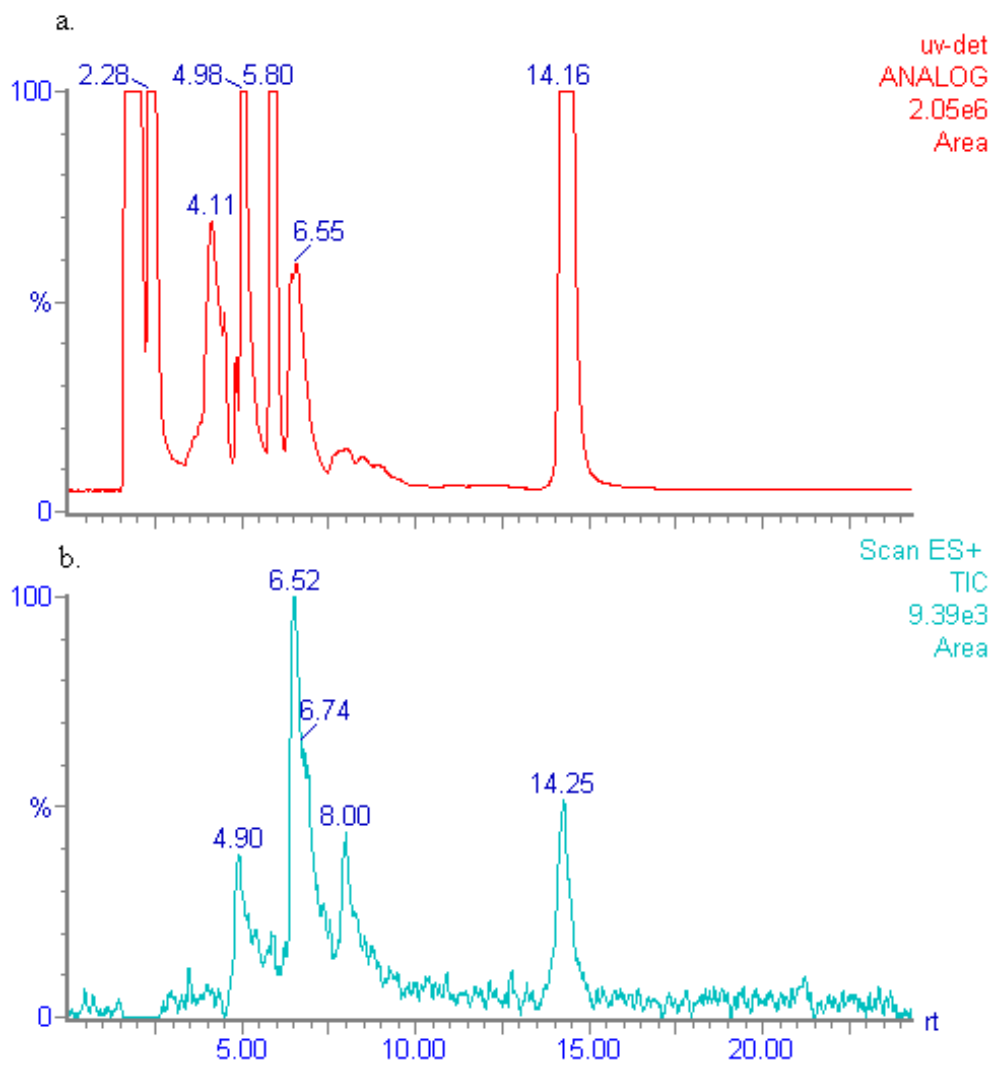


Figure 23. Mass Spectrum of MCPTP Obtained from LC-ESI/MS Analysis

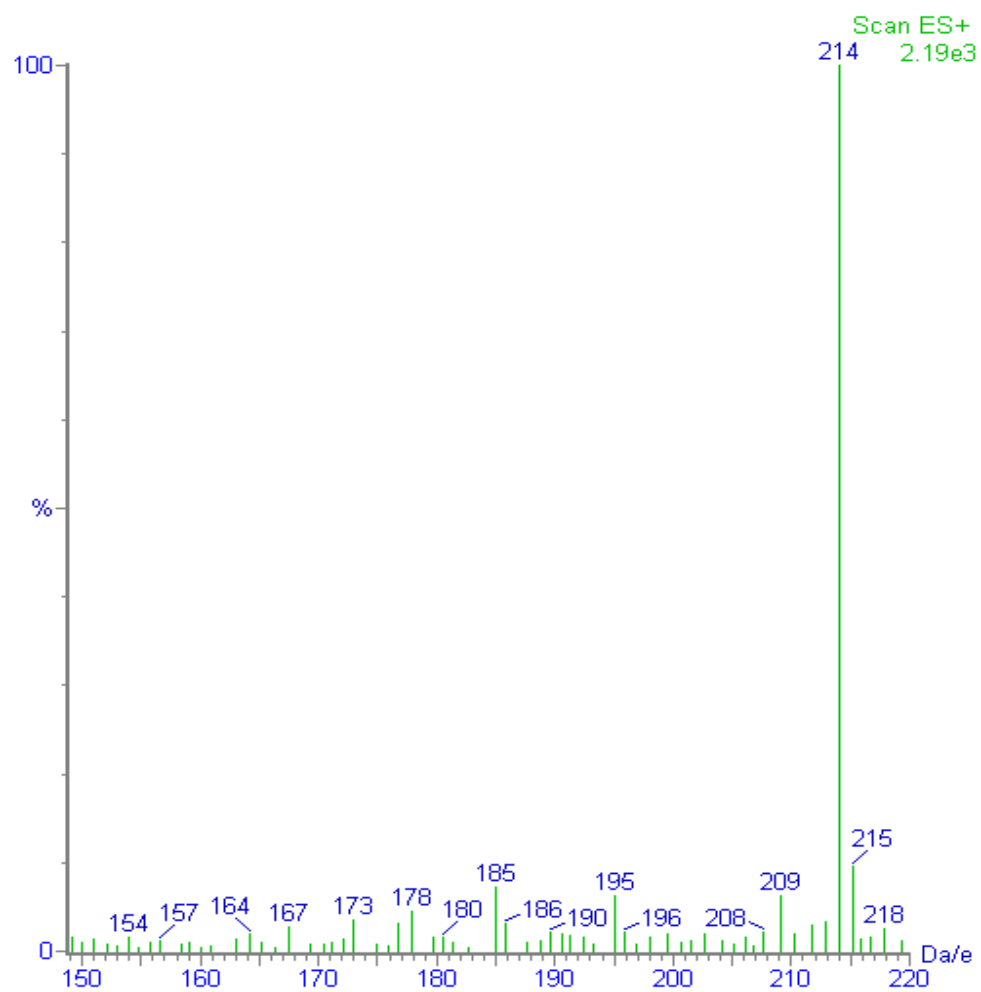
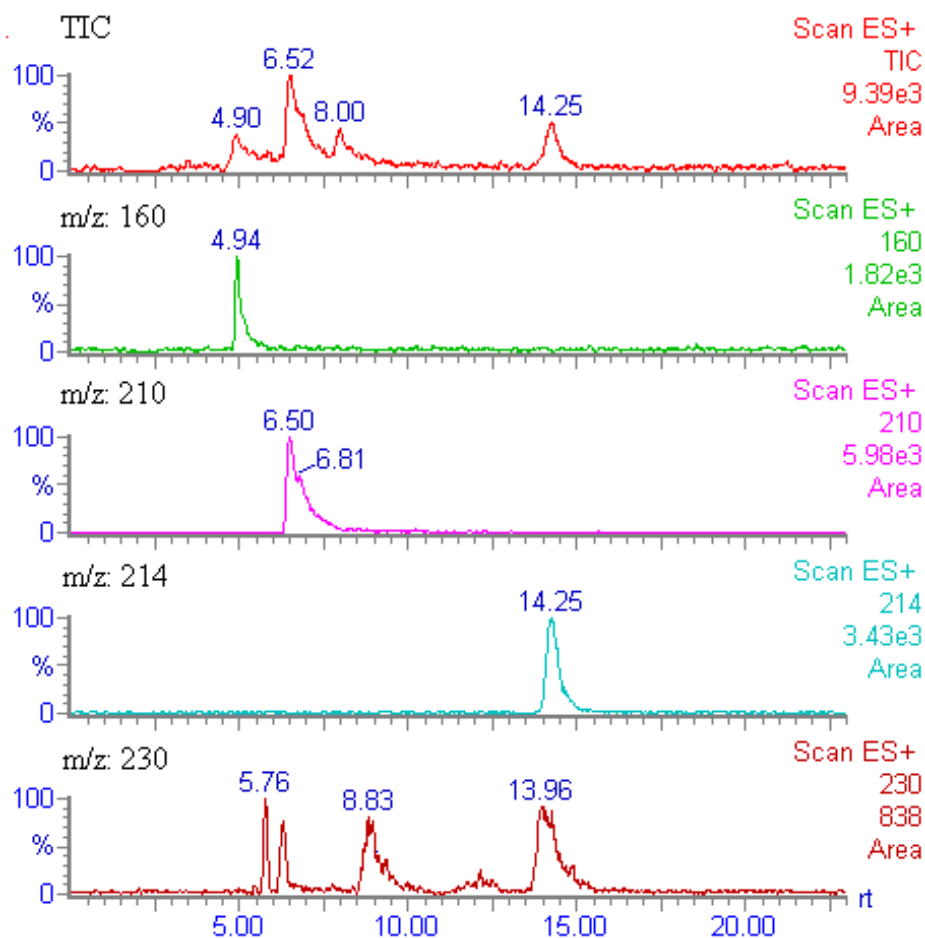


Figure 24 depicts the single ion current tracings obtained from the search of chromatographic peaks generated from base ion peaks and from pseudomolecular ions of likely metabolites. Our results gave several single ion traces with MH^+ of 160, 210, 214 and 230 Da. Obviously, the ion peak at m/z 214 corresponds to the substrate MCPTP.

Figure 24. Reconstructed ion Current Chromatograms from HPLC-ESI/MS Analysis of Liver Microsomal Incubation Mixture of MCPTP



M7 displayed an ion current trace at m/z 160 which corresponds to MH^+ of the N-despropyl species **40**. Its matched retention time, mass and UV spectroscopic properties with those of authentic PTP confirm this assignment. M9 displayed a single ion peak at m/z 210, 4 amu lower than that of parent drug (m/z 214), indicating the loss of four hydrogen atoms, and suggesting that this metabolite was pyridinium species **59** generated by the four electron oxidation of MCPTP. Its distinctive UV chromophore at 299 nm confirms this assignment. The single ion current trace analysis at m/z 212 corresponding to the ion peak of dihydropyridinium species **58**, a possible precursor of pyridinium product, did not result in a detectable peak. This is likely to be due to the fact that dihydropyridinium species is unstable and is quickly oxidized to the pyridinium species.

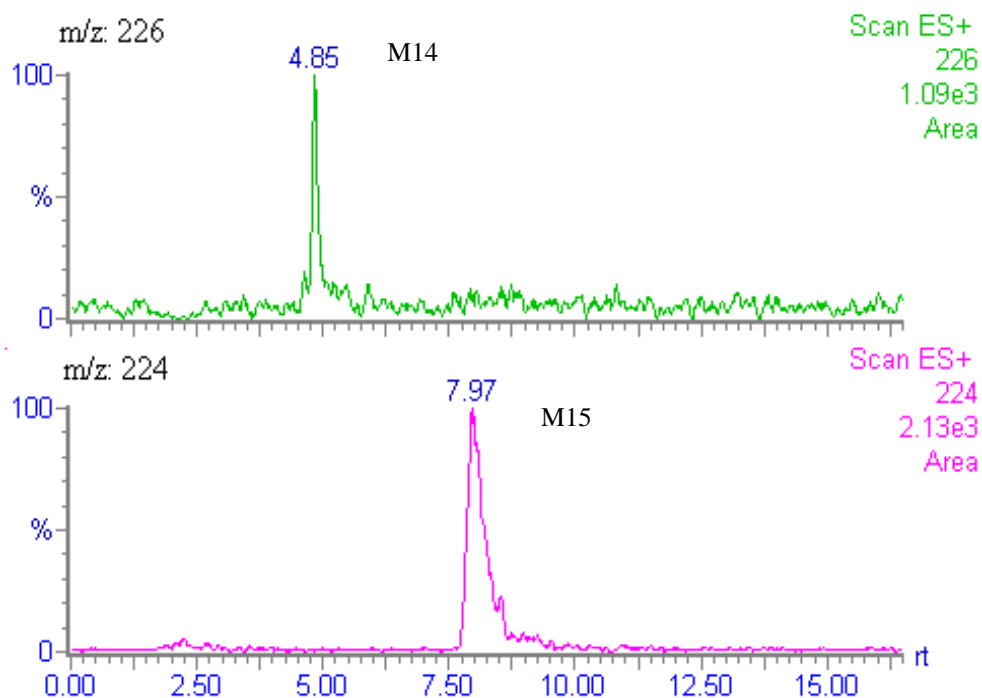
Single ion current traces at m/z 230 displayed four peaks at retention time 5.7 min, 6.1 min, 8.8 min and 13.9 min. The masses of these metabolites are 16 amu higher than the substrate, indicating monooxygenated products. From Scheme 12, several monooxygenated products, including the carbinols **66** and **67**, the phenol **68** and N-oxide **65**, are expected. The ion peak at 5.7 min corresponded to M8 from HPLC-DA analysis. M8 had a chromophore at 260 nm. This peak was previously assigned as the phenol **68** because of the longer wavelength, 260 nm, of the chromophore detected by DA. Its ion peak displayed m/z 230, which is 16 amu higher than that of the substrate, is consistent with this assignment. The ion peak at 13.96 min has almost the same retention time as that of the substrate. We did not observe a corresponding peak in the HPLC-DA tracing, possibly because it coeluted and has an identical UV chromophore with that of the substrate. This monooxygenated product was assigned as the N-oxide **65**. Since an authentic compound was not available, we were not able to confirm this assignment. We have tried to improve the resolution between the suspected N-oxide and substrate, but were not successful. By comparing the peak area of the ion current trace, this N-oxide product was present in a low yield compared to the N-oxide of CPTP. The other two ion traces at 6.10 min and 8.83 min with 16 amu increments suggest there might be other monooxygenated, possibly hydroxylated products. Hydroxylation may occur on the cyclopropyl ring to form **66** or on the methyl moiety to form **67**. However, the exact

position at which hydroxylation occurred was not possible to establish due to the limited information available.

Two minor ion current traces due to M14 and M15 at m/z 226 and 224 were extracted from the TIC (Figure 25). Similar to the patterns of the two minor peaks found from LC-ESI/MS analysis of metabolites generated from the substrate CPTP, these m/z values are also 12 and 10 amu higher than the parent substrate MCPTP. Based on our previous study on CPTP metabolites, these two minor metabolites were tentatively proposed to be **71** and **72** analogous to **52** and **53** generated from CPTP.

We also have attempted to obtain molecular ion information about metabolites M11-M13 appearing in the HPLC-DA chromatogram (Figure 17) but was not successful. This is probably because they are insensitive toward the electrospray mass detector or maybe they are present in very low concentrations. The identities of these metabolites remain unresolved.

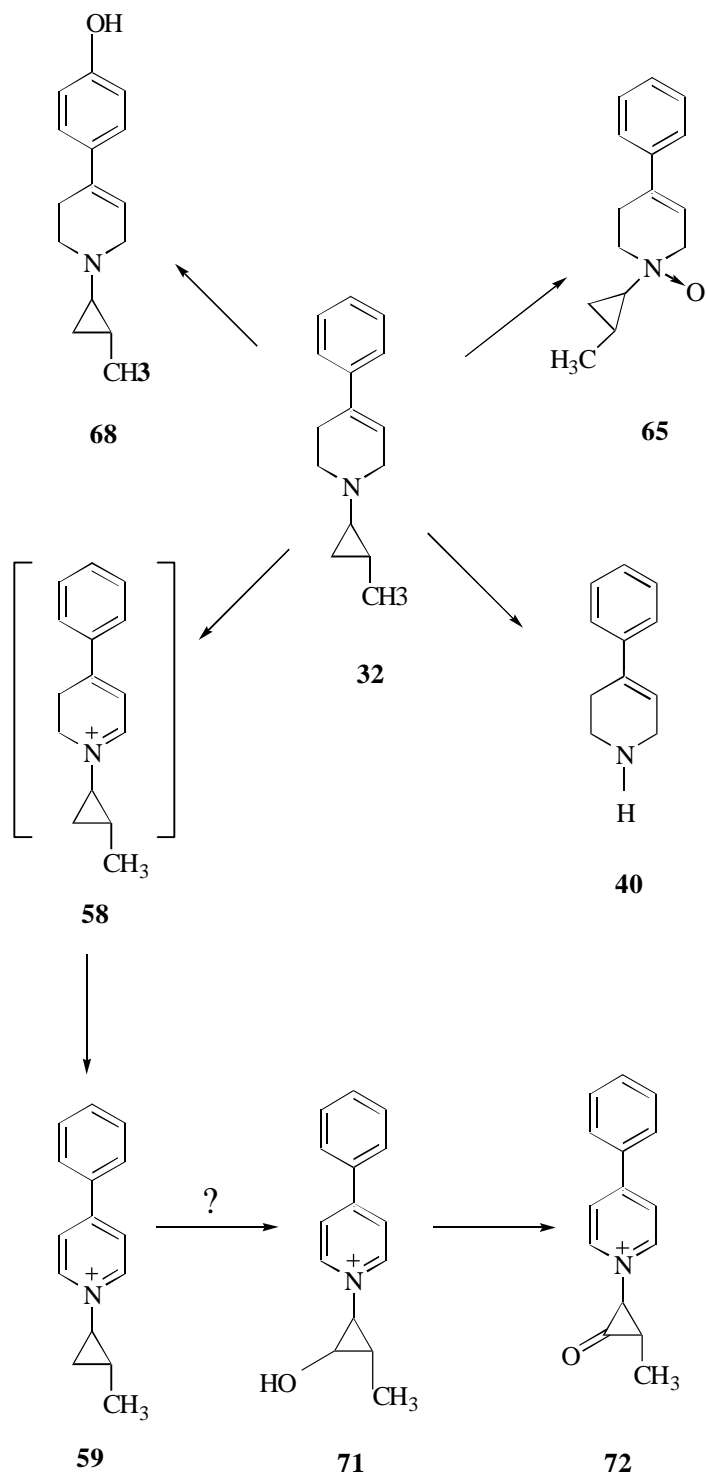
Figure 25. Reconstructed Ion Current Chromatograms of the two Minor Metabolites M14 and M15



3.4.2 Conclusions

Incubation of MCPTP with rat liver microsomes generated several metabolites with no evidence of significant enzyme inactivation. Several metabolites were identified by using HPLC coupled with electrospray mass spectrometry and by HPLC-diode array detection. Our results indicate that these metabolites are NADPH dependent and are formed by reactions catalyzed by cytochromes P450. The major metabolic pathways of the rat liver microsomal catalyzed oxidation of MCPTP include N-descyclopropylation to form **40**, aromatic hydroxylation to form **68**, and α -carbon oxidation to yield **58** and **59** (Scheme 13). The minor routes are due to N-oxidation and, perhaps, hydroxylation at the cyclopropyl moiety of the pyridinium species to form **71** followed by further oxidation of **71** to form keto derivative **72**. These pathways are similar to those of CPTP. Compared to the metabolic profile generated from CPTP, more metabolites are generated from MCPTP. Some of these might result from the ring opening pathway. Unfortunately we were not able to identify the fate of the cyclopropyl group. However, the conversion of CPTP and MCPTP to the N-descyclopropyl species may proceed via the ring opening pathway depicted in Scheme 12.

Scheme 13. Metabolic Pathways of Liver Microsomal Catalyzed Oxidation of MCPTP

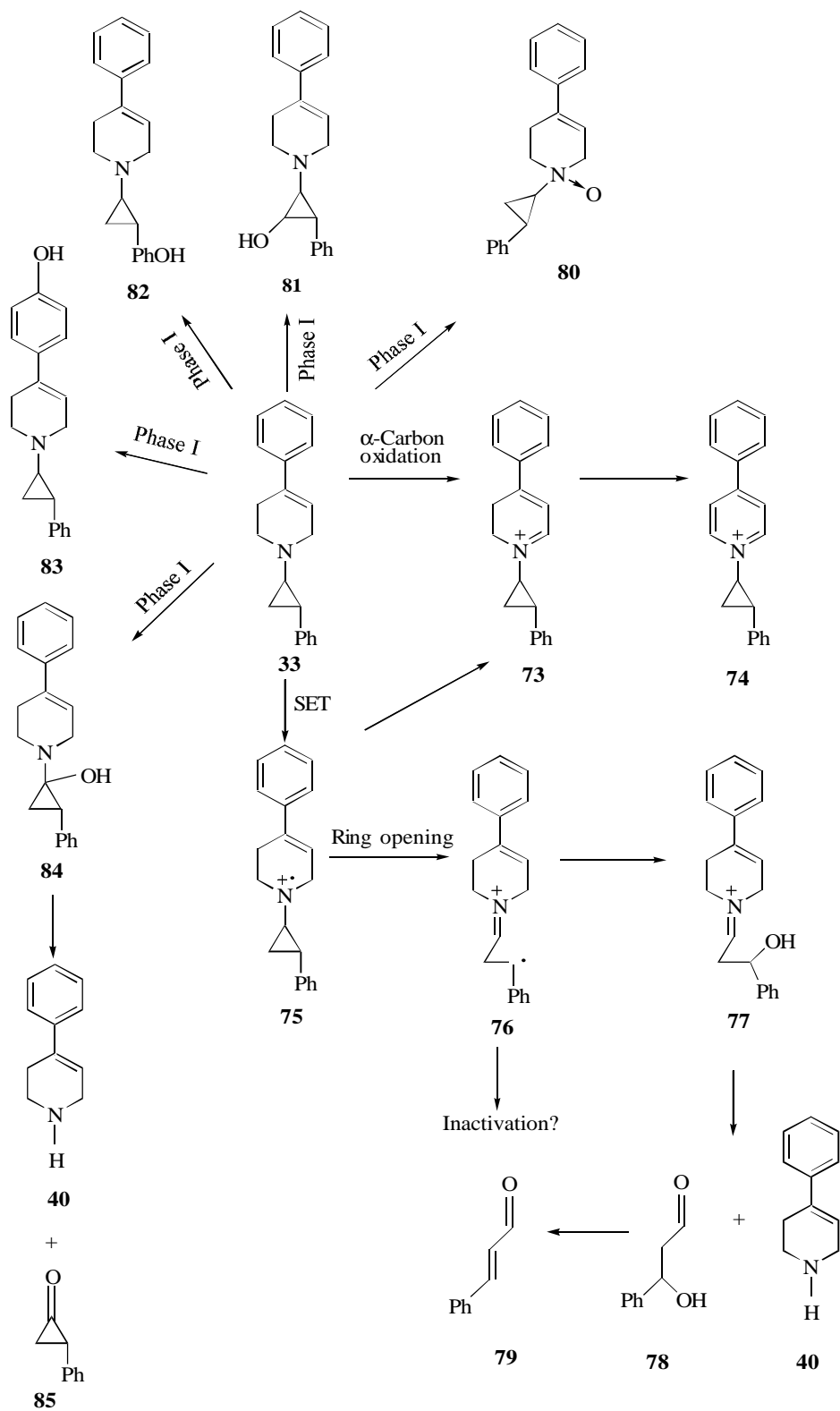


3.5. PCPTP

3.5.1. Results

Our studies on the liver microsomal catalyzed oxidation of CPTP and MCPTP still did not provide a clear distinction between the SET and HAT pathway. The formation of the dihydropyridinium species and pyridinium species can be rationalized by either the SET or HAT pathway. Although the formation of N-descyclopropyl product **40** can be rationalized to proceed via the ring opening pathway initiated by SET, the lack of direct observation of the fate of the cyclopropyl moiety limits our ability to describe the pathway. An examination of the metabolic fate of another CPTP analog, PCPTP (**33**), was undertaken. PCPTP was synthesized at our lab by Dr. Simon Kuttab [90] and was obtained as a mixture of *cis* and *trans* isomers. The compound we used here is the pure *trans* isomer: *trans*-1-(2-phenylcyclopropyl)-4-phenyl-1,2,3,6-tetrahydropyridine (**33**). Metabolic pathways analogous to those shown in Scheme 10 and Scheme 12 were proposed for PCPTP (Scheme 14). The substrate **33** may undergo α -carbon oxidation to form the dihydropyridinium species **73** and pyridinium species **74**. Alternatively it may undergo the ring opening reaction via the cyclopropylaminyl radical cation **75** to form the distonic radical cation **76** which may lead to the inactivation of the enzyme or may undergo subsequent radical recombination to form **77** and fragmentation of **77** will produce the N-descyclopropyl **40** and the β -hydroxylaldehyde **78**. Compound **78** can undergo dehydration to form cinnamaldehyde (**79**). Besides these reactions, PCPTP may undergo the common Phase I reactions to form the N-oxide **80** and hydroxylated products **81**, **82**, **83** and (or) **84**. Carbinolamine **84** is unstable and should undergo fragmentation to form the N-descyclopropyl product **40** and ketone **85**. The final metabolic profile might be the result of a combination of these pathways. We expected that the phenyl substituent on cyclopropyl ring would stabilize the ring opened radical cation **76** and favor the ring opening pathway leading to the formation of cinnamaldehyde (**79**). We will discuss our experimental results on characterizing these metabolic pathways below.

Scheme 14. Predicted Metabolic Pathways of PCPTP Catalyzed by Liver Microsomes



PCPTP was incubated with a rat liver microsomal preparation which had been supplemented with an NADPH generating system at 37°C. The samples were analyzed by HPLC-diode array at the incubation times of 0, 20, 40 and 60 min to see if any metabolites were generated and if their formation was time dependent. PCPTP was also incubated with rat liver microsomes in the absence of the NADPH. As we discussed in the CPTP section, the following five wavelength were employed to monitor the incubation mixture: 215 nm, 230 nm, 260 nm, 290 nm and 325 nm. This allowed us to detect simultaneously the unchanged substrate and the anticipated metabolites.

The incubation mixture was analyzed by the HPLC-DA assay as described in the Experimental Section. Figure 26 depicts the HPLC-DA tracings obtained when the sample had been incubated in the presence of NADPH generating system. Nine new peaks, M16 to M24, besides the substrate S3, appeared and their intensities were shown to gradually increase with the time of the incubation. The intensity of the substrate peak gradually decreased during this time. The HPLC-DA analysis of the control sample (containing no NADPH) showed only the substrate peak S3 which eluted at about 20 min (Figure 27). This established that the substrate was chemically stable under these conditions. Based on these data, the formation of M16 to M24 is likely to be cytochrome P450 mediated. The HPLC responses of the substrate and metabolites with the time of the incubation are depicted in Figure 28 and Figure 29. From these two plots we can see that the rate of the substrate consumption and the metabolite formation became slower with the the times of incubation, possibly reflecting substrate consumption. No significant enzyme inactivation was observed.

Figure 26. HPLC-DA Analysis of PCPTP Incubated with Liver Microsomes
Supplemented with NADPH System for 60 min

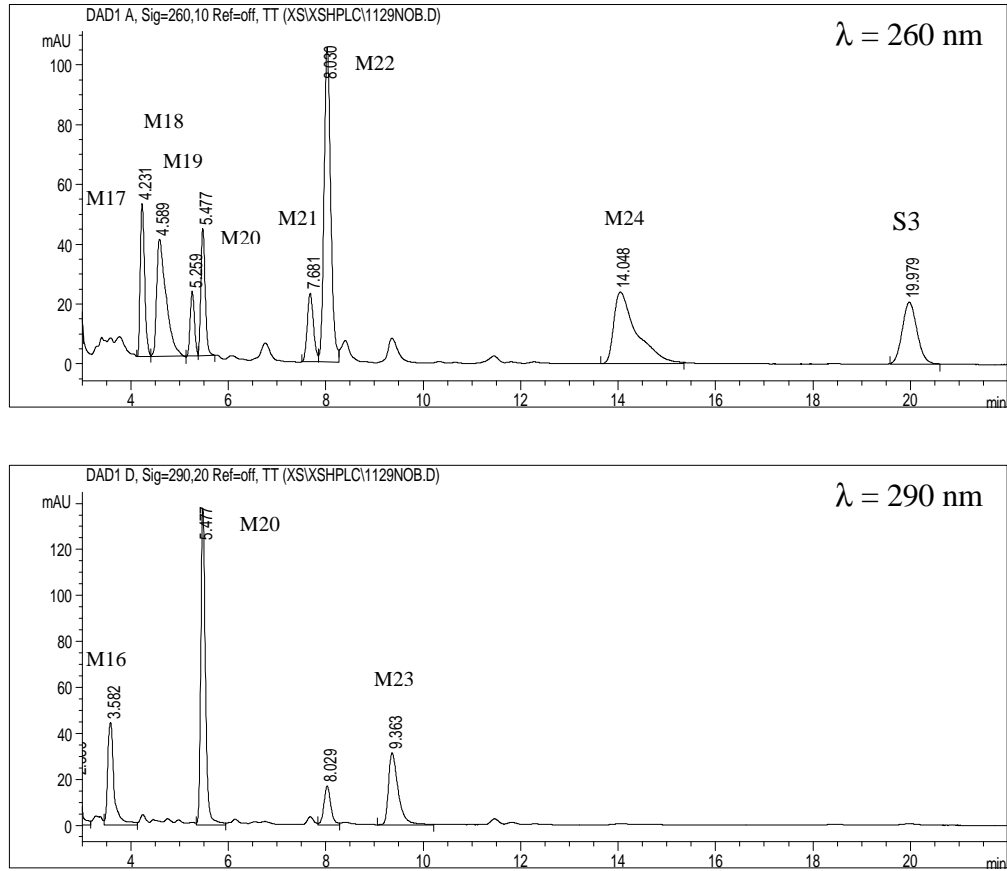


Figure 27. HPLC-DA Analysis of CPTP Incubated with Liver Microsomes
in the Absence of NADPH System for 60 min

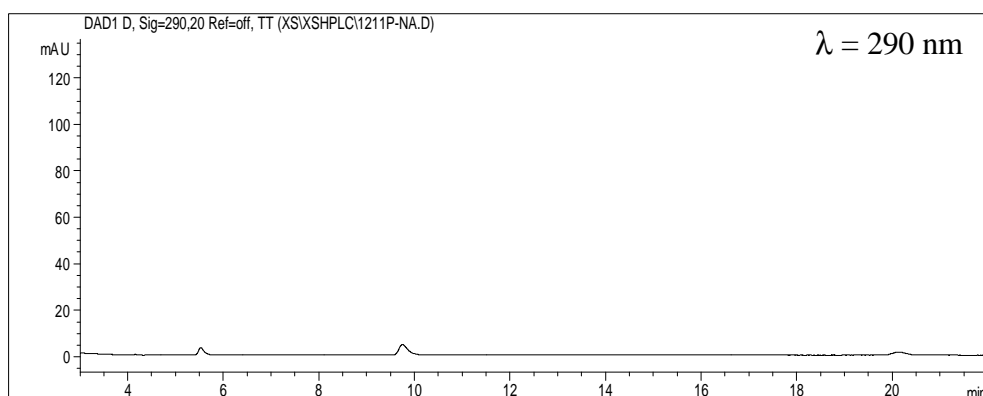
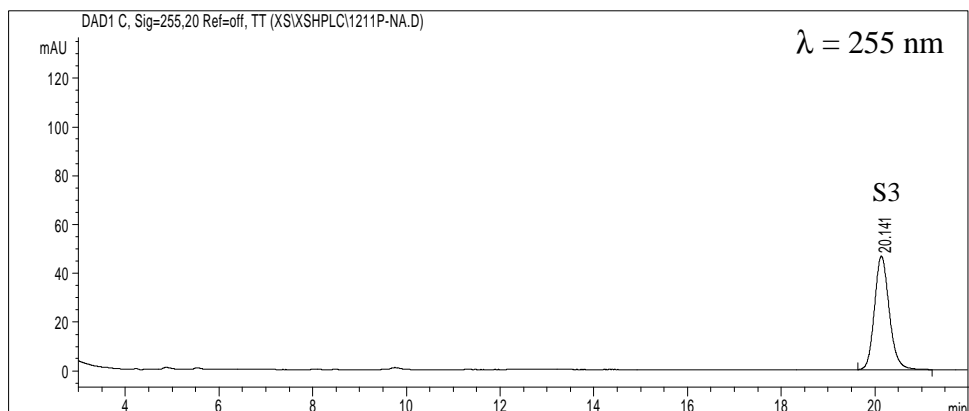


Figure 28. HPLC Response of the Substrate PCPTP vs. Incubation Time

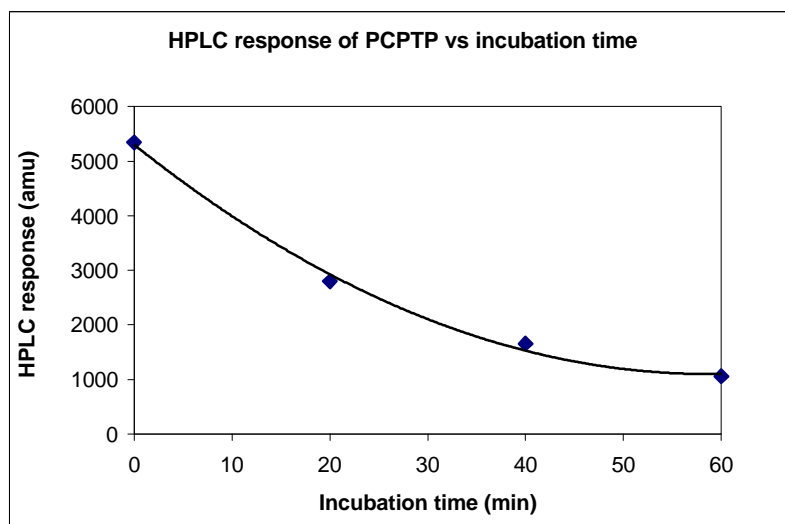
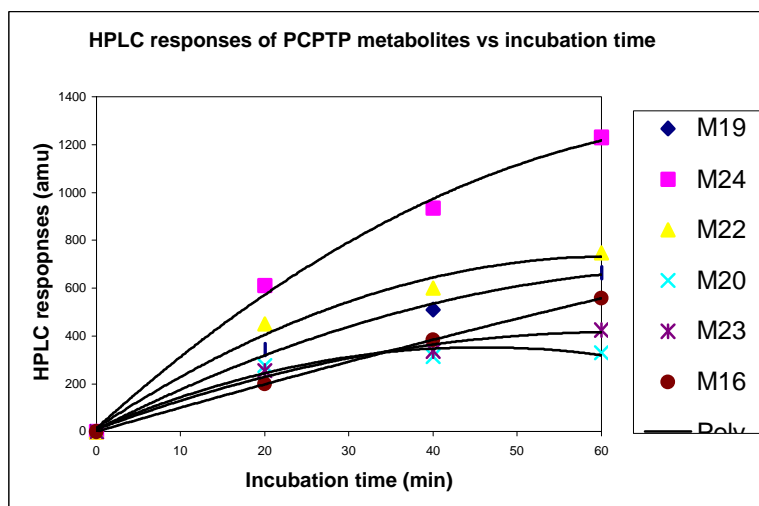


Figure 29. HPLC Responses of PCPTP Metabolites vs. Incubation Time



The substrate PCPTP (S3) eluted at 20.0 min and displayed the expected chromophore at 245 nm (Figure 30). Nine metabolites, M16-M24, were well resolved in the HPLC tracing: M16 (3.58 min, λ_{\max} 325 nm) , M17 (4.23 min, λ_{\max} 250 nm), M18 (4.59 min, λ_{\max} 245 nm), M19 (5.26 min, λ_{\max} 245), M20 (5.48 min, λ_{\max} 289 nm), M21 (7.68 min, λ_{\max} ?), M22 (8.03 min, λ_{\max} 260 nm), M23 (9.36 min, λ_{\max} 304 nm) and M24 (14.05 min, λ_{\max} 245 nm). The UV spectra are shown in Figures 31-39. The metabolic profile was more complicated compared to those of CPTP and MCPTP. Metabolites M16 and M20 received our greatest attention because of their long wavelength chromophores at 325 nm and 289 nm. Peaks with such UV absorptions were not observed with the metabolites generated from CPTP and MCPTP, suggesting an unusual pathway. The distinctive UV chromophore 304 nm of M23 led us to suspect that this metabolite might be the pyridinium species **74**.

Figure 30. UV Spectrum of S3

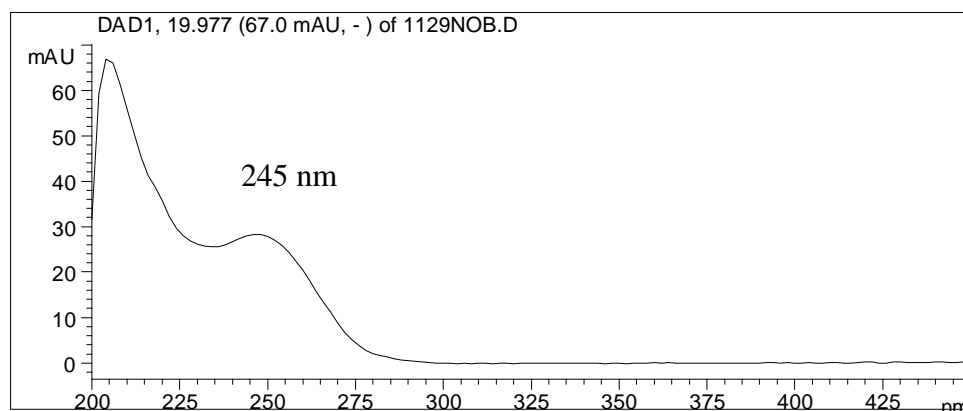


Figure 31. UV Spectrum of M16

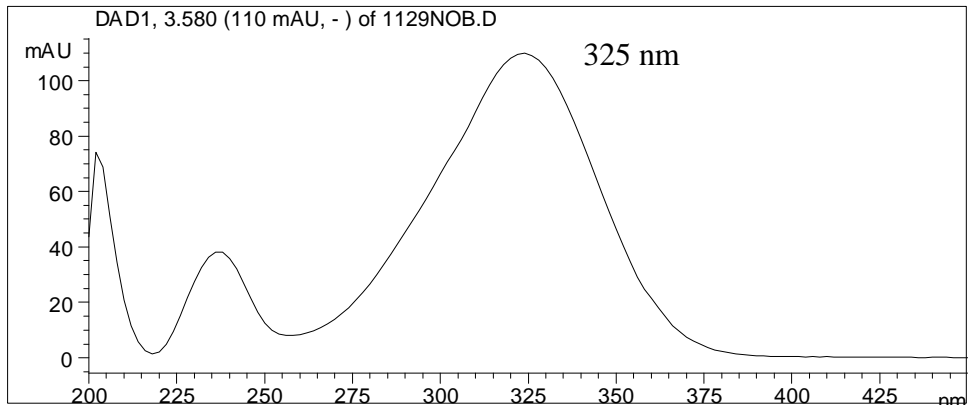


Figure 32. UV Spectrum of M17

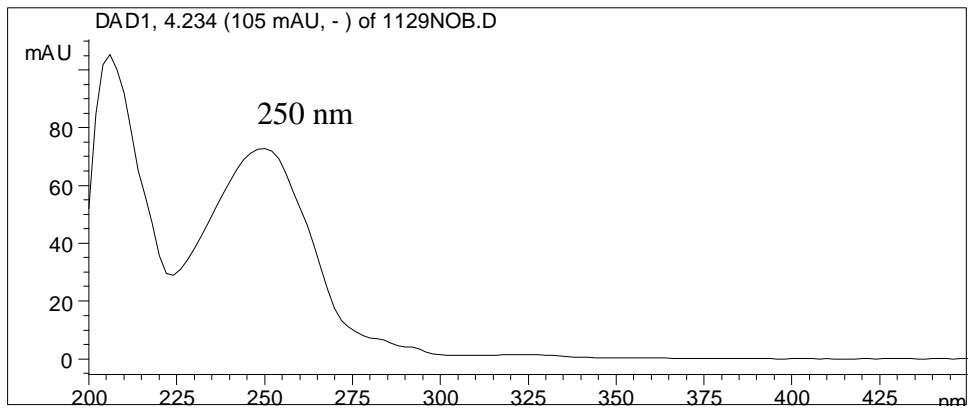


Figure 33. UV Spectrum of M18

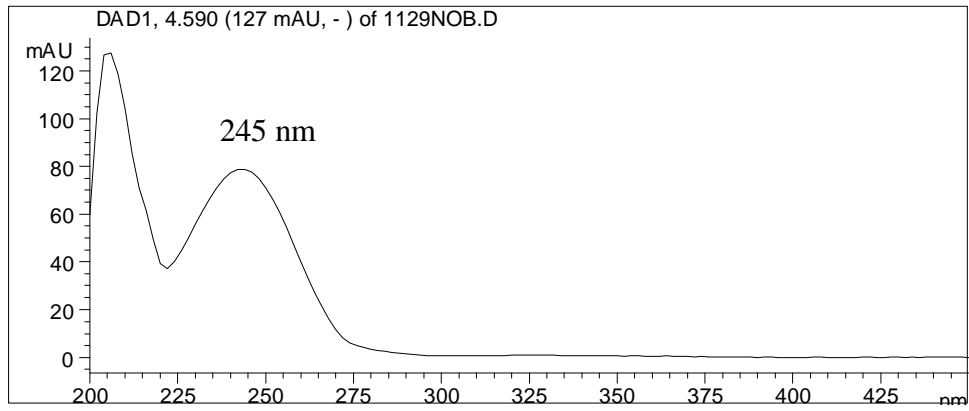


Figure 34. UV Spectrum of M19

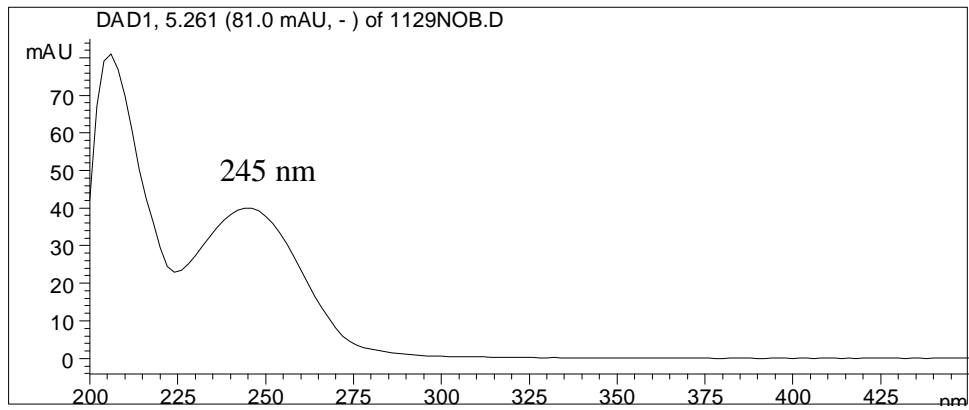


Figure 35. UV Spectrum of M20

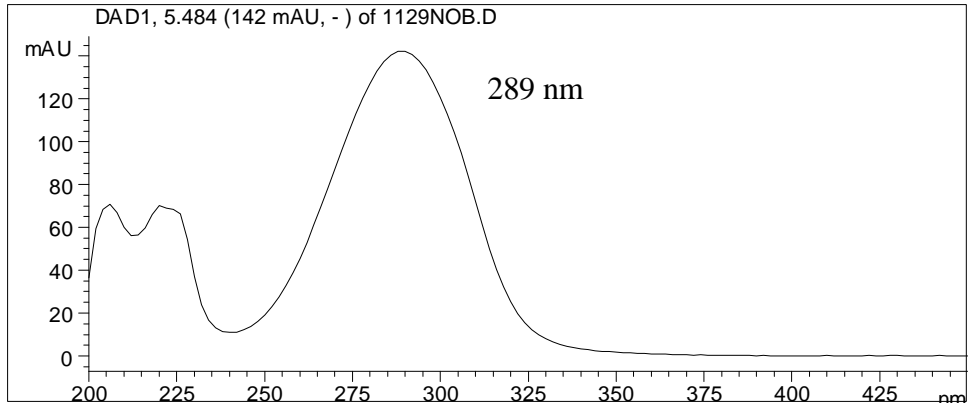


Figure 36. UV Spectrum of M21

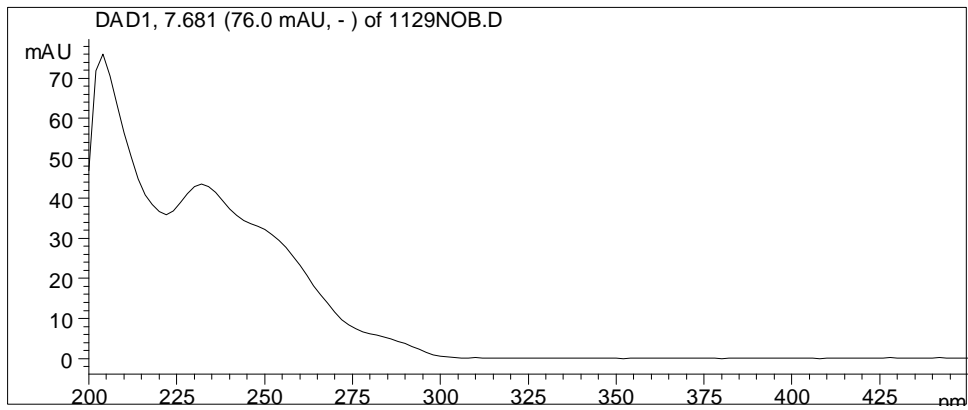


Figure 37. UV Spectrum of M22

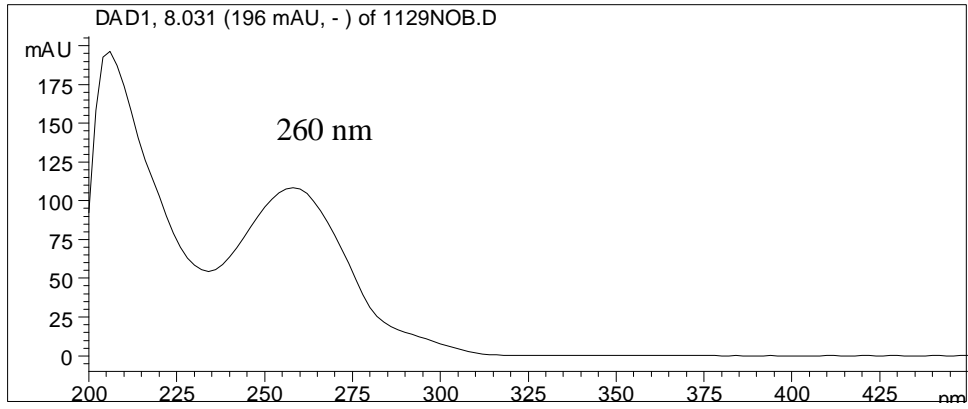


Figure 38. UV Spectrum of M23

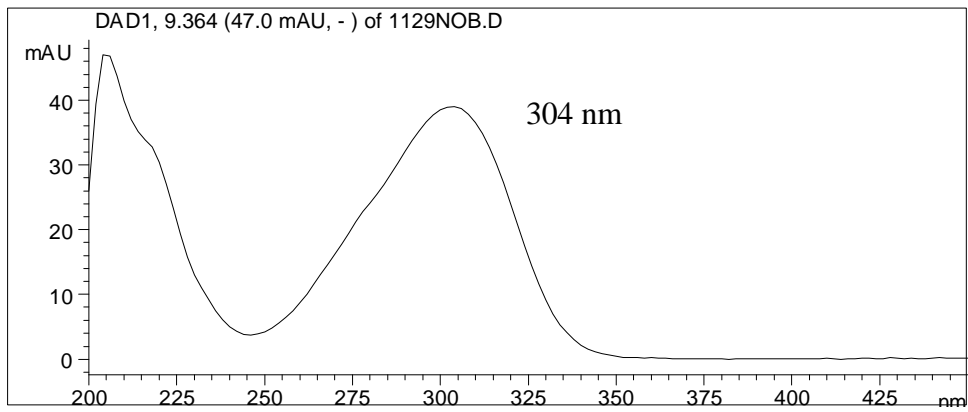
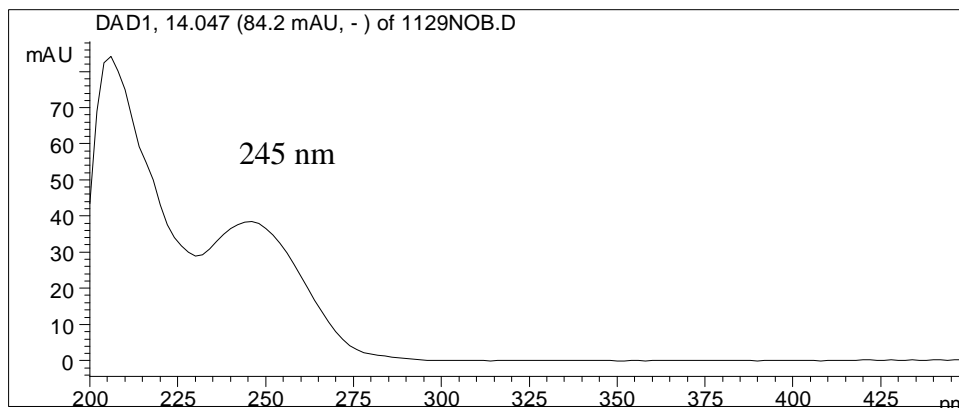


Figure 39. UV Spectrum of M24



In order to obtain additional structural information, LC-ESI/MS/UV analysis of the PCPTP liver microsomal incubation mixtures was pursued. We selected 250 nm to detect the unchanged substrate and most metabolites such as M17, M18, M19, M20, M21, M22 and M24. The metabolites M16 and M23 absorb very weakly at this wavelength and could not be detected. The HPLC/UV chromatogram served as a resource to let us correlate the retention times of the peaks between the HPLC/DA chromatogram and TIC obtained from HPLC-ESI/MS analysis. Figure 40 shows HPLC/UV chromatogram and positive ion TIC obtained from HPLC-ESI/MS/UV analysis of the incubation mixture. Searching single ion current signals generated several peaks at m/z 160, 133, 272, 276 and 292 (Figure 41).

Figure 40. HPLC/MS/UV Analysis of Liver Microsomal Incubation Mixture of PCPTP.

a. HPLC/UV Chromatogram, b. TIC Obtained from LC-ESI/MS

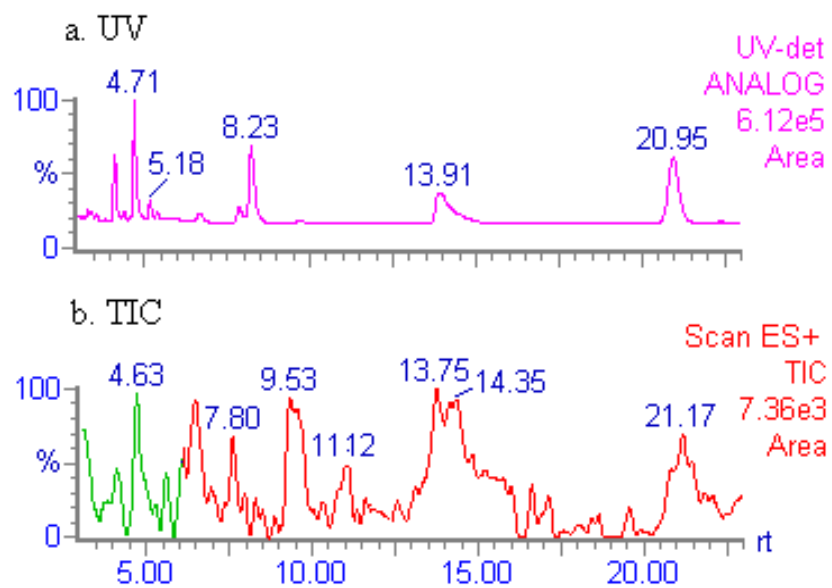
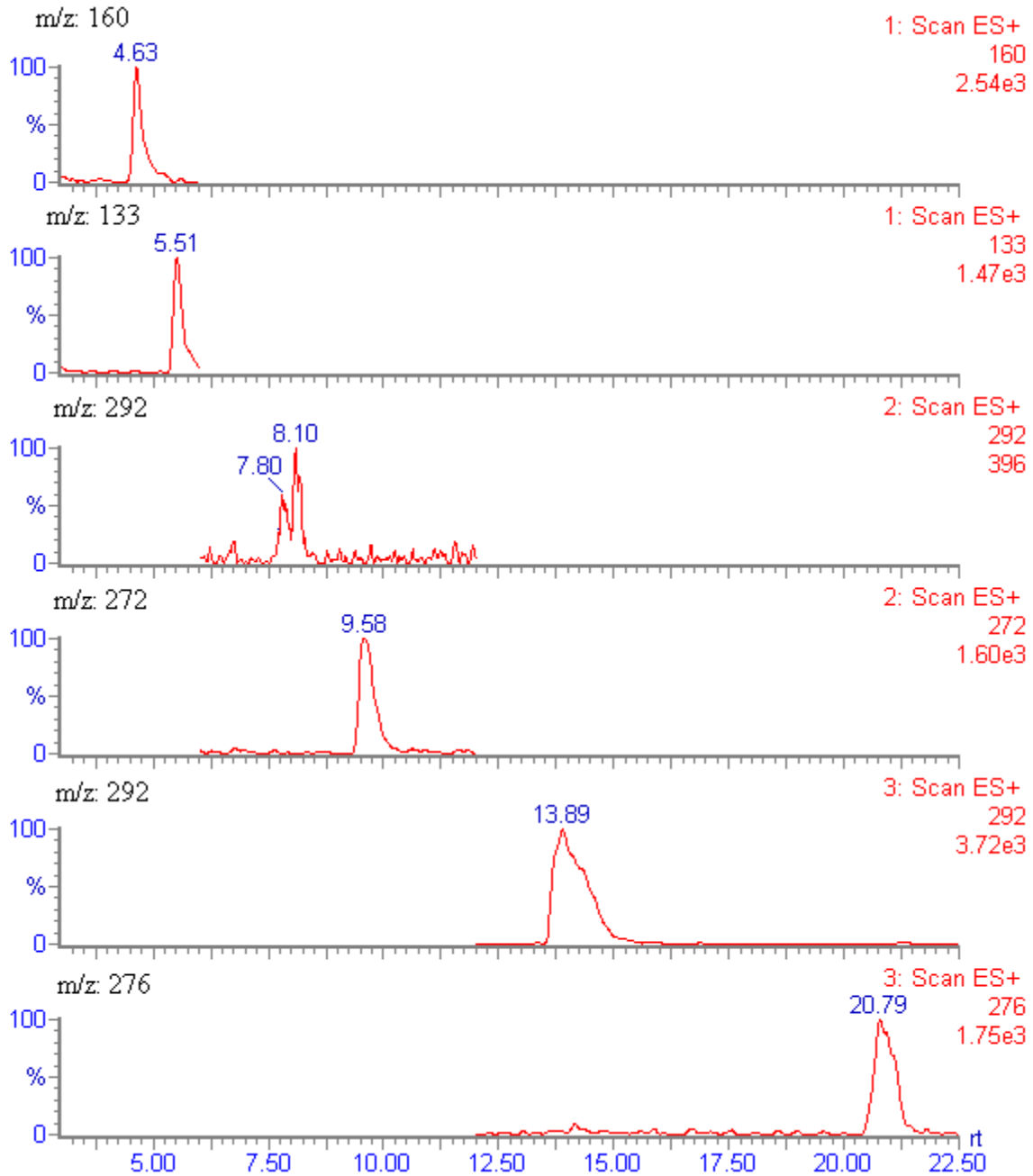
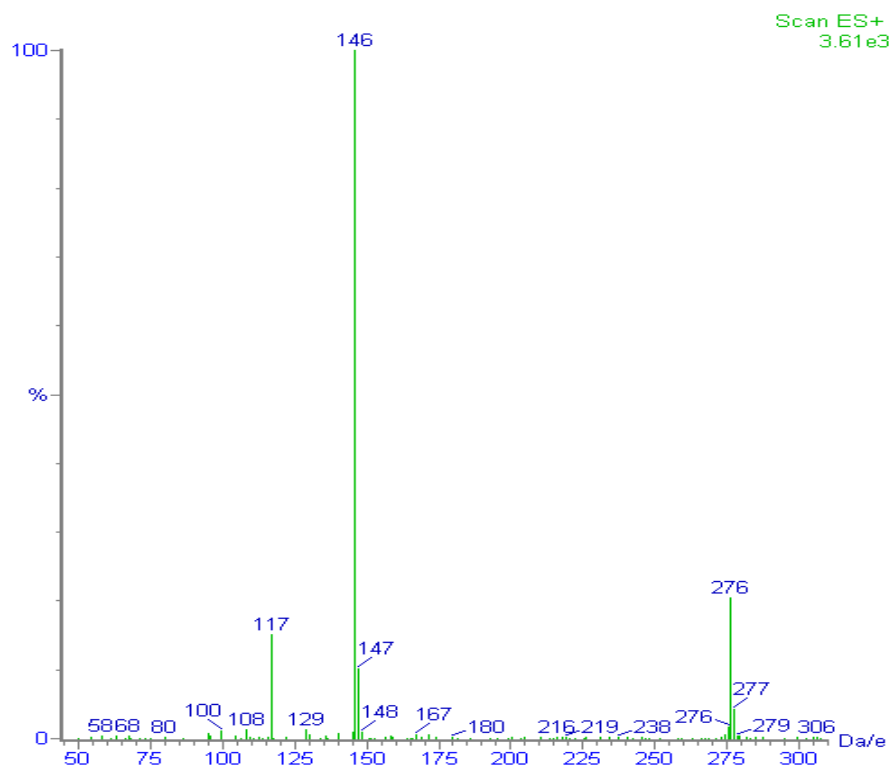


Figure 41. Reconstructed Ion Current Chromatograms of
Liver Microsomal Incubation Mixture of PCPTP

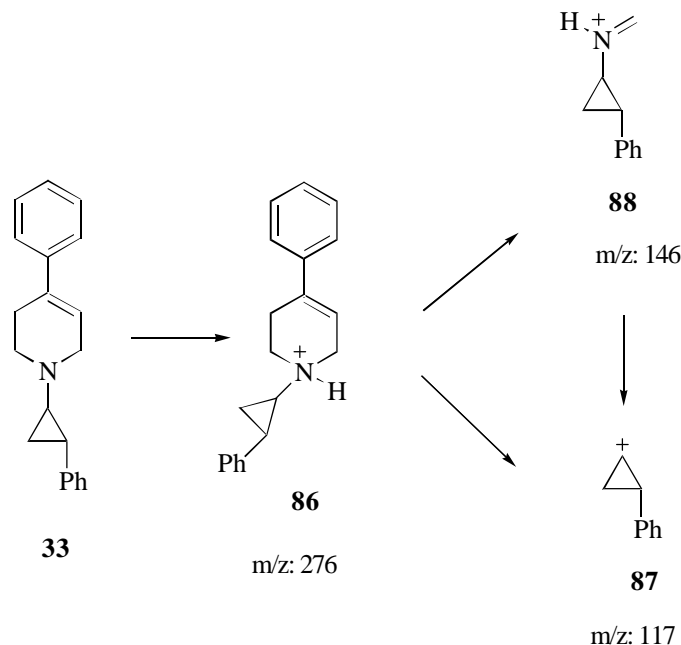


The mass spectrum of PCPTP displays several peaks including the pseudomolecular ion and two strong fragmentation ion peaks (Figure 42). The ion at m/z 276 corresponds to MH^+ (**86**) (Scheme 15). The fragment ion at m/z 117 is assigned to **87** and the fragment ion at m/z 146 is assigned to **88**.

Figure 42. Mass Spectrum of PCPTP

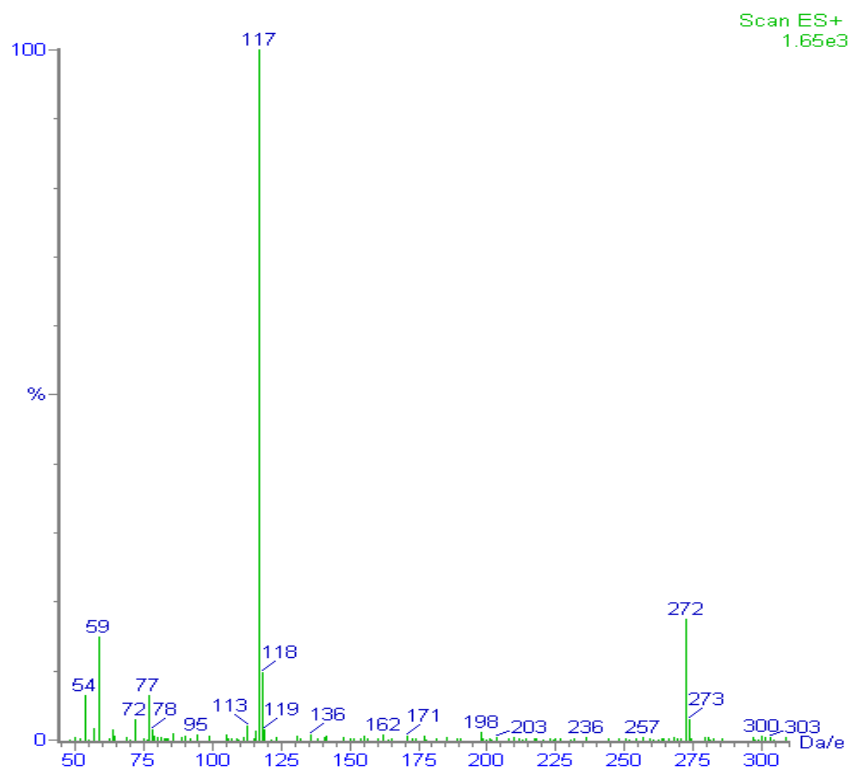


Scheme 15. The Fragmentation Generated from PCPTP

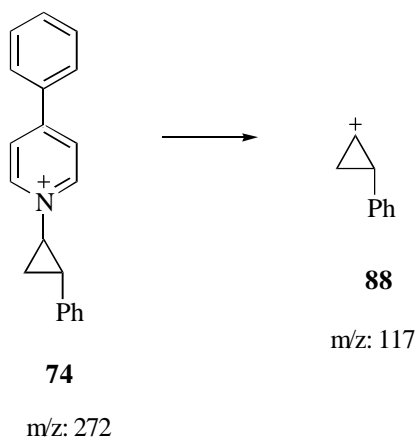


M18 displayed an ion at m/z 160, which corresponded to the N-despropyl species **40**, the common metabolite generated from CPTP and MCPTP as well. This was confirmed as PTP by comparing the spectral properties with the standard compound. M18 and standard PTP had the same retention time and identical UV spectra. M23 displayed an ion at m/z 272, 4 amu lower than that of the substrate PCPTP (m/z 276), indicating the loss of four hydrogens and suggesting that this metabolite was pyridinium species **74** generated by the four electron oxidation of PCPTP. The mass spectrum of M23 (Figure 43) shows a molecular ion at m/z 272 and major fragment at m/z 117 which was assigned to **88** (Scheme 16). M23 displayed a UV chromophore at 304 nm, consistent with this assignment. In order to identify M23 unambiguously, compound **74** was synthesized in our lab by Dr. Simon Kuttub [90]. M23 was confirmed as the pyridinium species **74** by the matched chromatographic and spectroscopic properties with the synthetic standard **74**.

Figure 43. Mass Spectrum of M20



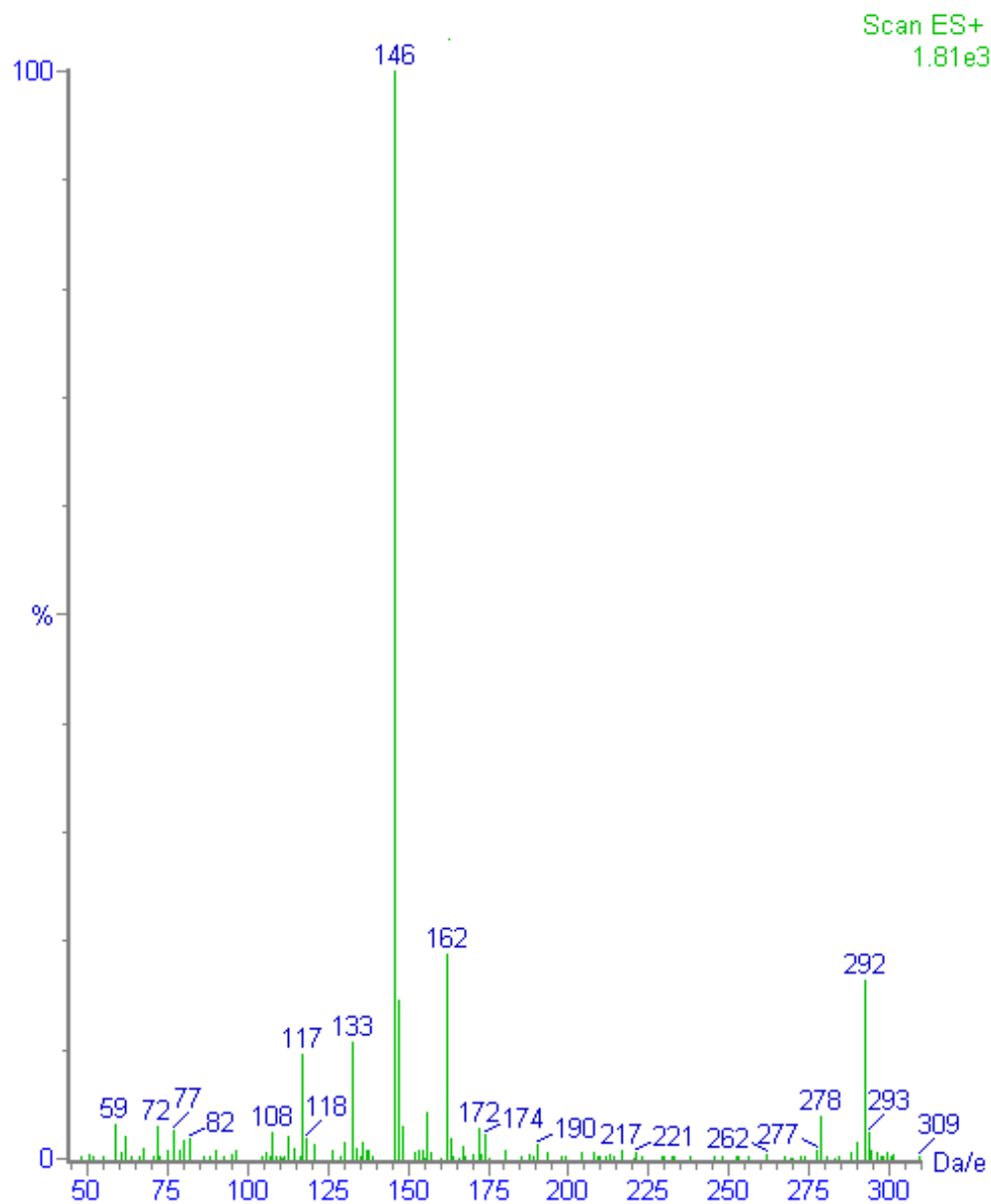
Scheme 16. The Fragmentation Generated from M23



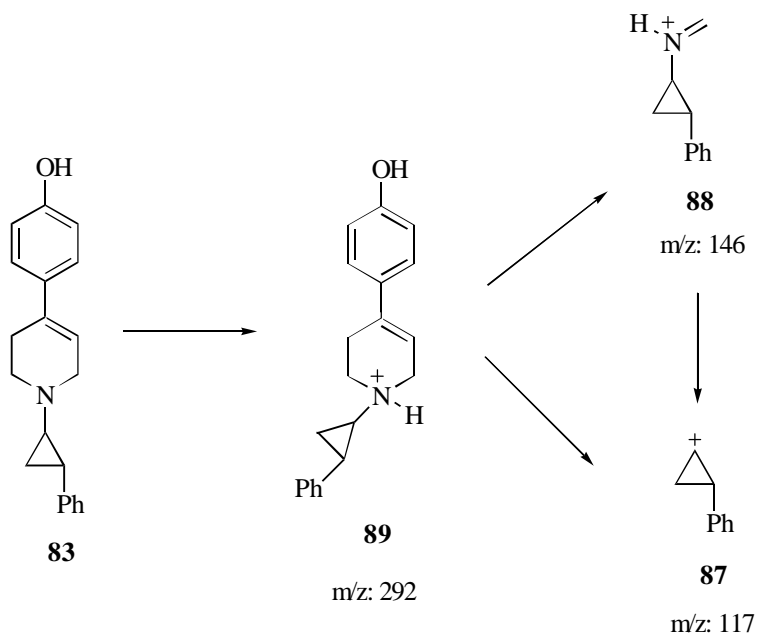
Three metabolites, M21, M22 and M24, displayed ion intensities at m/z 292, 16 amu higher than the substrate (m/z 276). The difference of 16 amu suggested monooxygenated products. Addition of oxygen can be either at the phenyl moiety, to form **82** and/or **83**, or at cyclopropyl ring, to form **81**, or at the nitrogen atom, to form N-oxide **80**. The UV chromophore of 260 nm for M22 indicated that hydroxylation had occurred at the *para*-position of the 4-phenyl moiety (metabolite **83**), similar to the phenolic products **43** and **68** generated from CPTP and MCPTP which have the same UV chromophore at 260 nm. M24 displayed the same chromophore (245 nm) as the substrate, suggesting that it might be the N-oxide **80** or carbinol **81** since the formation of these two monooxygenated products would not change the chromophore of the styrene moiety. M21 displayed a broad chromophore from 220 nm to 275 nm, eliminating the possibility of **81**. Possibly this metabolite is **82** because **82** would have a UV spectrum resulting from the overall contribution of the chromophore of both the phenol group (275 nm) and styrene group (245 nm).

In order to distinguish between these isomers, additional mass spectral information was obtained. The mass spectrum of M22 (Figure 44) shows one molecular ion peak at m/z 292 and several fragment ion at m/z 117, m/z 133, m/z 146 and m/z 162. The formation of the fragments at m/z 146 and m/z 117 has been rationalized in Scheme 17. This is consistent with our assignment of M22 as **83**. For fragments at m/z 133 and m/z 162, they are both 16 amu higher than **87** and **88**. It is difficult to rationalize that they are fragments coming from the same molecule **83**. Since the two ions for M21 and M22 which eluted at 7.8 min and 8.1 min (Figure 41) did not seem well resolved, the mass spectrum (Figure 44) for M22 might come from the unresolved mixture of M21 and M22. The fragment ions at m/z 133 and 162 can be rationalized as being generated from M21 (Scheme 18). These assignments supported our assignment of M21 as **82**.

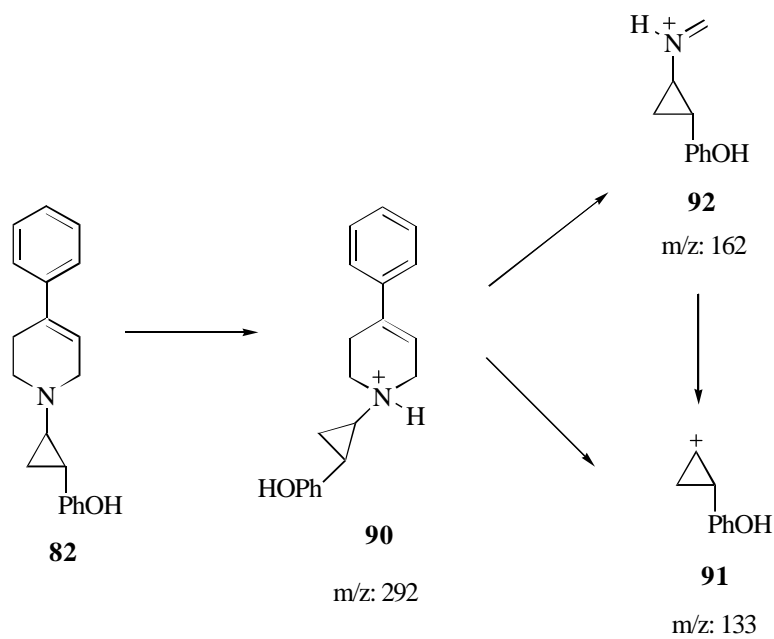
Figure 44. Mass Spectrum of the Mixture of M21 and M22



Scheme 17. The Fragmentation Generated from M22



Scheme 18. The Fragmentation Generated from M21



The mass spectrum of M24 shows one protonated molecular ion peak at m/z 292 and two fragment at m/z 117 and m/z 162 (Figure 45). The major fragment at m/z 117 is assigned as **87** which is generated by C-N bond cleavage, and the fragment at m/z 162 is assigned as **108** (Scheme 19). It seems for tertiary amine species, C-N is easily broken and leading to an intense m/z 117 ion. The abundance of the ion at m/z 117 was also high among the fragments generated from pyridinium species (Figure 43). The absence of the fragment at m/z 133 ruled out the possibility that M24 might be **81** because m/z 133 will be the possible fragment of **81**. Although the mass spectral data are consistent with N-oxide product **80**, these data are not unequivocal. Unambiguous identification of the metabolites was made with an authentic standard N-oxide PCPTP (**80**) which was synthesized in our lab by Dr. Simon Kuttub [90]. The mass spectrum of standard N-oxide PCPTP (Figure 46) is identical with that of M24 (Figure 45). Therefore, M24 is confirmed as N-oxide **80** by its corresponding matched retention times, UV chromophores and mass spectral data with those of the synthetic standard.

Figure 45. Mass Spectrum of M24

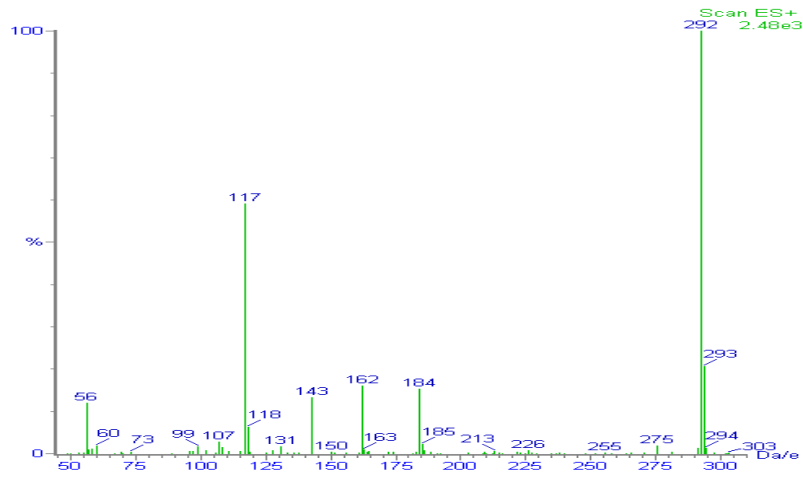
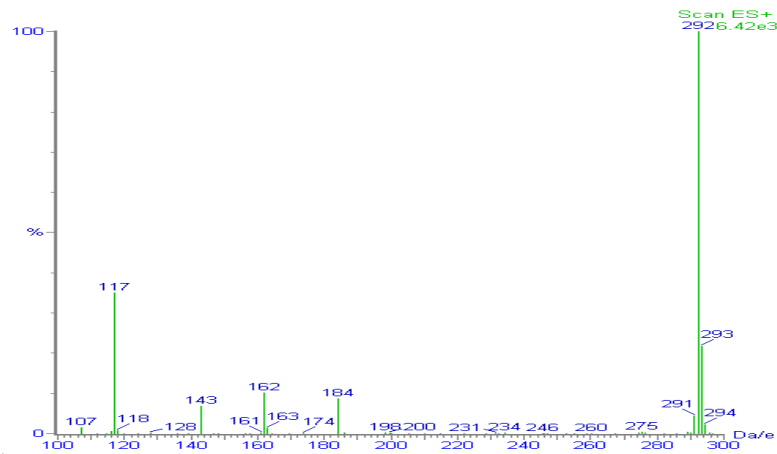
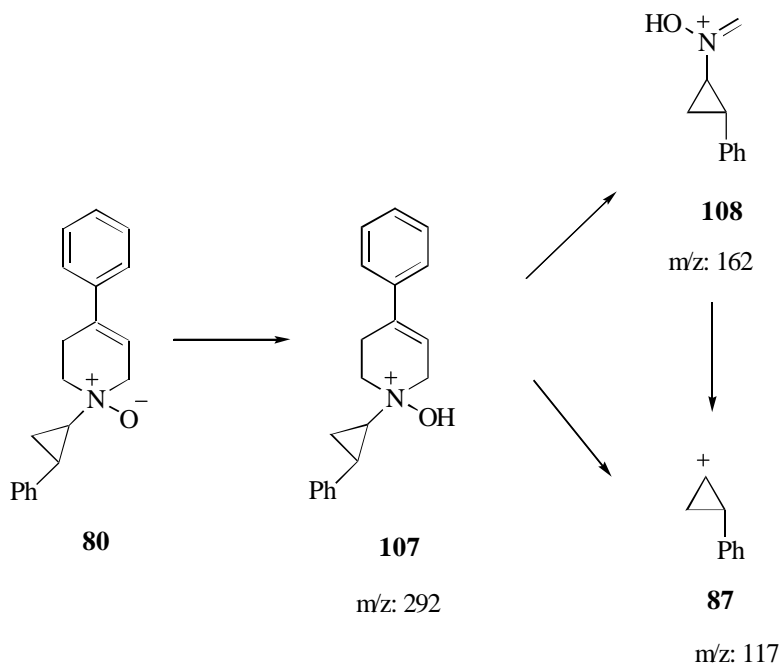


Figure 46. Mass Spectrum of Synthetic N-oxide PCPTP

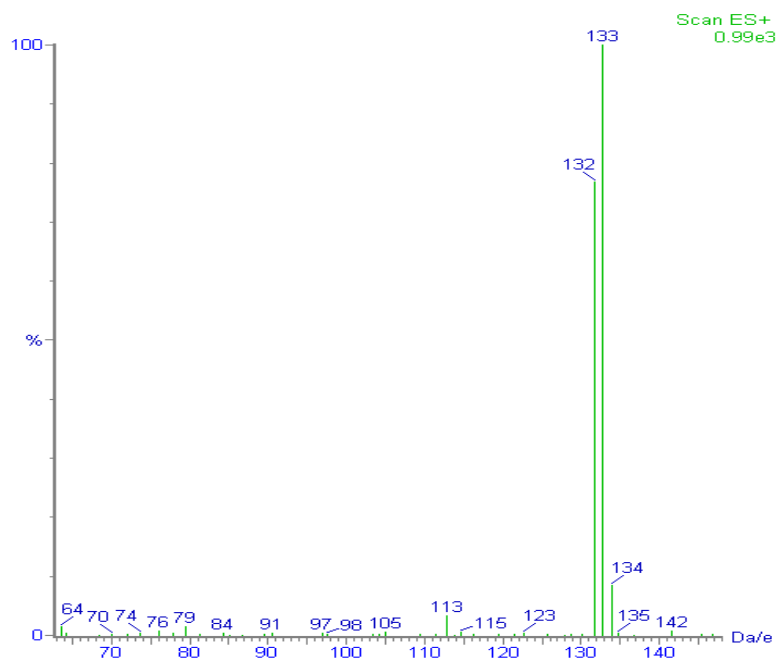


Scheme 19. The Fragmentation Generated by M24

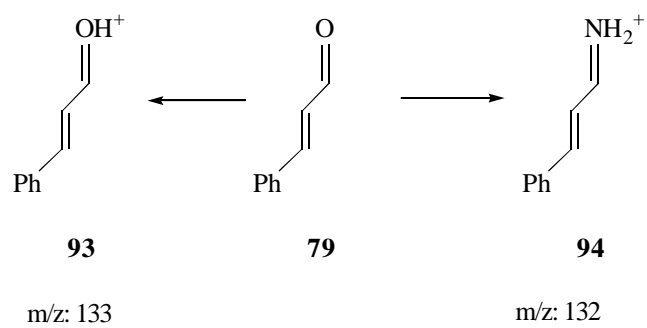


M20 displayed a protonated molecular ion peak at m/z 133 (Figure 41). The UV chromophore for M20 is at 289 nm. The 289 nm chromophore is very curious since such a UV chromophore was not observed for metabolites generated by CPTP and MCPTP. Consideration of the ring opening pathway and the mass of MH^+ for this metabolite led us to consider cinnamaldehyde (**86**). Mass spectrum of M20 shows two major ion peaks at m/z 133 and m/z 132 (Figure 47). The ion at m/z 133 is the protonated molecular ion MH^+ (**93**, Scheme 20) while the ion at m/z 132 is assigned as $PhCHCHCHNH_2^+$ (**94**), and may be generated by the reaction between cinnamaldehyde and the ammonia present in the mobile phase. This assignment was further confirmed by comparing the retention time, and UV characteristic (287 nm) with that of standard cinnamaldehyde.

Figure 47. Mass Spectrum of M20

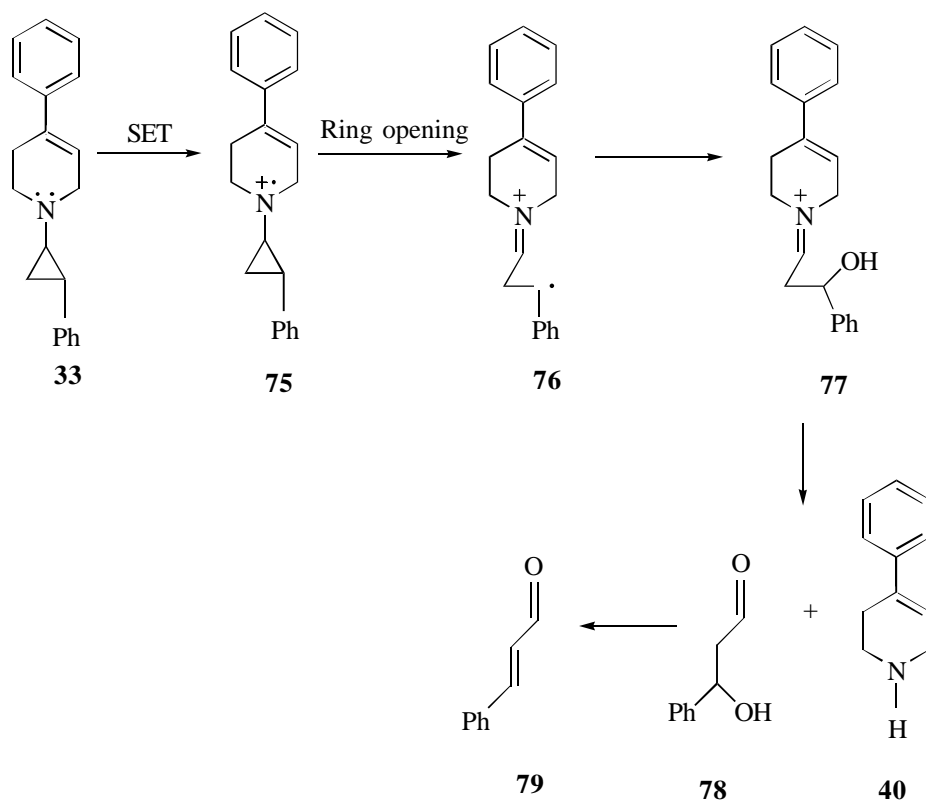


Scheme 20. The Fragmentation Generated from M20



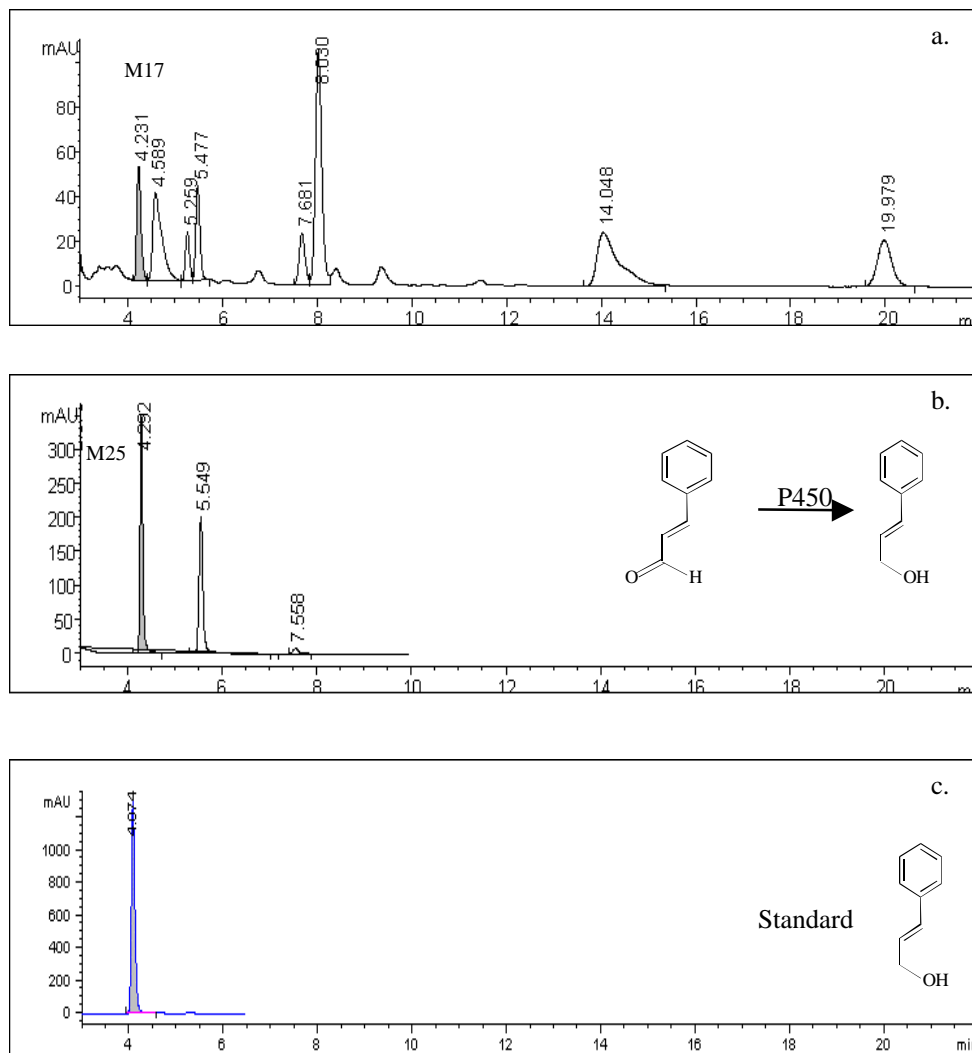
The mechanism proposed to account for the formation of cinnamaldehyde is depicted in Scheme 21. The catalytic pathway is proposed to proceed by an initial single electron transfer step from the lone pair of amine substrate **33** followed by cyclopropyl ring opening of the resulting aminyl radical cation **75** to form the reactive distonic carbon centered radical **76**. Subsequent free radical recombination yields **77** which undergoes further cleavage to form the N-decyclopropylated species **40** and the β -hydroxylaldehyde **78**. Compound **78** is unstable and undergoes dehydration to form cinnamaldehyde (**86**). This pathway accounts for both N-decycloproplation and cinnamaldehyde formation.

Scheme 21. A Catalyzed Pathway Proposed to Account for the Formation of Cinnamaldehyde



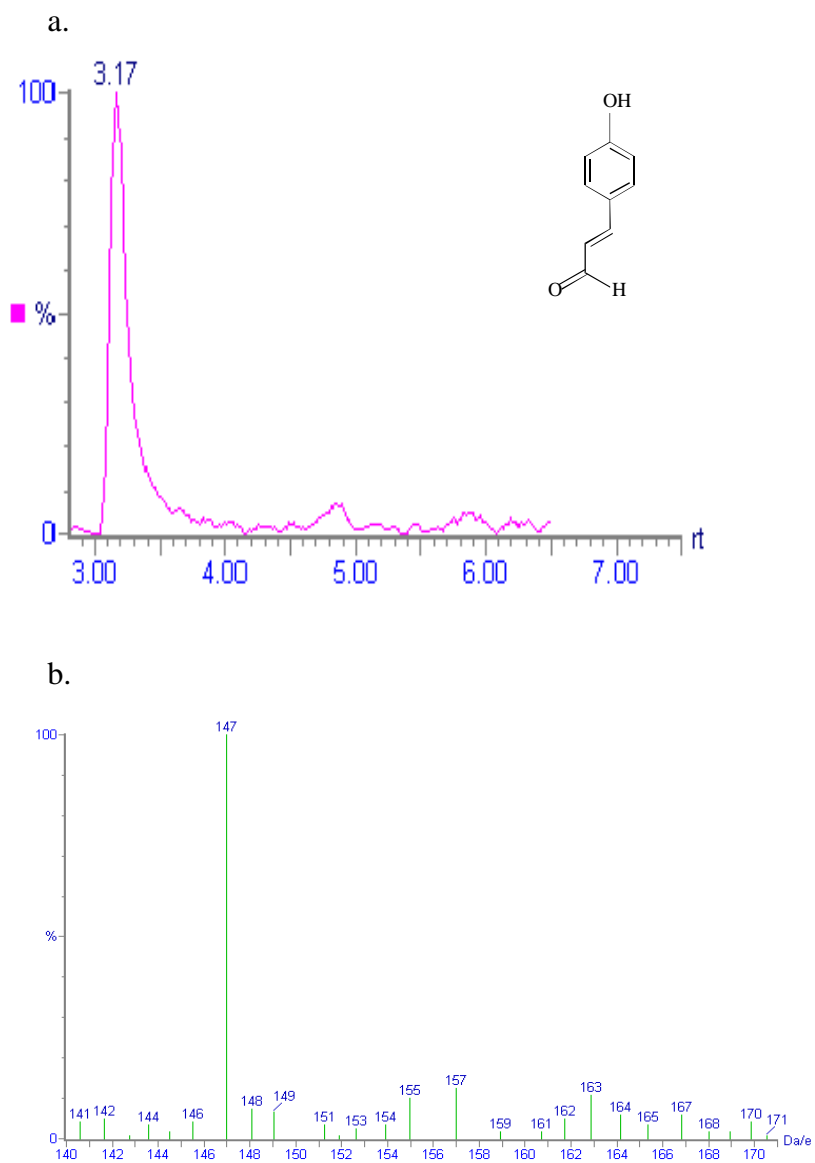
M17 eluted at 4.2 min and has a UV chromophore of 250 nm. Since a similar metabolite was not observed in CPTP and MCPTP, we suspected that this metabolite was associated with cinnamaldehyde. Cinnamic acid was tentatively assigned to M17. Comparison of HPLC-DA behavior of standard cinnamic acid with M17 eliminated this possibility. Neither its retention time (3.6 min) nor its UV chromophore (275 nm) was consistent with M17. Incubation of cinnamaldehyde with rat liver microsomes yielded a metabolite which had the same retention time and identical chromophore with M17 (Figure 48), suggesting that M17 is a product of cinnamaldehyde formed in a reaction catalyzed by liver microsomes. Reduction of cinnamaldehyde with NaBH₄ yielded cinnamyl alcohol (**95**). This compound has the same retention time and UV chromophore as those of M17, suggesting this structure for M17. M17 was fully confirmed as cinnamyl alcohol by its matched retention time and UV spectrum with those of the standard cinnamyl alcohol.

Figure 48. HPLC-DA Chromatograms of (a). Incubation Mixture of PCPTP, (b). Incubation Mixture of Cinnamaldehyde, (c), Authentic Cinnamyl Alcohol.

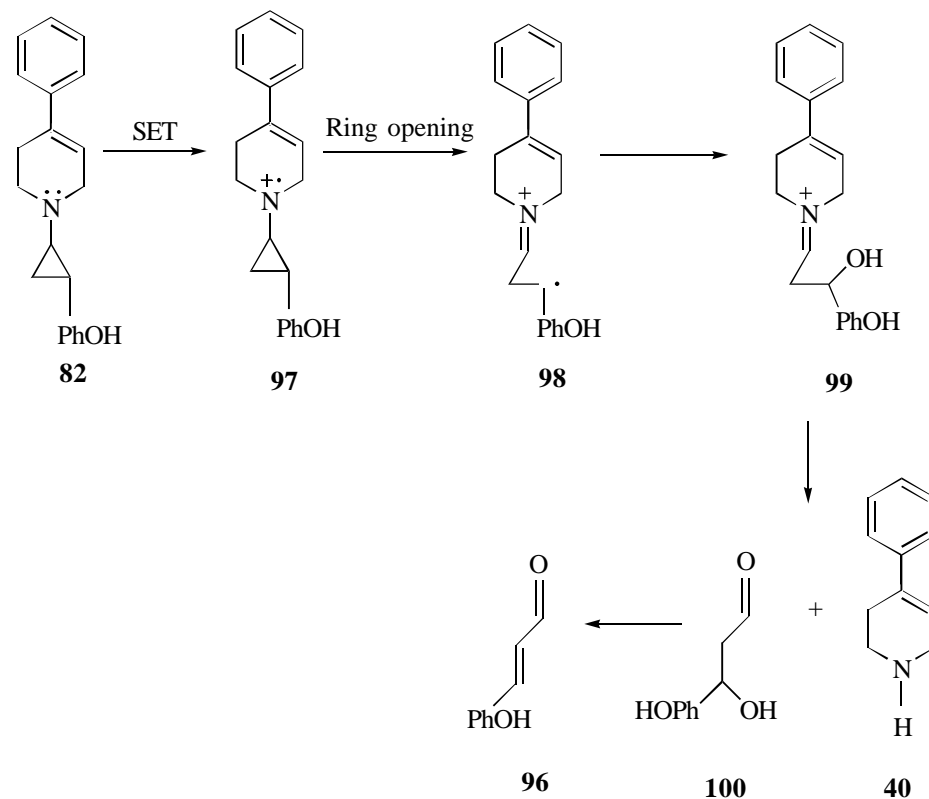


The distinctive UV chromophore at 325 nm (Figure 31) of M16 also is of considerable interest. Its long wavelength chromophore suggests a new metabolite associated with the ring opening pathway. It was first suspected to be *p*-hydroxycinnamaldehyde (**96**). Since LC-ESI/MS analysis in the positive ion mode didn't generate any molecular ion information about M16, LC-ESI/MS analysis in the negative ion mode was attempted. Searching for a base peak of negative ion TIC revealed an (M-H)⁻ of 147 (Figure 49). This mass matched with that of *p*-hydroxycinnamaldehyde. In order to identify this metabolite unambiguously, authentic *p*-hydroxycinnamaldehyde were synthesized in our lab by Mr. Sean Hislop. M16 had the identical retention time and UV chromophore as those of synthetic **96**. The route of the formation of **96** was first thought to be via the hydroxylation of cinnamaldehyde catalyzed by liver microsomes. But the absence of the peak at 3.5 min from LC-DA analysis of incubation mixtures of cinnamaldehyde suggests that this is not the actual pathway. This metabolite might be generated from **82** via the ring opening pathways. This alternative pathway, which is analogous to the pathway leading to form cinnamaldehyde, was proposed to account for the formation of *p*-hydroxycinnamaldehyde (Scheme 22).

Figure 49. Negative Ion Current Trace (a) and Mass Spectrum (b) of M16

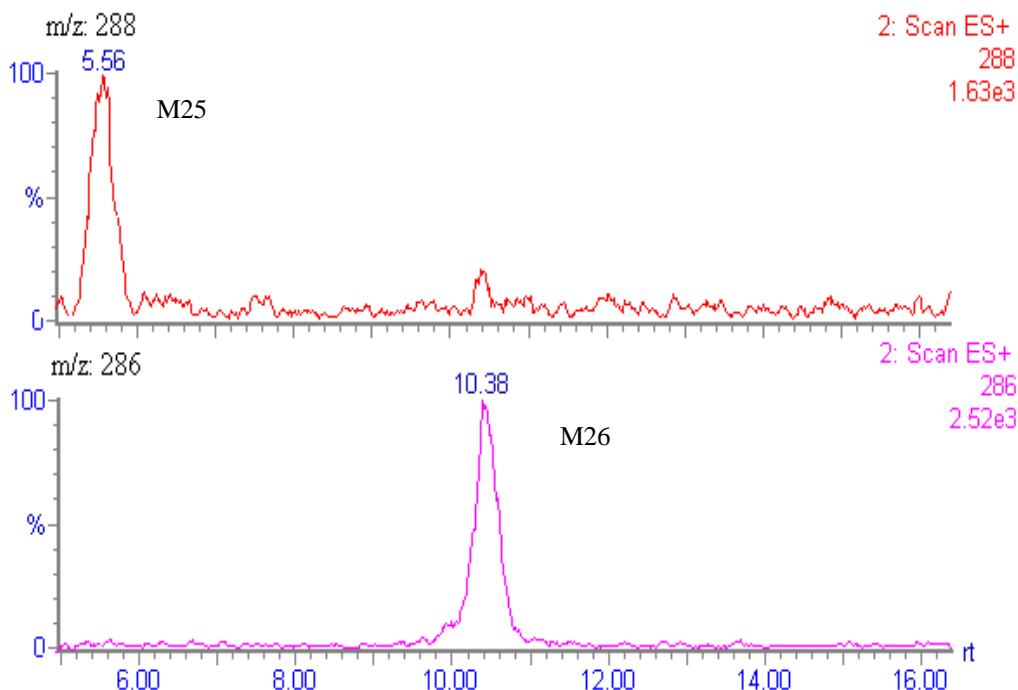


Scheme 22. A Catalyzed Pathway Proposed to Account for the Formation of *p*-Hydroxycinnamaldehyde



Searching the base peaks from the positive ion TIC also yielded two ions at m/z 288 and 286 (Figure 50) that are 12 and 10 amu higher than the parent substrate. These two metabolites are proposed to be the hydroxyl (**101**) and keto (**102**) species analogous to **52** and **53** generated from CPTP and **71** and **72** generated from MCPTP.

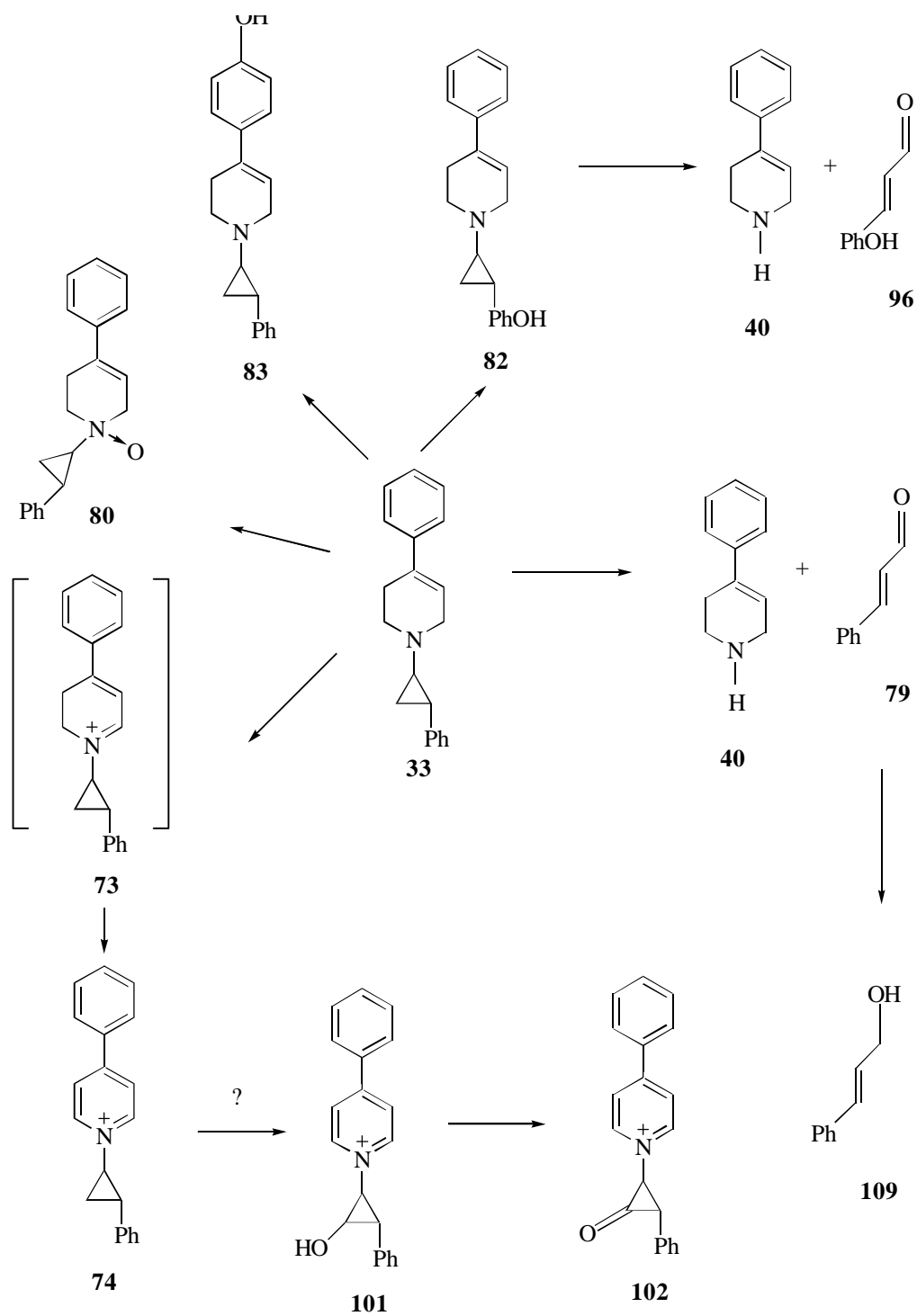
Figure 50. Reconstructed Ion Current Chromatograms of two Minor Metabolites M25 and M26



3.5.2. Conclusions

Incubation of CPTP with rat liver microsomes generated several metabolites with no evidence of significant inactivation. These metabolites were identified by using HPLC coupled with electrospray mass spectrometry and by HPLC equipped with diode array detection. Our results indicate that formation of these metabolites is NADPH dependent and cytochrome P450 mediated. The formation of the N-oxide metabolite might be mediated by FMO. The pathways of these biotransformations are depicted in Scheme 23. PCPTP undergoes four major pathways. 1). Hydroxylation to form hydroxyl products **82** and **83**; 2). N-oxidation to form N-oxide **80**; 3) ring opening to form N-despropyl metabolite **40** and cinnamaldehyde (**86**) and *p*-hydroxycinnamaldehyde (**96**); and 4). α -carbon oxidation to form the dihydropyridinim **73** and pyridinium species **74**. Compound **74** undergoes further hydroxylation to form **101** and oxidation of **101** leads to the keto metabolite **102**.

Scheme 23. Metabolic Pathway of Liver Microsomal Catalyzed Oxidation of PCPTP



Chapter 4. Metabolism of CPTP Derivatives Catalyzed by cDNA Expressed Forms of Human Hepatic Cytochrome P450

4.1. Introduction

Our previous studies on the rat liver microsomal catalyzed oxidation of CPTP and derivatives generated several metabolites, including the N-descyclopropyl, pyridinium, hydroxylated, and N-oxide metabolites. For the N-(2-phenylcyclopropyl) analog, the cyclopropyl ring opened product cinnamaldehyde was also identified. The NADPH dependence on the formation of these metabolites has shown that they are catalyzed by cytochrome P450. The cytochrome P450s form a superfamily of enzymes. Which form of the enzymes participating in these biotransformations is unknown. In order to get a better understanding about these metabolic pathways, the forms of the enzymes involved in these biotransformations were investigated next. For this purpose, we examined human cDNA expressed cytochrome P450s. In human liver, CYP3A4 and CYP2D6 are the most active forms. They are known to mediate a variety of substrate oxidations [51]. It has been reported that CYP2D6 is responsible for metabolizing MPTP to N-desmethyl MPTP and *p*-hydroxyphenyl-MPTP [91, 92]. CYP3A4 and CYP2A6 are reported to be involved in metabolizing the tetrahydropyridinyl moiety to the pyridinium species [93]. We anticipated that these three forms are the likely forms of the enzymes mediating the oxidation of CPTP and its derivative.

This study aims at identifying which particular P450 enzymes are responsible for metabolizing CPTP and its derivatives to the N-descyclopropyl metabolite and pyridinium metabolite. We are particularly interested to find out whether the two competing pathways are catalyzed by the same or different forms of the enzyme. We will discuss our results in the following paragraphs.

4.2. Experimental

Chemicals. CH₃CN (EM scientific, Gibbstown, NJ), CH₃OH, glacial CH₃COOH (Fisher Scientific, Fair Lawn, NJ), ammonium acetate (Fisher Scientific, Fair lawn, NJ) were HPLC grade. Mono and dibasic potassium phosphate (Fisher Scientific, Fair lawn, NJ), ethylenediamine tetraacetic acid (EDTA) (Sigma Chemical Co., St. Louis, MO),

MgCl₂ (Fisher Scientific, Fair Lawn, NJ), trisodium isocitrate (Sigma Chemical Co., St. Louis, MO), β-Nicotinamide adenine dinucleotide phosphate (NADP) (Sigma Chemical Co., St. Louis, MO) and isocitrate dehydrogenase (Sigma Chemical Co., St. Louis, MO) were purchased as indicated. CPTP, MCPTP and PCPTP were synthesized in our lab by Dr. Simon Kuttab.

Human CYP2A6, CYP2D6, CYP3A4 were purchased from Gentest Corp. (Woburn, MA). They were shipped on dry ice and stored in a freezer -70 °C until used.

Incubation of CPTP derivatives with human c-DNA expressed enzymes. Stock solution (25 mM in methanol) of CPTP, MCPTP, PCPTP, 50 mM pH 7.4 potassium phosphate buffer with 0.1 mM EDTA and 5 mM NADPH generating system (50 mM MgCl₂, 50 mM trisodium isocitrate, 5 mM NADP⁺, and 5 unit isocitrate dehydrogenase) were prepared. Typical incubations were conducted in a final volume of 0.5 mL 50 mM potassium phosphate buffer at 37 °C. The protein concentration for CYP2A6 and CYP2D6 were at 1 mg/mL and the protein concentration for CYP3A4 was at 0.76 mg/mL. A 5 μL aliquot of the substrate (25 mM) in methanol was added into the incubation mixtures to make a final concentration of 250 μM of each substrate. The reaction was initiated by addition of 50 μL of the NADPH generating system to maintain a steady state concentration of 0.5 mM NADPH in the incubation mixture. The reactions were quenched by adding an equal volume of acetonitrile. The resulting mixtures were centrifuged at 10,000g for 5 min. The supernatant (100 μL) was injected on the column for HPLC-DA analysis. Control incubations were conducted in the absence of the NADPH generating system. No evidence of metabolite formation was observed.

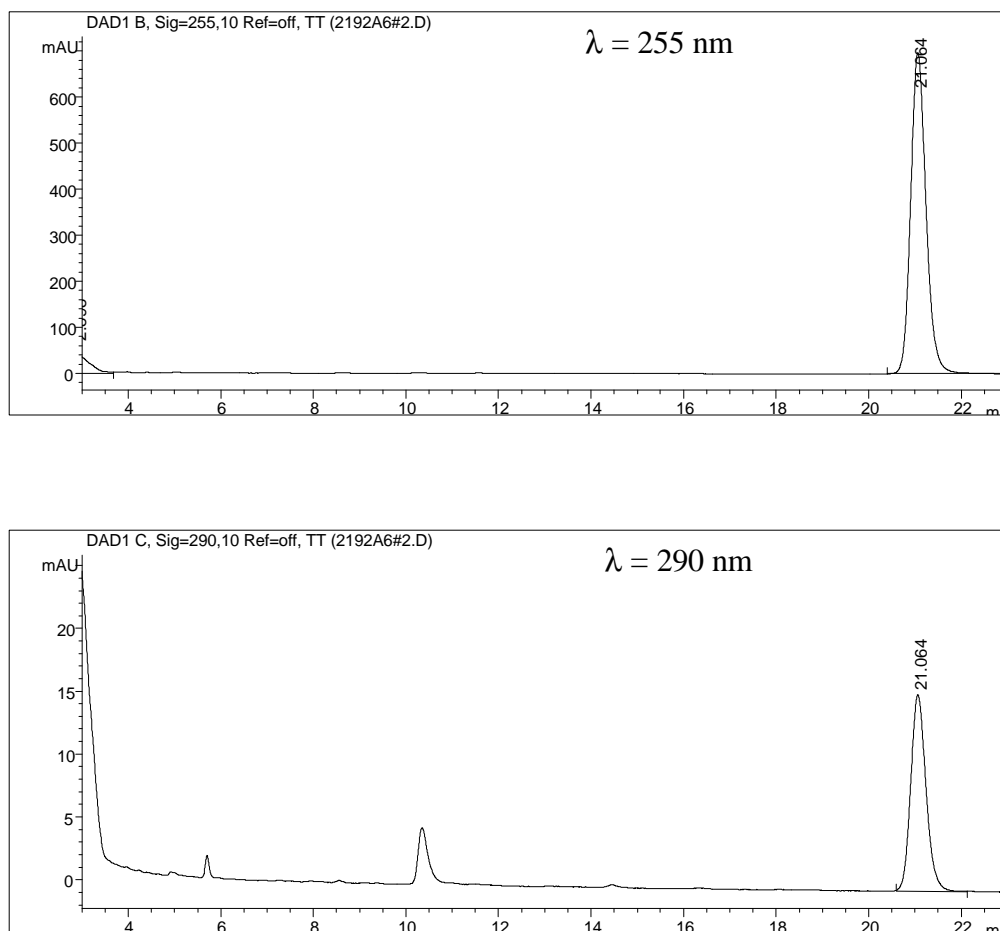
HPLC-DA assay. The HPLC-DA assays used in these studies were those described in the Experimental Section of Chapter 3. The same assays used to analyze the liver microsomal incubation mixtures were employed to analyze the incubation mixtures of PCPTP in the presence of CYP2A6, CYP2D6 or CYP3A4, and incubation mixtures of CPTP, MCPTP in the presence of CYP3A4.

4.3. Results

Since the incubation of PCPTP with the liver microsomal preparations generated more metabolites than incubations of either CPTP or MCPTP, PCPTP was used as a

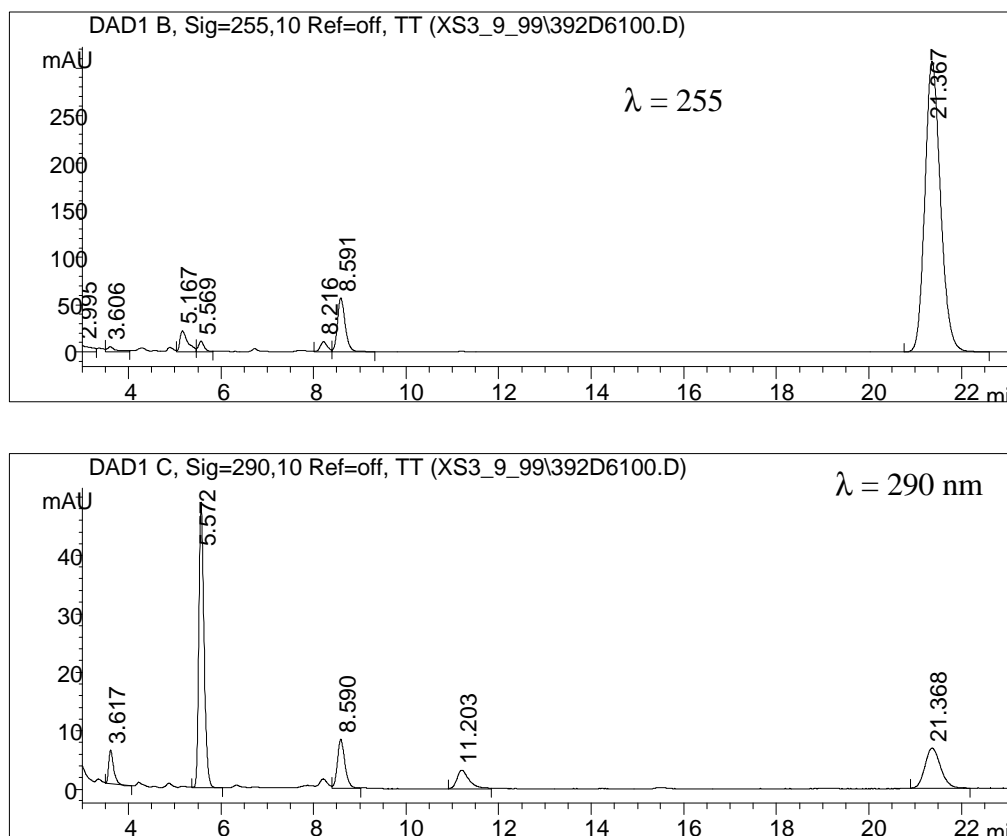
substrate to examine the three enzymes. Our first experiment was to incubate PCPTP with CYP2A6 in the presence and the absence of NADPH. For easy comparison, we used the same HPLC assay as we used to analyze the liver microsomal incubation mixture of PCPTP. Figure 51 displays the HPLC analysis of the incubation mixtures of PCPTP with CYP2A6 supplemented with NADPH. To our surprise, only two peaks appeared, one at 5.5 min and the other at 10.5 min. These small peaks were also observed in the control incubations and therefore are not likely to be metabolites.

Figure 51. HPLC-DA Chromatogram of Metabolic Fates of PCPTP by CYP2A6

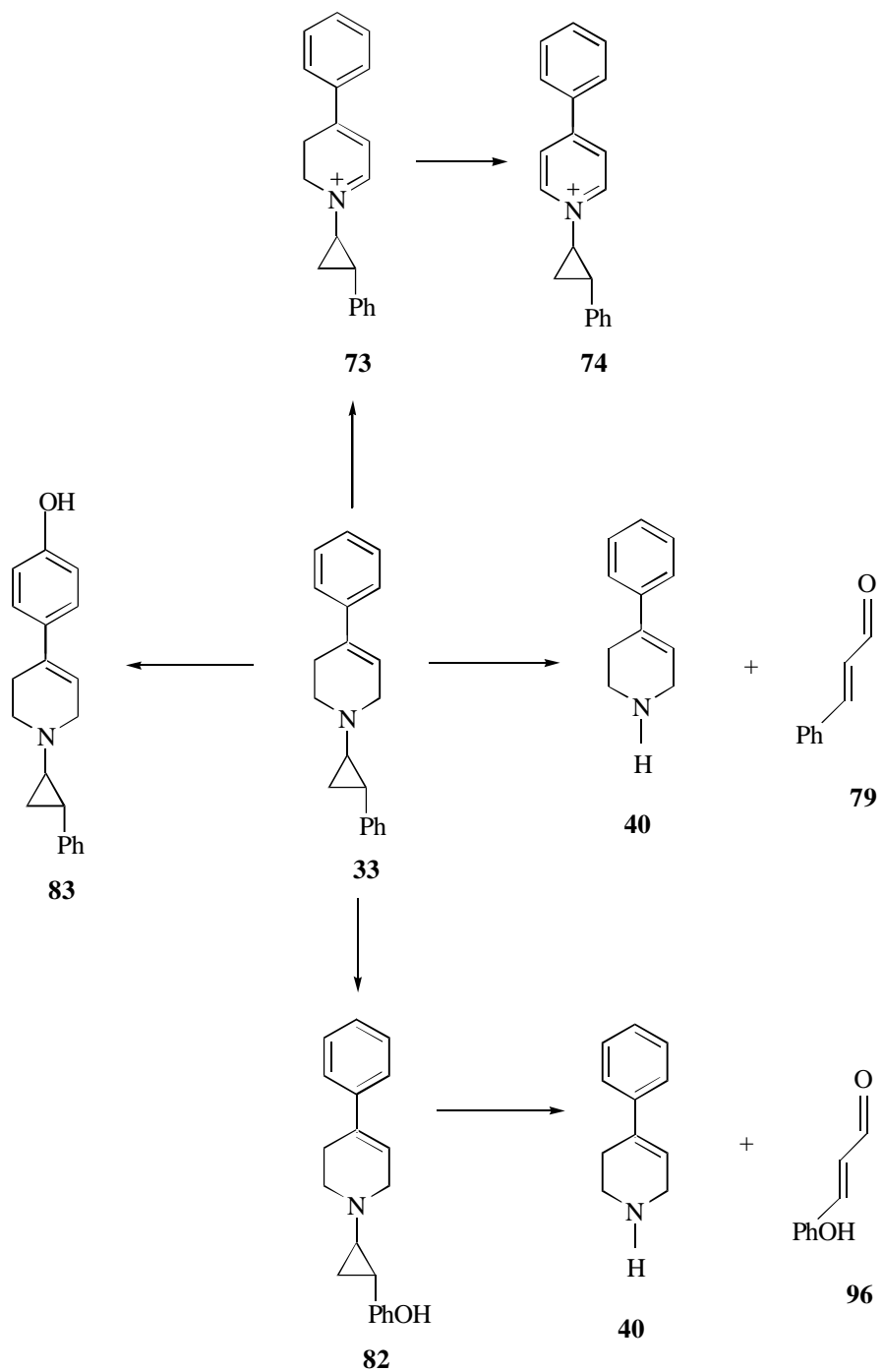


Incubation of PCPTP with CYP2D6 was attempted next. Metabolites were generated. Figure 52 displays the HPLC tracings with PCPTP incubated with CYP2D6 supplemented with NADPH. By comparing the retention times of the resulting metabolites with those of the PCPTP metabolites generated by liver microsomes, the peak eluting at 5.2 min was identified as N-descyclopropyl **40**, the peak eluting at 5.6 min was identified as cinnamaldehyde (**79**), the peak eluting at 3.6 min was identified as *p*-hydroxycinnamaldehyde (**96**), the peak eluting at 8.2 min was identified as the hydroxyl product **82**, the peak eluting at 8.6 min was identified as the hydroxyl product **83**, and the peak eluting at 11.2 min was identified as the pyridinium species **74**. Scheme 24 depicts the metabolic pathway catalyzed by CYP2D6. CYP2D6 is the form catalyzing both the α -carbon pathway leading to the pyridinium metabolite and the ring opening pathway leading to cinnamaldehyde and N-descyclopropylated metabolites.

Figure 52. HPLC-DA Chromatogram of Metabolic Fates of PCPTP by CYP2D6

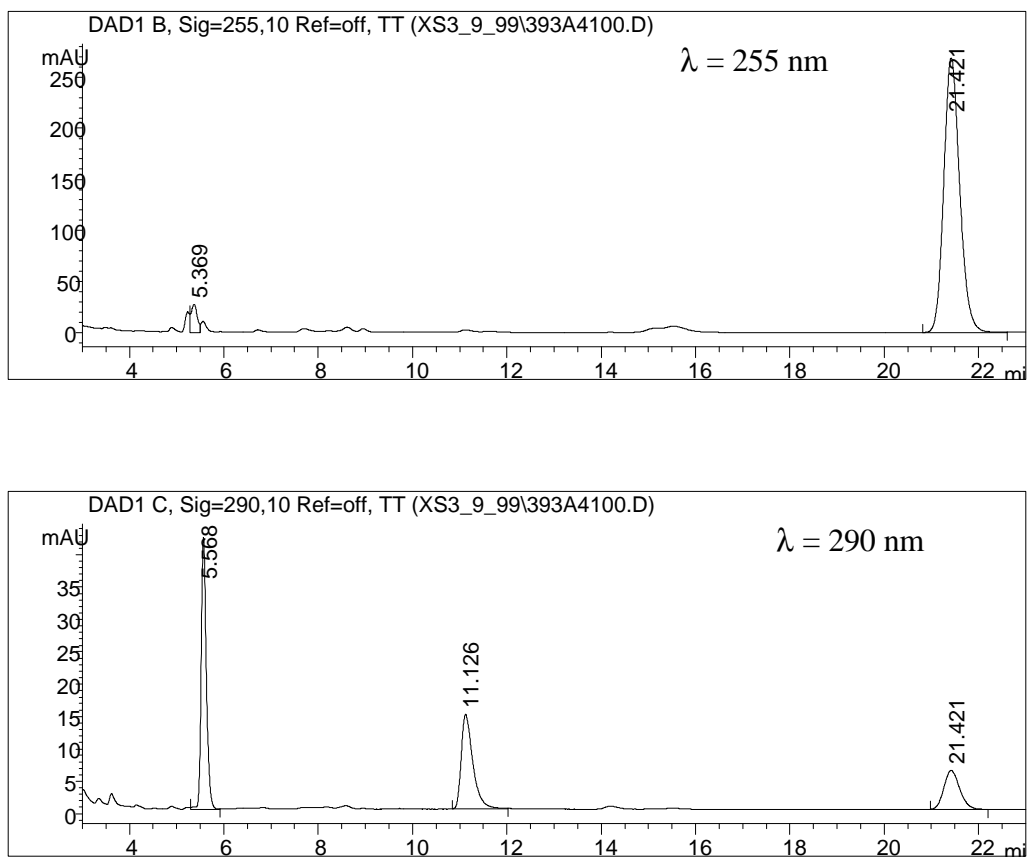


Scheme 24. Metabolic Pathway of PCPTP Catalyzed by CYP2D6

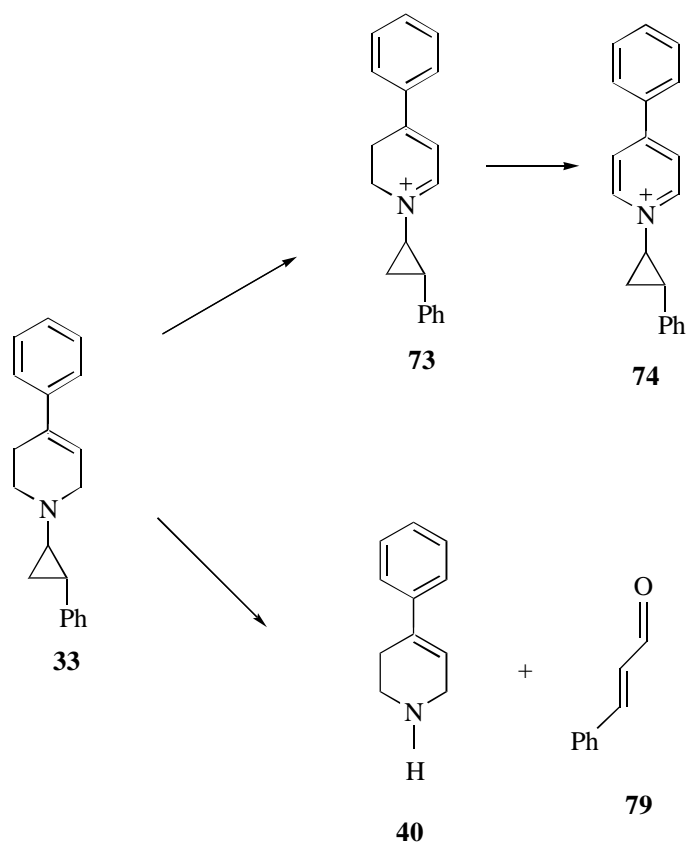


We next examined the metabolic fate of PCPTP incubated with CYP3A4 (Figure 53). The metabolic profile of PCPTP by CYP3A4 looks much simpler than that observed with CYP2D6. By comparison with the HPLC tracings of metabolites generated with liver microsomes, the peak eluting at 5.2 min was identified as N-descyclopropyl species **40**. The peak eluting at 5.5 min was identified as cinnamaldehyde (**79**). The peak eluting at 11.12 min was identified as pyridinium species **74**. Scheme 25 depicts the metabolic pathways catalyzed by CYP3A4.

Figure 53. HPLC-DA Chromatogram of Metabolic Fates of PCPTP by CYP3A4



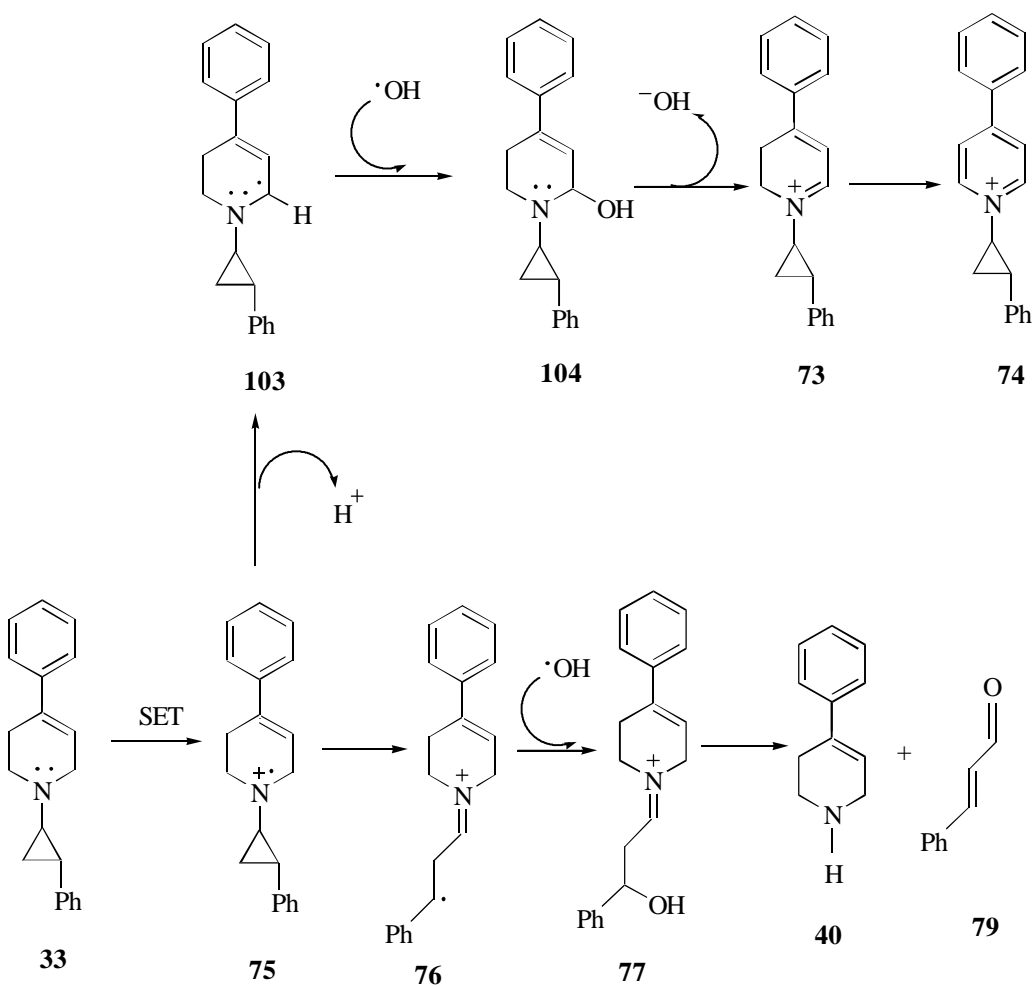
Scheme 25. Metabolic Pathway of PCPTP Catalyzed by CYP3A4



CYP3A4 also was involved in both the α -carbon oxidation and ring opening pathways. The ring opening pathway is generally thought to proceed via the SET generated cyclopropylaminyl radical cation **75**. The α -carbon oxidation pathway to form the dihydropyridinium species **73** can be proceeded via either SET or HAT. That both the α -carbon oxidation and N-despropylation are mediated by a single enzyme suggests they proceed through the same radical cation intermediate **75** generated by SET. This intermediate will partition between the α -carbon oxidation pathway leading to dihydropyridinium species **73** and the ring opening pathway leading to N-despropylated pyridine **40** and cinnamaldehyde (**79**) (Scheme 26). The amount of pyridium formed will be dependent on the result of the partitioning between these two pathways. Since the phenyl

substituent on the cyclopropyl ring will stabilize the ring opened radical cation **76** and favor the ring opening pathway, one would predict less pyridinium formation.

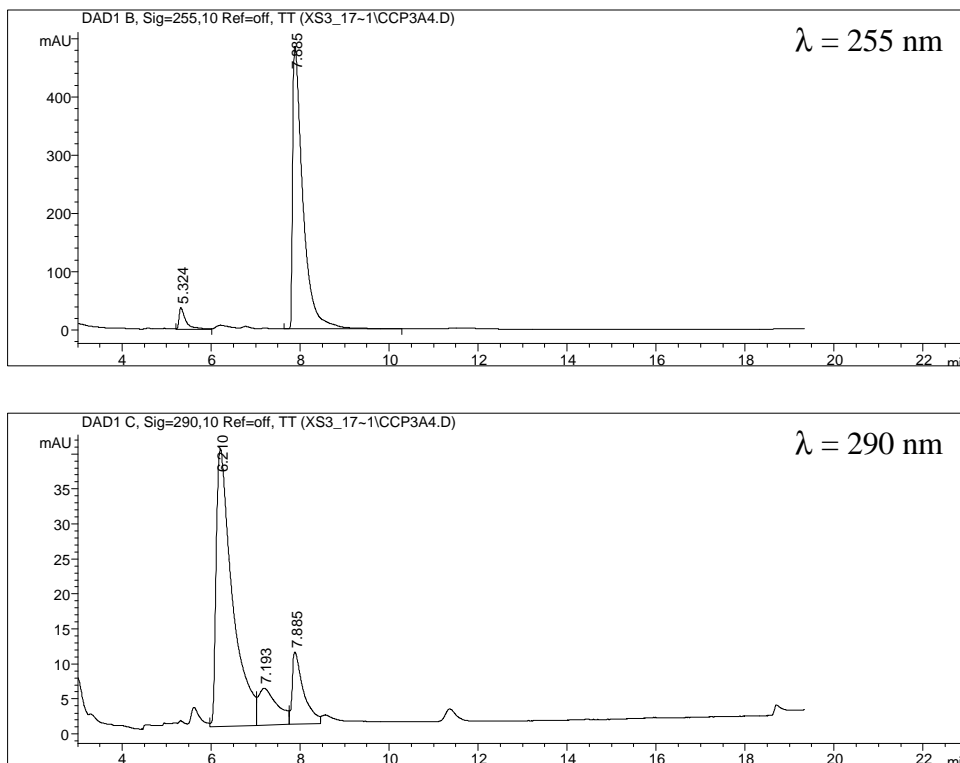
Scheme 26. Mechanism Proposed to Account for the α -carbon Oxidation and N-Descyclopropylation



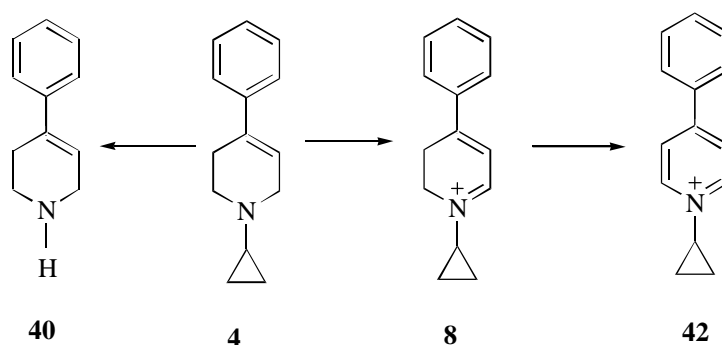
In order to determine the effect of the cyclopropyl substituent on the partitioning between the ring opening pathway and the α -carbon oxidation pathway, the metabolic fates of CPTP and MCPTP were also examined. Both pathways are catalyzed by CYP3A4 or CYP2D6. By simply comparing the chromatographic area of pyridinium species generated by CYP2D6 and CYP3A4, it was concluded that CYP3A4 produced more of the pyridinium than CYP2D6 did. For easy detection, CYP3A4 was incubated with CPTP and MCPTP to compare the yields of pyridinium metabolites generated for these two compounds.

HPLC-DA analysis of CPTP incubation mixture showed three major peaks which eluted at 5.3 min, 6.2 min and 7.9 min (Figure 54). The peak eluting at 5.3 min was identified as N-descyclopropyl **40**, and the peak eluting at 6.2 min was identified as the pyridinium species **42**. The peak eluting at 7.9 min was substrate CPTP. Scheme 27 depicts the metabolic pathway of CPTP generated by CYP3A4.

Figure 54. HPLC-DA Chromatogram of Metabolic Fates of CPTP by CYP3A4

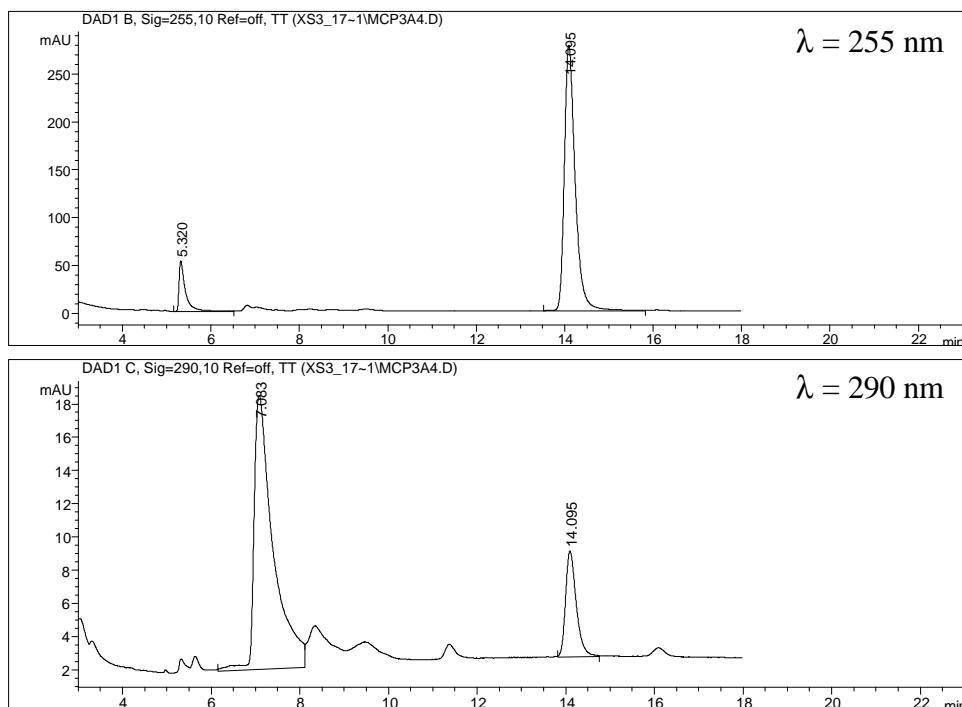


Scheme 27. Metabolic Pathway of CPTP Catalyzed by CYP3A4

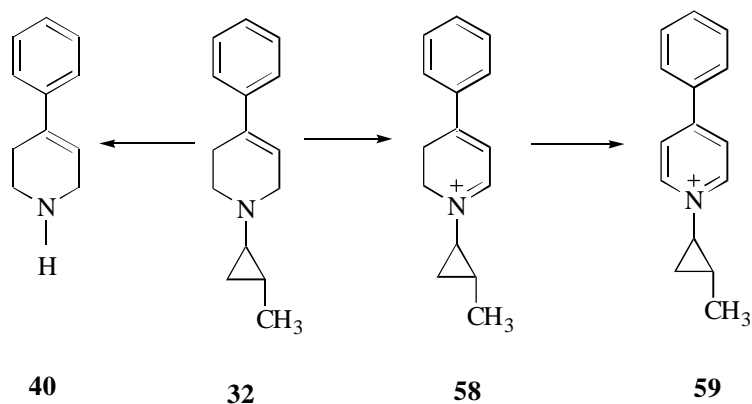


PLC-DA analysis of the MCPTP incubation mixture showed three major peaks at 5.3 min, 7.1 min and 14.1 min (Fig. 55). The peak eluting at 5.3 min was identified as N-descyclopropyl **40**, the peak at 7.1 min was identified as pyridinium species **59**, and the peak at 14.1 min was substrate MCPTP. Scheme 28 depicts the metabolic pathway of MCPTP generated by CYP3A4.

Figure 55. HPLC-DA Chromatogram of Metabolic Fates of MCPTP by CYP3A4

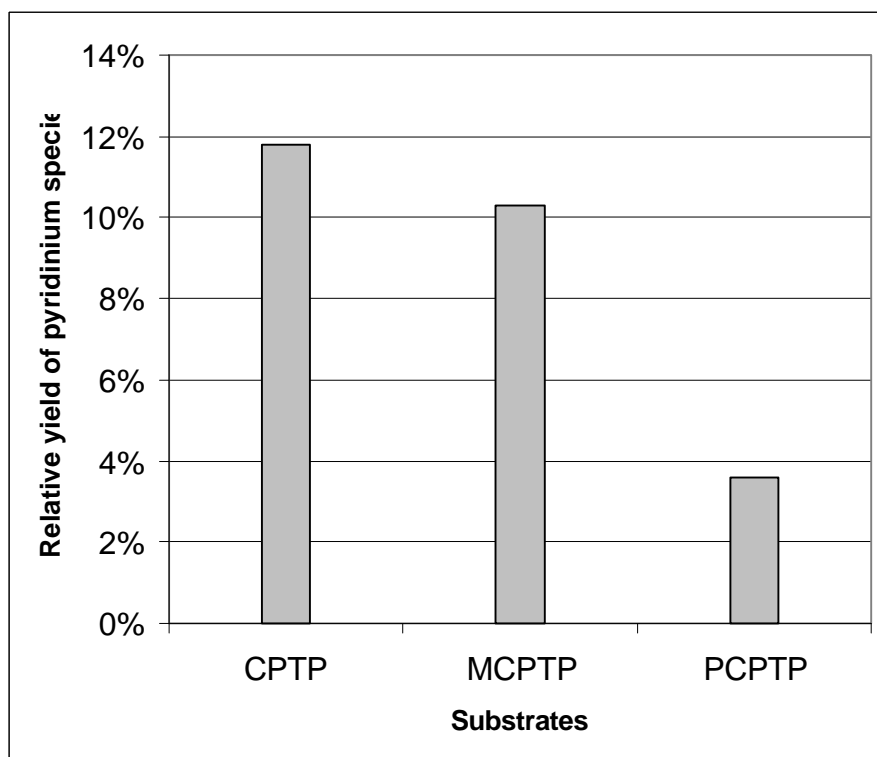


Scheme 28. Metabolic Pathway of CPTP Generated by CYP3A4



In order to estimate the influence of the cyclopropyl substituent on the fate of the putative cyclopropylamine radical cation, we compared the yields of the pyridinium species generated by the three substrates. Each substrate was incubated with CYP3A4 at the same concentration (250 μ M). The yields of the pyridinium species were roughly calculated by using the ratios of the chromatographic peak areas of pyridinium species over the corresponding substrates. Figure 56 displays the relative yields of pyridinium species generated from the three CPTP derivatives. We see from this plot that most pyridinium species are formed from CPTP (12.8%) and less from MCPTP (10.3%), and least from PCPTP (3.6%). The data are only semiquantitative. More accurate analysis involving actual rate measurement needs to be performed. The results, however, are consistent with the proposed partitioning of these cyclopropylaminy radical cations.

Figure 56. Comparison of the Pyridinium Metabolite Formation from CPTP and its Derivatives by CYP3A4



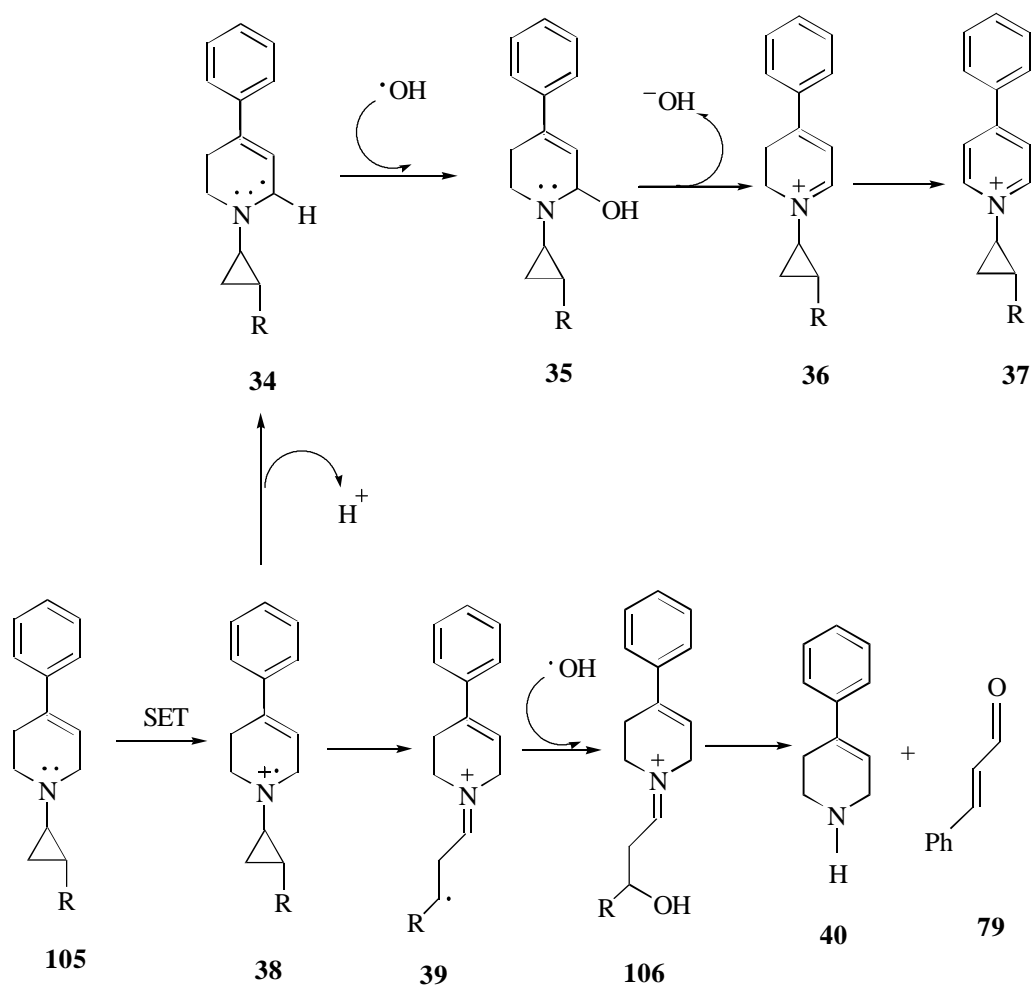
4.4. Conclusions

Incubation of CPTP and its derivatives with CYP2A6, CYP2D6, CYP3A4 has shown that CYP2A6 is not involved in this metabolism. CYP2D6 catalyzes the formation of the N-despropyl, pyridinium, cinnamaldehyde and hydroxylated products. CYP3A4 is responsible for the formation of the N-despropyl, pyridinium species and cinnamaldehyde but it does not mediate any hydroxylation reactions.

That both the α -carbon oxidation and N-despropylation were mediated by a single enzyme (either CYP2D6 or CYP3A4) suggests that they proceed through a common intermediate (**38**, scheme 26) generated by the SET pathway. This intermediate partitions between the α -carbon oxidation pathway, leading to dihydropyridinium species **36**, and the ring opening pathway, leading to N-despropyl **40** and aldehyde species **79** (Scheme 29). The phenyl substituent on the cyclopropyl ring stabilizes the ring opened radical cation **39** and favors the ring opening pathway. This results in less pyridinium

species while the proton and methyl groups on the 2-position favoring the α -carbon oxidation pathway, favoring the formation of dihydropyridinium species and subsequently, pyridinium species.

Scheme 29. Proposed Partitioning of the Cyclopyoaminyl Radical Cation



Chapter 5. Conclusions

Incubation of CPTP, MCPTP and PCPTP with rat liver microsomal preparations generated several metabolites with no evidence of significant inactivation. We developed HPLC and LC-ESI/MS methods to separate and characterize these metabolites. Our results indicate that the major biotransformation pathways of these CPTP derivatives proceed via: the following routes: 1) N-descyclopropylation to form PTP, 2) aromatic hydroxylation to form *p*-hydroxyphenyl metabolites, 3) N-oxidation to form N-oxide metabolites, and 4) ring α -carbon oxidation to form dihydropyridinium and pyridinium species. Besides these reactions, PCPTP and its *p*-hydroxyphenylcyclopropyl metabolite **82** also are biotransformed to cinnamaldehyde and *p*-hydroxycinnamaldehyde, respectively. The formation of these aldehyde species can be rationalized via a mechanism involving initial SET followed by ring opening pathway of the resulting cyclopropylaminyl radical cation. Although we don't have direct observation of ring opened metabolites from CPTP and MCPTP, the formation of N-descyclopropyl species in these cases can be rationalized via the same pathway. Since no significant inactivation of the enzyme catalyzing these reactions was observed, the distonic radical cation **39** generated via the ring opening pathway interacts differently with MAO-B and cytochrome P450. When interacting with MAO-B, it alkylates the active site and inactivates the enzyme. When interacting with cytochrome P450, it seems that this distonic radical cation does not bind with the active site of cytochrome P450. Instead it undergoes rapid free hydroxyl radical recombination to a carbinol intermediate. Hydrolytic cleavage of the iminium group generates the desmethyl compound and a β -hydroxyaldehyde that dehydrates to the corresponding cinnamaldehyde. The different fates of the reactive distonic radical cation intermediates may be accounted for by the competing radical recombination chemistry but also may reflect different orientations within the active sites of the two enzymes.

Our studies on the CPTP and derivatives with human cDNA expressed cytochrome P450s have shown that the α -carbon oxidation pathway and the pathway leading to N-descyclopropylation are catalyzed by a single enzyme (either CYP3A4 or CYP2D6). This suggest that the two pathways might proceed via a common intermediate.

We propose this common intermediate to be the cyclopropylaminyl radical cation **38** generated by the SET pathway. The intermediate then partitions between the α -carbon oxidation pathway and the ring opening pathway.

The comparative studies on pyridinium formation generated from the three CPTP derivatives have shown that the most pyridinium species is formed from CPTP (12.8%), with intermediate amounts from MCPTP (10.3%) and the least amount from PCPTP (3.6%). These results are consistent with the cyclopropylaminyl radical cation intermediate partitioning between the α -carbon oxidation and the ring opening pathways. The phenyl substituent on the cyclopropyl ring stabilizes the ring opened radical cation **39** and favors the ring opening pathway resulting in the formation of less pyridinium species. The proton and methyl substituent on the cyclopropyl ring favor will stabilize the ring opened radical cation less and therefore favor the pyridinium formation less. On the other hand, the possibility that the α -carbon oxidation may proceed via the HAT pathway cannot be ruled out at this time. But in this case, the partitioning would have to take place at the initial oxidation step--hydrogen atom transfer leading to the dihydropyridinium and pyridinium metabolite formation and single electron transfer leading to the decyclopropylation and the formation of the desmethyl metabolite.

Chapter 6. References

1. Montastruc, J. L., Llan, M. E., Rascol, O., Senard, J. M. Drug induced parkinsonism: a review. *Fundam. Clin. Pharmacol.* **8**, 293-306, 1994.
2. Ehringer, H., Hornykiewicz, O. Verteilung Von Noradrenalin und Dopamin (3-Hydroxytryamin) in Gehirn des Menschen und ihr Verhalten bei Erkrankungen des extrapyramidalen System. *Klin. Wochenschr.* **38**, 1236-1239, 1960.
3. Kurland L. T., Kurtzke, J. F., Goldberg, I. D., Choi N. W., Williams, G. Parkinsonism. In: *Epidemiology of neurologic and sense organ disorders*. Cambridge: Harvard University Press, 1973.
4. Tanner C. M., Langston J. W. Do environmental toxins cause Parkinson's disease? A critical review. *Neurology* **40** (10, suppl 3): 17-30, 1990.
5. Langston, J. W., Ballard, P., Tetrud, J. W., and Irwin, I. Chronic Parkinsonism in humans due to a product of meperidine-analogy synthesis. *Science* (Washington D. C.), **219**, 979-980, 1983.
6. Sanchez-Romos, J., Barrett, J. N., Gioldstein, M., Weiner, W. J., Hefti, F., 1-Methyl-4-phenylpyrdinium (MPP+) but not 1-methyl-4-phenyl-1,2,3,6-tetrahydropyridine (MPTP) selectively destroys dopaminergic neurons in cultures of dissociated rat mesencephalic neurons. *Neurosci. Lett.* **72**, 215-220, 1986.
7. Langston, J. W., Irwin, I., Langston, E. B. and Forno, L. S., Perglyline prevents MPTP-induced parkinsonism in primates. *Science* (Washington D. C.) **225**, 1480-1482, 1984.
8. Heikkila R. E., and Manzino, L., Behavioral properties of GBR 12,909, GBR 13,098: Specific inhibitors of dopamine uptake. *Eur. J. Pharmacol.* **103**, 241-248, 1984.
9. Markey, S. P., Johannessen, J. N., Chiueh, C. C., Burns, R. S. and Herkenham, M. A., Intraneuronal generation of a pyridinium metabolite may cause drug-induced Parkinsonism. *Nature (London)* **311**, 464-467, 1984.
10. Chiba, K., Peterson, L.A.; Castagnoli, K., Trevor, A. J., Castagnoli, N., Jr. Studies on the molecular mechanism of bioactivation of the selective nigrostriatal neurotoxin 1-methyl-4-phenyl-1,2,3,6-tetrahydropyridine. *Drug Metab. Dispo.*, **13**, 342-347, 1985.

11. Trevor, A. J., Castagnoli, N. Jr., Singer, T. P. The formation of reactive intermediates in the MAO-catalyzed oxidation of the nigrostriatal toxin 1-methyl-4-phenyl-1,2,3,6-tetrahydropyridine. *Toxicology*, **49**, 513-519, 1988.
12. Peterson, L. A., Caldera, P. S., Trevor, A. J., Chiba, K., Castagnoli, N. Jr. Studies on the 1-methyl-4-phenyl-1,2,3,6-tetrahydropyridine species 2,3-MPDP⁺, the monoamine oxidase catalyzed oxidation product of the nigrostriatal toxin 1-methyl-4-phenyl-1,2,3,6-tetrahydropyridine. *J. Med. Chem.* **28**, 1432-1436, 1985.
13. Langston, J. W., Irwin, I., Langston, E. B., Forno, L. S., 1-methyl-4-phenylpyridinium ion (MPP⁺): identification of a metabolite of MPTP, a toxin selective to the substantia nigra. *Neurosci. Lett.* **48**, 87-92, 1984.
14. Castagnoli, N., Jr., Chiba, K., Trevor, A. J., Potential bioactivation pathways for the neurotoxin 1-methyl-4-phenyl-1,2,3,6-tetrahydropyridine (MPTP). *Life Sci.*, **36**, 225-230, 1985.
15. Trevor, A. J., Castagnoli, N., Jr., Caldera, P. S., Ramsay, R. R., Singer, T. P. Bioactivation of MPTP: reactive metabolites and possible biochemical sequelae. *Life Sci.*, **40**, 713, 1987.
16. Javitch J. A., D'Amata, R. J., Strittmatter, S. M., Snyder, S. H. Parkinsonism-inducing neurotoxin 1-methyl-4-phenyl-1,2,3,6-tetrahydropyridine: uptake of the metabolite N-methylpyridine by dopaminergic neurons explains selective toxicity. *Proc. Natl. Acad. Sci. U.S.A.* **82**, 2173-2177, 1985.
17. Chiba, K., Trevor, A. J., Castagnoli, N., Jr. Active uptake of MPP⁺, a metabolite of MPTP by brain synaptosomes. *Biochem. Biophys. Res. Commun.*, **128**, 1228-1232, 1985.
18. Ramsay, R. R., Salach, J. I., Singer, T. P. Uptake of the neurotoxin 1-methyl-4-phenylpyridine by mitochondria and its relation to the inhibition of the mitochondrial oxidation of NAD⁺-linked substrates by MPP⁺. *Biochem. Biophys. Res. Commun.* **134**, 743-748, 1986.
19. Silverman, R. B., Zieske, P. A. Mechanism of inactivation of monoamine oxidase by 1-phenylcyclopropylamine. *Biochemistry*, **24**, 2128-2138, 1985.
20. Silverman, R. B. Radical ideals about monoamine oxidase. *Acc. Chem. Res.* **28**, 335-342, 1995.

21. Hall, L., Murray, S., Castagnoli, N., Jr. Studies on 1,2,3,6-tetrahydropyridine derivatives as potential monoamine oxidase inactivators. *Chem. Res. Toxicol.*, **5**, 625-633-1992.
22. Yamasaki, R. B., Silverman, R. B. Mechanism for reactivation of N-cyclopropylbenzylamine-inactivated monoamine oxidase by amines. *Biochemistry*, **24**, 6543-6550, 1985.
23. Musa, O. M., Horner, J. H., Shahin, H., Newcomb, M. A kinetic scale for dealkylaminy radical reactions. *J. Amer. chem. Soc.*, **118**, 3862-3868, 1996.
24. Rinne, U. K. *J. Neural Trans.*, **25** (Suppl.), 149-155, 1987.
25. Tetrud, V. W., Langston, J. W. The effect of deprenyl (selegiline) on the natural history of Parkinson's disease. *Science*, **245**, 519-522, 1989.
26. Guengerich, F. P., Okazaki, O., Seto Y., MacDonald T. L. Radical cation intermediates in N-dealkylation reactions. *Xenobiotica* **25**, 689-709, 1995.
27. Karki, S. B., Dinnocenzo, J. P. On Mechanism of amine oxidations by P450. *Xenobiotica* **25**, 711-724, 1995.
28. Guengerich, F. P., Yun, C. H., MacDonald, T. L. *J. Biol. Chem.* 271, 27321-27329, 1996.
29. Hanzlik, R. P.; Tullman, R. H. *J. Amer. Chem. Soc.* **104**, 2048-2050, 1982.
30. Macdonald, T. L.; Zirvi, K.; Burka, L. T.; Peyman, P.; Guengerich, F. P. *J. Amer. Chem. Soc.* , **104**, 2050-2052, 1982;
31. Guengerich, F. P.; Willard, R. J.; Shea, J. P.; Richards, L. E.; Macdonald, T. L. *J. Amer. Chem. Soc.* **106**, 6446-6447, 1984;
32. Bondon, A.; Macdonald, T. L.; Harris, T. M.; Guengerich, F. P. *J. Biol. Chem.* **264**, 1988-1997, 1989.
33. Zhao, Z., Mabic S., Kuttab S., Franot, C., Castagnoli, K., Castagnoli, N. Jr. Rat liver microsomal enzyme catalyzed oxidation of 1-cyclopropyl-4-phenyl-1,2,3,6-tetrahydropyridine *Bioorg. Med. Chem.*, **6**, 2531-2539, 1998.
34. Miller, E. C., Miller, J. A., 1966, Mechanism of Chemical carcinogenesis: nature of proximate carcinogen and interactions with macromolecules. *Pharmacol. Rev.* **18**, 805-838, 1966.

35. Weisburger, J. H., Yamamoto, R. S., Williams, G. M., Grantham, P. H., Matsushima, T., Weisburger, E. K. On the sulfate ester of N-hydroxy-N-2-fluorenylacetamide as a key ultimate hepatocarcinogen in the rat. *Cancer Res.*, **32**, 491-500, 1972.
36. Guengerich, F. P., Oxidation of toxic and carcinogenic chemicals by human cytochrome P450 enzymes. *Chem. Res. Toxicol.* **4**, 391-401, 1991.
37. Gibson, G., Skett, P. *Introduction to Drug Metabolism*. Chapman and Hall, 1-38, 1986.
38. Hogeboom, G. H., Schneider, W. C., *Nature*, **166**, 302, 1950.
39. Phillips, A. H., Langdon, R. G., *J. Biol. Chem.*, **237**, 2652, 1962.
40. Masters, B. S., Kamin, H., Gibson, Q. H., Williams, C. H., *J. Biol. Chem.*, **240**, 921, 1965.
41. Kingenber, *Arch. Biochem. Biophys.* **75**, 376, 1958.
42. Garfinkel, D., *Arch. Biochem. Biophys.* **77**, 493, 1958.
43. Strittmatter, P., Velick, *J. Biol. Chem.*, **221**, 227, 1956.
44. Garfinkel, D., *Arch. Biochem. Biophys.* **71**, 111, 1957.
45. Strittmatter, P., Ball, E. G. *Proc. U. S. Natl. Acad. Sci.* **38**, 19, 1952.
46. Strittmatter, P., Ball, E. G. *J. Cell. Physiol.* **43**, 57, 1954.
47. Chance, B., Williams, G. R. *J. Biol. Chem.* **209**, 945, 1954.
48. Guengerich, F. P., *Mammalian Cytochromes P450*, Vols. **1** and **2**, CRC press, Boca Raton, Florida, 1987.
49. Nelson, D. R., kamataki, T., waxman, D. J., Guengerich, F. P., Estabrook, R. W., Feyereisen, R., Gonzales, F., J., Coon, M. J., Gunsalus, I. C., Gotoh, O., Okuda, K., Nebert, D., W. The P450 superfamily: Update on new sequences, gene mapping, accession numbers, early trivial names of enzymes, and nomenclature. *DNA Cell Biol.* **12**, 1-51, 1993.
50. Gonzales, F. J. Human cytochromes P450: problems and prospects. *Trends Pharmacol. Sci.* **13**, 346-352, 1994.
51. Guengerich, F. P. Catalytic selectivity of human cytochrome P450 enzymes: relevance to drug metabolism and toxicity. *Toxicol. Lett.* **70**, 133-138, 1994.

52. Halpert, J. R., Guengerich, F. P., Bend, J. R., Correia, M. A. Contemporary issues in toxicology. Selective inhibitors of cytochrome P450. *Toxicol. Appl. Pharmacol.* **125**, 163-175, 1994.
53. Guengerich, F. P. Analysis and characterization of enzymes. *In principles and Methods of Toxicology*, Chap. 35 (Hayes, W. Ed.), pp. 1259-1313. Raven Press, Ltd. New York, 1994.
54. Cooper, D., Schleyer, H., Rosenthal, O. Chemistry of cytochrome P450 purified from endocrine systems. *Drug Metab. Dispos.* **1**, 21-28, 1973.
55. Bend, J., Hook, G., Gram, T. Characterization of lung microsomes as related to drug metabolism. *Drug Metab. Dispos.* **1**, 358-367, 1973.
56. Mukhtar, H., Khan, W. A. Cutaneous cytochromes P450. *Drug Metab. Rev.* **20**, 657-673, 1989.
57. Orrenius, S., Ellin, A., Jakonsson, S., Thor, H., Cinti, D., Schenkman, J., Estabrook, R. The cytochromes P450 containing monooxygenase system of rat kidney cortex microsomes. *Drug Metab. Dispos.* **1**, 350-357, 1973.
58. Vessey, D. Hepatic metabolism of drugs and toxins. *In Hepatology*, Philadelphia, pp. 197-230, 1982.
59. Guengerich, F. P., Cytochromes P450 enzymes and drug metabolism. In *Progress in Drug Metabolism*, Vol. **10**, Chap. 1 (Bridges, J. W., Chasseaud, L. F., Gibson, G. G., Eds.) pp. 1-54. Taylor & Francis, London, 1987.
60. White, R. E., Coon, M. J., *Annu. Rev. Biochem.*, **49**, 315, 1980.
61. Ullrich, V., *Top. Current Chem.*, **83**, 67, 1979.
62. Sato, R., Omura, "Cytochrome P450", Academic Press, New York, 1978.
63. Guengerich, F. P., *Biochemistry*, **22**, 2811, 1983.
64. Guengerich, F. P., MacDonald, T. L., Chemical Mechanisms of Catalysis by Cytochromes P450: A Unified View. *Acc. Chem. Res.* **17**, 16-22, 1984.
65. Guengerich, F. P. *J. Biol. Chem.*, **253**, 7931, 1978.
66. Guengerich, F. P., Ballou, D. P., Coon, M. J., *J. Biol. Chem.*, **252**, 4431, 1977.
67. Peterson, J. A., White, R. E., Yasukochi, Y., Coomes, M. L., O'Keefe, D. H., Ebel, R. E., Masters, B. S., Ballou, D. P., Coon, M. J., *J. Biol. Chem.*, **252**, 4431, 1977.

68. Guengerich, F. P., Ballou, D. P., Coon, M. J., *Biochem., Biophys. Res. Commun.*, **70**, 951, 1976.
69. Bonfils, C., Balny, Maurel, P., *J. Biol. Chem.*, **256**, 9457, 1981.
70. Hildebrandt, A., Estabrook, R. W., *Arch. Biochem. Biophys.*, **143**, 66
71. McMahon, R. E., Microsomal dealkylation of drugs. *J. Pharmaceut. Sci.* **55**, 457-466, 1966.
72. Smith, D. A., Jones, B. C., Speculation on the substrate structure-activity relationship (SSAR) of cytochrome P450 enzymes. *Biochem. Pharmacol.*, **44**, 2089, 1992.
73. Guengerich, F. P. Reaction and Significance of cytochrome P450 enzymes. *J. Biol. Chem.*, **266**, 10019-10022, 1991.
74. Seto, Y., Guengerich, F. P. Partitioning between N-dealkylation and N-oxygenation in the oxidation of N,N-dialkylarylamines catalyzed by cytochromes P450 2B1. *J. Biol. Chem.*, **266**, 9986-9997, 1993.
75. Dunford, H. B., *Xenobiotics*, **25**, 725-733, 1995.
76. Everse, J. Everse, K. E., Grisham, M. B. (eds) *Peroxidase in Chemistry and Biochemistry*, Vols. I and II., CRC Press, Boca Raton, FL.
77. Ortiz de Montellano, P. R., in *Cytochrome P450: Structure, Mechanism, and Biochemistry* (Ortiz de Montellano, P. R., ed) 2Ed., pp. 245-303, 1995.
78. McMahon, R. E., Culp, H. W., Occolowitz, J. C. Studies on the hepatic microsomal N-dealkylation reaction: molecular oxygen as the source of the oxygen atom. *J. Amer. Chem. Soc.*, **91**, 3389-3390, 1969.
79. Narisada, M., Yoshida, T., Onoue, H., Ohtani, M., Okada, T., Tsuji, T., Kikkawa, I., Haga, N., Satoh, H., Itani, H., Nagata, W. Cyclopropylamines as suicide substrates for cytochromes P450, *J. Med. Chem.*, **22**, 759-760, 1979.
80. Hanzlik, R. P., Tullman, R. H. Suicide inactivation of cytochrome P450 by cyclopropylamines. Evidence for cation-radical intermediates, *J. Amer. Chem. Soc.*, **104**, 2048-2050, 1982.
81. Macdonald, T., Zirvi, K., Burka, L. T., Peyman, P., Guengerich, F. P. Mechanism of cytochrome P450 inhibition by cyclopropylamines, *J. Amer. Chem. Soc.*, **104**, 2050
82. Bruins, A. P. " Atomespheric-pressure-ionization mass spectrometry II. Applications in Pharmacy, Biochemistry and General Chemistry", *Trends Anal. Chem.* **13**, 2, 1994.

83. Gelpi, E. "Biomedical and biochemical applications of liquid chromatography-mass spectrometry", *J. Chromatogr. A*, **703**, 59-80, 1995.
84. Castagnoli, N., Jr., Chiba, K., Trevor, A. J., Potential bioactivation pathways for the neurotoxin 1-methyl-4-phenyl-1,2,3,6-tetrahydropyridine (MPTP). *Life Sci.*, **36**, 225-230, 1985.
85. Chiba, K., Trevor, A. J., and Castagnoli, N., Jr., Metabolism of the neurotoxic tertiary amine, MPTP, by brain monoamine oxidase. *Biochem. Biophys. Res. Commun.*, **120**, 574-578, 1984.
86. Castagnoli, N., Jr., Chiba, K. and Trevor, A. J., Potential bioactivation pathways for the neurotoxin 1-methyl-4-phenyl-1,2,3,6-tetrahydropyridine (MPTP). *Life Sci.*, **36**, 225-230, 1985.
87. Shinka T. N., Castagnoli, N. Jr., Wu, E. Y., Hoag, K. P., Trevor, A. J., Cation-exchange high performance assay for the nigrostriatal toxicant 1-methyl-4-phenyl-1,2,3,6-tetrahydropyridine and its monoamine oxidase generated metabolites in brain tissues, *J. Chromatogr.*, **398**, 279-287, 1987.
88. Wu, E., Shinka, T., Caldera-Munoz, P., Yoshizumi, H., Trevor, A., Castagnoli, N., Jr., Metabolic studies on the nigrostriatal toxin MPTP and its MAO B generated dihydropyridinium metabolite MPDP⁺. *Chem. Res. Toxicol.*, **1**, 186-194, 1988.
89. Zhiyang Zhao reported that the presence of the dihydropyridinium species in the light of the results that LC-DA analysis of incubation mixture at $t < 15$ min revealed a peak with the same retention time and UV spectrum (345 nm) as those observed with the synthetic standard.
90. Kuttub, S., Shang, J. X., Castagnoli, N., Jr., manuscript in preparation.
91. Narimatsu, S., Tachibana, M., Masubuchi, Y., Suzuki, T., Cytochrome P450_{2D} and -2C enzymes catalyze the oxidative N-demethylation of the parkinsonism-inducing substance 1-methyl-4-phenyl-1,2,3,6-tetrahydropyridine in rat liver microsomes. *Chem. Res. Toxicol.*, **9**, 93-98, 1996.
92. Modi, S., Gilham, D. E., Sutcliffe, M. J., Lian, L. Y., Primrose, W. U., Wolf C. R., Roberts, G. C., 1-methyl-4-phenyl-1,2,3,6-tetrahydropyridine as a substrate of cytochrome P450_{2D6}: allosteric effects of NADPH-cytochrome P450 reductase, *Biochemistry*, **36**, 4461-70, 1997.

93. Jensen, K., G., Dalgaard, L., In vitro metabolism of the M1-Muscarinic Agonist 5-(2-Ethyl-2H-tetrazol-5-yl)-1-methyl-1,2,3,6-tetrahydropyridine by human hepatic cytochromes P450 determined at pH 7.4 and 8.5, *Drug. Metab. Dispos.*, **27**, 125-132, 1999.

Vita

Xueqin Shang was born in December 1965 in Shandong province, P. R. China. She received her B.S. degree in Chemistry from Shandong University in July 1986. She worked as an analytical chemist in Bioanalytical Division, Institute of Biology, Shandong Academy of Science from 1986 to 1994. She received her M.S. degree in Physical Chemistry from East Carolina University in July 1996. She joined the graduate program in the Department of Chemistry at Virginia Polytechnic Institute and State University in the Spring of 1997 under the direction of Professor Neal Castagnoli, Jr. Her research was sponsored by the Harvey W. Peters Research Center for Parkinson's Disease and Disorders of the Central Nervous System. She received her M.S. degree in Analytical Chemistry in the Summer of 1999.